Università Politecnica delle Marche
Scuola di Dottorato di Ricerca in Scienze dell'Ingegneria
Corso di Dottorato in Ingegneria Industriale

Experimental Dynamic Characterization of Tire/Tire Components

Ph.D. Dissertation of:

Stefano Galeazzi

Supervisor:

Prof. Enrico Primo Tomasini

Assistant Supervisor:

Prof. Paolo Chiariotti

Prof. Milena Martarelli

Ph.D. Course coordinator:

Prof. F. Mandorli

XVII edition - new series

Università Politecnica delle Marche
Scuola di Dottorato di Ricerca in Scienze dell'Ingegneria
Corso di Dottorato in Ingegneria Industriale

Caratterizzazione dinamica sperimentale dello pneumatico e di suoi componenti

Ph.D. Dissertation of:

Stefano Galeazzi

Supervisor:

Prof. Enrico Primo Tomasini

Assistant Supervisor:

Prof. Paolo Chiariotti

Prof. Milena Martarelli

Ph.D. Course coordinator:

Prof. F. Mandorli

XVII edition - new series

Università Politecnica delle Marche
Dipartimento di Meccanica
Via Brecce Bianche — 60131 - Ancona, Italy

Abstract

The reduction of the noise generated by rolling tire is becoming one of the most important and difficult challenges for tire manufactures. The increasing interest in tire noise performance is related both to the requirements coming from the car industry and to new regulations that impose a significant reduction of the noise emitted by tires in order to reduce the acoustic pollution of our cities. Rolling tire is the second noise source of a car; the first one is the engine. During last years, a lot of work has been done in order to make the interior of the cars as comfortable as possible and the current insulation can significantly reduce the noise coming from the engine, so, in order to increase the comfort level, the car manufacturers ask for silent tires. Rolling tire generates also noise propagating in the surroundings causing unpleasant noise for the people outside the car. From this short introduction it is clear how complex the phenomenon is and that there is a double problem, because both the in-vehicle (noise perceived by car passengers) and the exterior noise (noise propagating in the environment) must be considered, but, even if the noise source is the same, they are different phenomena and require dedicated countermeasures.
To obtain the noise reduction, it is necessary to consider the effect on noise emission of every components and materials used in tire construction. To do this it is necessary to better understand the noise generation mechanisms, in fact even if a lot of researchers have studied this phenomenon for decades, it is still not completely clear how noise is generated. For sure, one of the most important causes are the vibrations of the rolling tire.

This project deals with the study of tire vibrations using an innovative set-up based on the Digital Image Correlation technique. This technique has several advantages if compared with the current techniques among which the possibility to perform significative measurement of tire crown. This is one of the innovations introduced in this work, since this measurement can provide new information not available in the past years. In fact, all the other vibration measurement set-ups cannot perform this kind of measurement because of the presence of tire pattern generating an inhomogeneous surface. The new dynamic characterization of tire crown and its comparison with sidewall provide new information about rolling tire vibrations that suggest some countermeasures for the development of a noise-oriented tire structure. Two case studies are described to demonstrate the potentialities of the new set-up and demonstrating how an important noise reduction can be achieved.

In the second part of this PhD Project, the same set-up has been used to characterize some tire components with a dynamic noise-oriented characterization. It represents a completely new approach to the problem since the current characterization is performed in quasi-static condition or dynamically on small samples of rubber only: with these tests it is possible to completely characterize the rubber used for tire compound and the cords used as reinforcing fabric, but there are no physical or mechanical properties useful for the noise emission prediction. This lack of information is related to approach used: in the past years, tire silence was a secondary requirement. Nowadays, the reduction imposed is so strong, that tire developers are forced to consider it from the first stages of the development and the

absence of such a characterization has emerged. The proposed approach considers samples produced in the same way they can be found on the final tire: they are slabs made of a calendered rubber layer with embedded cords. Currently, rubber and reinforcing materials are separately characterized and it is not possible to predict the effect of a material on noise. The only way to know it is producing a tire and acoustically test it. In this way a lot of time and money are spent. The new proposed approach tries to evaluate the mobility of the samples and uses it as criterion to select the materials which are supposed to have a positive effect in terms on noise reduction. For sure, the final response comes from the test of the prototype, but in this way the selection of the proper materials is faster and, at the same time, the number of tests on tire and the prototypes produced is significantly reduced. In order to obtain good and useful results it important to define the correct structure of the samples, in fact even if the idea is to characterize the cap ply or body ply layers, the sample must contain also the belt package for global stiffness and mass reasons: if the belt is not used, the slab produced is very lightweight and the variation of the cord cause significant variations in terms of mass with a shift in terms of resonance frequencies that it is not related to mechanical properties of the cord materials or sample thickness, but it is related to the mass variation. When the belts are applied, the samples have almost the same mass and stiffness and the effect of the different cap ply layers is a variation of the mobility. The performed measurements suggest that the new approach produce interesting results correlating with vibration measurement on rolling tires.

In conclusion it can be said that an innovative measurement set-up for the characterization of rolling tire has been developed and validated and an innovative approach for noise reduction based on the characterization of tire components has been proposed.

Riassunto

La riduzione del rumore generato dagli pneumatici in rotolamento rappresenta una delle sfide principali e più difficili per le case produttrici e per gli ingegneri di sviluppo. Negli ultimi anni, infatti, c'è stato un sempre crescente interesse verso questo argomento a causa di richieste provenienti sia dal mondo automobilistico che dalle nuove normative in termini di inquinamento acustico, che impongono un forte abbattimento del rumore generato dagli pneumatici. Il rotolamento degli pneumatici sull'asfalto genera un rumore che viene percepito in maniera fortemente sgradevole all'interno del veicolo ed è piuttosto fastidioso. La richiesta di pneumatici silenziosi da parte delle case automobilistiche è legata al crescente livello di comfort degli abitacoli: col passare degli anni, infatti, c'è stato un notevole abbattimento del rumore generato dal sistema di propulsione, principalmente attraverso l'isolamento acustico dell'abitacolo e, dal momento che la seconda fonte di rumore dopo il motore è rappresentata proprio dagli pneumatici, si capisce come mai ci sia questo tipo di richiesta. Inoltre, la diffusione della mobilità elettrica e dei motori ibridi rende questa tematica sempre più importante, dal momento che il rumore del motore è fortemente ridotto o del tutto eliminato. Dall'altro lato ci sono le nuove normative riguardo la riduzione dell'inquinamento acustico delle nostre città che impongono anch'esse un forte abbattimento delle emissioni sonore dello pneumatico da raggiungere anche in tempi molto stretti.

Quando si parla di rumore generato dagli pneumatici occorre distinguere "in-vehicle noise" and "exterior noise": il primo rappresenta il rumore percepito dagli individui all'interno dell'abitacolo, mentre il secondo si riferisce al rumore emesso nell'ambiente e che quindi viene percepito dalle persone all'esterno della vettura. Da questa breve introduzione si capisce come il fenomeno analizzato sia molto complesso, in quanto comprende due componenti che sono molto diverse tra loro, sia in termini di meccanismo che di range di frequenza, e pertanto richiedono studi e contromisure dedicate. La somma di queste due richieste richiede un drastico cambio nel modo in cui il problema del rumore viene approcciato, in quanto per ottenere una così consistente riduzione del rumore è necessario considerare questo aspetto fin dalle prime fasi dello sviluppo di un nuovo pneumatico. Per fare ciò, è necessario in primo luogo approfondire la conoscenza dei meccanismi di generazione del rumore, in modo da definire le linee guida delle cosiddette "noise-oriented tires".

Tra i tanti meccanismi di generazione del rumore, il più importante è rappresentato sicuramente dalle vibrazioni dello pneumatico in rotolamento, pertanto gran parte del lavoro è stata dedicata allo sviluppo di un set-up di misura che permette di superare i limiti dello stato dell'arte, mentre la seconda parte è incentrata su un approccio innovativo allo studio del rumore, basato sull'analisi di singoli componenti.

La prima parte di questa tesi è dedicata allo sviluppo di un innovati sistema di misura basato sulla tecnica 3D Digital Image Correlation. Questa tecnica ha diversi vantaggi e permette di superare i limiti dello stato dell'arte, rappresentato dalle misure effettuate con il Vibrometro Laser Doppler. L'utilizzo di tale set-up ha richiesto un lungo lavoro di

ottimizzazione per valutare l'influenza di tutti i parametri di misura. Le moderne fast cameras usate in questo progetto sono caratterizzate da frame rate molto elevati, ragion per cui è possibile misurare spostamenti estremamente piccoli e, quindi, è possibile usare tale tecnica anche per misure di vibrazioni ad alta frequenza. Tuttavia, per poter avere un frame rate così alto, la risoluzione non è estremamente elevata e questo richiede un adattamento dell'inquadratura a seconda del range di frequenze che si vuole studiare: le vibrazioni a bassa frequenza (fino a circa 250 Hz) sono caratterizzate da spostamenti ampiezza elevata che investono tutta la struttura dello pneumatico e per questo sono detti modi di carcassa, mentre ad alta frequenza, le vibrazioni sono generate dagli impatti dei blocchetti di battistrada sull'asfalto che causano spostamenti molto piccoli dei punti localizzati intorno la zona di contatto. Nel primo caso, l'inquadratura dell'intero fianco può essere utilizzata, ma se si vogliono studiare le alte frequenze è necessario usare un'inquadratura focalizzata sulla zona di contatto, che è stato dimostrato essere la zona più rappresentativa del comportamento vibrazionale dell'intero pneumatico. Sempre nell'ambito della misura di vibrazioni, è stata inserita anche una delle principali innovazioni di questo lavoro, ovvero la misura sulla corona dello pneumatico, non possibile con altre tecniche a causa delle discontinuità introdotte dal pattern. In questo modo è possibile avere una caratterizzazione dinamica completa dello pneumatico e, attraverso due casi studio, è stato dimostrato come è possibile usare questa tecnica per fornire nuove utili informazioni agli ingeneri di sviluppo. Infine, il set-up di misura è stato validato sia in condizioni statiche che dinamiche attraverso il confronto con il vibrometro laser.

La seconda parte del lavoro introduce un innovativo approccio allo studio del rumore, considerando l'effetto di alcuni componenti della struttura dello pneumatico. Tale metodo vuole far fronte alla difficoltà degli ingegneri di scegliere quale sia il materiale più adatto, in particolare per quanto riguarda i materiali di rinforzo. L'approccio attuale è estremamente dispendioso sia i termini di denaro che di tempo perché basata sulla produzione e sul test di molti prototipi. Alla base di questo approccio c'è l'assenza di una caratterizzazione dinamica di campioni di gomma e corde dei materiali di rinforzo. Il nuovo approccio invece si basa sulla caratterizzazione dei materiali di rinforzo, fatta su campioni di gomma e corde realizzati allo stesso modo di come si troverebbe nello pneumatico. In questo modo si possono selezionare i materiali che rispettano determinate condizioni e i test su pneumatico servono solo per conferma, quindi il loro numero sarà ridotto. Il confronto di misure acustiche su pneumatico in rotolamento, caratterizzazione dinamica dello pneumatico e misure vibrazionali sui campioni ha permesso di definire che i materiali di rinforzo da preferire sono quelli che aumentano la mobilità della corona, in quanto si riduce la mobilità del fianco che è la principale sorgente di rumore. Tutto questo ragionamento è supportato da un caso studio presentato nell'ultimo paragrafo.

In conclusione, un nuovo sistemata per la misura delle vibrazioni dello pneumatico in condizioni di rotolamento è stato sviluppato, ottimizzato e validato attraverso il confronto con il Vibrometro Laser Doppler, sia in condizioni statiche che dinamiche. Il nuovo set-up permette di eseguire misure anche sulla corona, non realizzabili con nessun'altra tecnica. Lo stesso set-up è stato utilizzato per la caratterizzazione dinamica di componenti dello penumatico.

This page intentionally left blank.

Contents

This page intentionally left blank.

List of Figures

List of Tables

Chapter 1.

Introduction

The reduction of the noise generated from a rolling tire is becoming more and more important and it is probably the biggest and the most difficult challenge for tire designers because it is not easy to understand how noise is generated and which countermeasures can be adopted to reduce or control it. During last years, there has been a growing interest on this topic that has become one of the main performances considered during the development of a new tire. Until a few years ago, tires were developed trying to find the optimal balance between the main performances, such as dry handling, wet braking or low rolling resistance, and silence was an optional. If there were some noise problems, for example related to a car manufacturer's claim, the problem was solved with some design changes. The approach to the problem was empirical and based on slight changes in the design of tire pattern and every claim had an ad hoc solution. Nowadays, the scenario is completely different both for the new severe acoustic limits imposed by regulations and for the NVH requirements coming from car manufacturers. According to these new requirements, tire industry understood that the unique way to produce a silent tire is considering this feature since from the first stages of the development, studying a tire structure that is also noise-oriented in addition to all other standard performances. So, in order to design silent tires, it is necessary to understand how tire noise is generated.

Even though a lot of researchers have worked on this topic, the phenomenon is still not completely understood because it involves several mechanisms which interact with each other. The complexity of the phenomenon is well described by Figure 1.

Although the noise source is the same, i.e. the rolling tire, two noise components are generally distinguished: in-vehicle noise and exterior noise. The *in-vehicle noise* is the noise perceived inside the car; the *exterior noise* is the noise heard by the people outside the car, i.e. the noise propagated by the tire in external environment. In-vehicle and exterior noise are two completely different phenomena as can be seen from the spectra shown in the lower part of Figure 1: the exterior noise has a strong contribution at high frequency, while the in-vehicle noise decays above about 250 Hz. This difference depends on the nature of the phenomenon considered. The exterior noise depends only on the rolling tire while the in-vehicle noise depends on the interaction between tire and car which acts like a filter or an amplifier according to the frequency range: the noise reduction at high frequency is related to the cockpit insulation, while the amplification at lower frequency depends on the coupling of tire vibrations with car components (more details in Chapter 2).

In addition to this, a second classification must be done considering the mechanism involved in the noise generation. According to this classification, Structureborne noise and Airborne noise can be distinguished [1], as described in Figure 2.

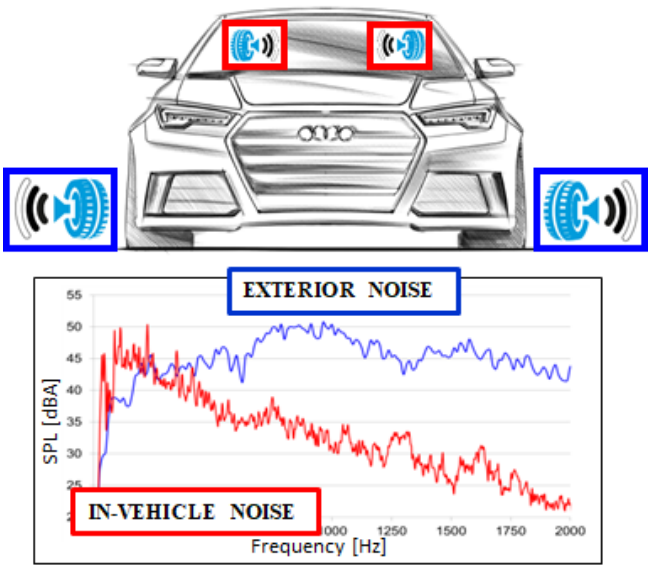

Figure 1 – In-vehicle and Exterior noise spectra of a rolling tire

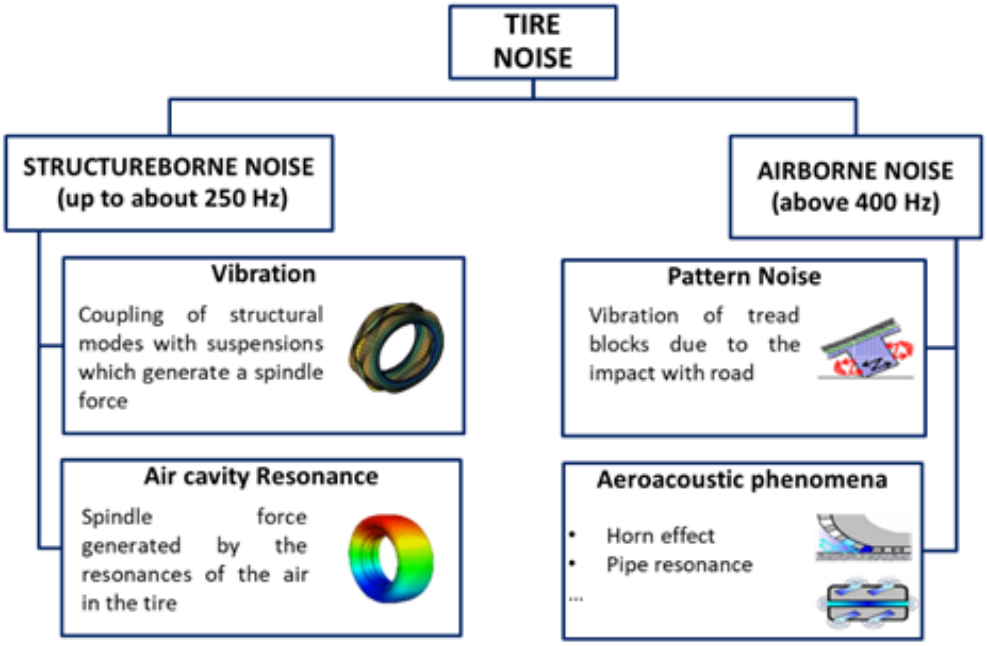

Figure 2 – Noise generation mechanisms

The so-called *Structureborne noise* is related to the spindle force generated by the interactions of tire and vehicle's components, such as the suspensions. The spindle force can be generated by:

- the coupling of tire carcass vibration with car suspension;
- the resonance of the air cavity enclosed between tire and rim.

The *Airborne noise*, instead, depends on the interaction between tire and road because, when the tire is rolling, the impacts of the tread blocks cause high frequency vibrations. Moreover, there are some aero-acoustic effect like horn effect or pipe resonances in the grooves of the tire responsible of the high frequency noise. The airborne component is mainly responsible of the exterior noise, but it generates also an annoying high frequency noise component that enters inside the cockpit.

It must be also considered that tire structure is very complex because it contains rubber and cords of other materials and their combination determines tire behaviour: this makes the understanding of noise generation mechanisms quite tough and, therefore, the definition of general rules for tire design become a difficult task.

From this short introduction, it is clear how complex the phenomenon analysed is and why both the regulations and the car's manufacturers require silent tire. From one side there is the car industry which requires silent tires because, over the years, ever higher levels of comfort have been reached inside the car through soundproofing of the cockpit that reduces the noise coming from the engine. Since the second main noise source on a car is the rolling tire, it can be easily understood how there is the requirement of quieter tires and this aspect will be more and more important with electric engines. The noise generation from the interaction of rolling tires with the road surface is the dominant source of vehicle noise for driving speeds above approximately 50-60 km/h for passenger cars [2], [3]. With new hybrid and electric engines, the effect is even amplified since the main noise source is removed.

On the other side there are the new regulations in terms of noise pollution reduction that impose a drastic tire noise abatement for the next years. Noise resulting from road traffic has a severe impact on the environmental quality in urban areas all over the world. In the European Union, it is estimated that approximately 80 million people are exposed to unacceptably high noise levels [4] and tire is one of the causes.

Moreover, it must be considered that, in order to produce "eco-friendly" tires, there is a progressive mass loss because of rubber reduction with an increase of the noise emitted: the vibrations of the modern lightweight tires are amplified due to the reduction of the damping material and consequently the noise emitted is magnified.

Another problem in the development of a noise-oriented tire structure is the absence of a dynamic characterization of tire materials that make impossible to predict if a material changes in one of the several layers making up the structure can be positive or negative in terms of noise emission. Nowadays the unique way to know the effect of a material change is the construction of a prototype and the execution of an acoustic test. This procedure is very expensive both in terms of money and time, because if the engineer must decide among several different technical solutions, it is necessary to produce a tire for each technical specification and execute a lot of tests. In this PhD project, a new approach based on the dynamic characterization of new tire samples is proposed in order to facilitate the material selection: the idea is to use the new characterization to select a small group of promising samples among a large group of materials and produce a smaller number of prototypes reducing the costs and the number of tests on tires.

This work focuses on tire and tire component vibration as noise generating driver. Since tire vibrations involves low and high frequency phenomena, an experimental characterization of tire and tire materials requires first of all the identification of a measurement technique able to cope with this frequency range (10 – 800 Hz) and with highly dynamic vibration amplitudes.

The aim of this PhD project is the understanding of noise generation mechanisms related to tire vibrations through the characterization of tire and tire components in order to define the guidelines for the design of the silent tires.

To dynamically characterize the rolling tire, an innovative measurement set-up for vibration measurement has been developed, optimized and validated both in static and dynamic conditions as well as the measurement procedure. The set-up is based on the *3D-Digital Image Correlation (DIC)* technique to overcome the limits of the current state of art techniques for this kind of measurement, as described in detail in Paragraph 2.3. The new set-up has several advantages, among which the measurement on tire tread can be considered as the most important innovation introduced by this work. The new set-up can be useful also for other activities, such as the validation of the *Finite Element Method (FEM)* models of tires or using the vibration maps obtained by a DIC measurement as input for the simulation of the radiated noise.

The same set-up is used to characterize the dynamic behaviour of tire samples in terms of mobility to define a criterion for a noise-oriented material selection. In this way the effect of tire vibrations on noise is studied from a global point of view (rolling tire) and a more detailed point of view (vibration of a single component/layer). The rationale behind this PhD project is illustrated in Figure 3 where the parallel strands are introduced.

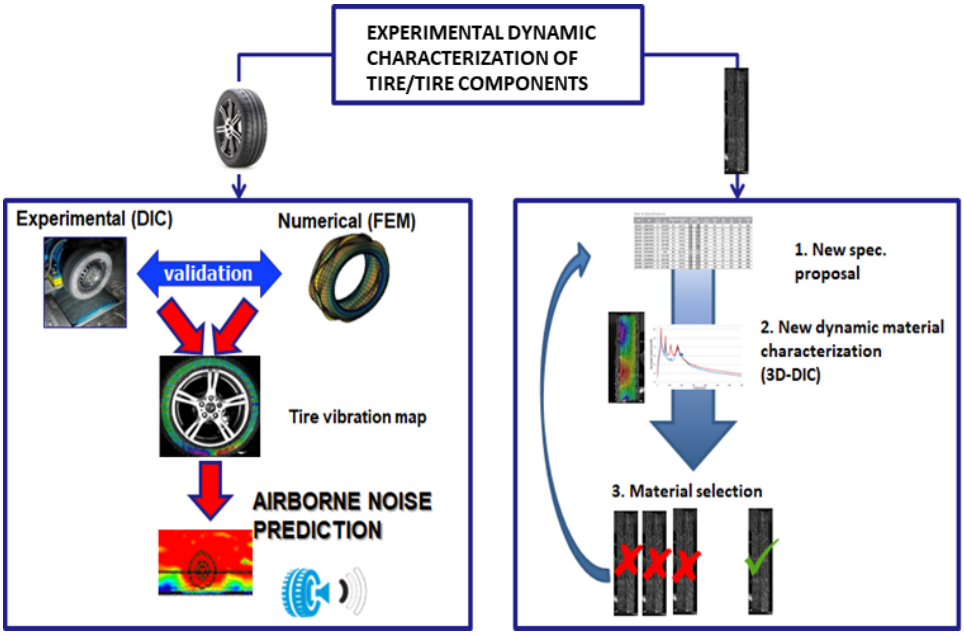

Figure 3 – PhD Project rationale

According to Figure 3, the thesis is organized in order to describe the two mainstreams.

Chapter 2 is the introductory chapter, so it is divided into several sections each of which describes a topic to give the reader a global point of view of the problem. In fact, the first section introduces tire structure in terms of its most important components; the second one describes the current status in the comprehension of the noise mechanisms with a brief description of them. The state of art techniques regarding the measurement of the vibrations of the rolling tire are introduced, analysed and compared in the third section as well as the innovative approach used in this work based on DIC technique. The fourth section deals with a focus on the state of art regarding the dynamic characterization of the materials highlighting which are limits related to a separate characterization of rubber and reinforcing cords. In the same section the new cord-rubber composite characterization is presented. The following section is dedicated to a brief theoretical introduction on DIC and the explanation of the different algorithms used and in the last paragraph the test benches used are described.

Chapter 3 is divided into two main parts. The first one describes what has been done to optimize the new 3D-DIC measurement set-up, describing which are the best configurations both for sidewall and crown measurement, both in static and rolling conditions. The chapter contains also the validation of the DIC technique made by a comparison with LDV both for the static and the dynamic case. The second part presents two case studies to describe the main outcomes of this works and how it can be obtained with two different technical solutions, because in one case a sidewall construction change is considered, while in the second one a crown change is applied, but the effect produced is the same.

Chapter 4 deals with the optimization of the 3D-DIC set-up to measure the vibration of tire slabs and a case study is described. The optimization of the measurement set-up, in terms of measurement technique is not described in detail, as done for the rolling tire case, because the static measurement and the experience of the author made the process of finding the best measurement conditions quicker. It was more difficult to find the optimal geometry and configuration of the samples, so this process is widely described concluding with a test case on the final samples. In the final paragraph the noise-oriented material selection is validated considering a test case in which acoustic and vibration measurements on tires are compared with the dynamic characterization of the new tire samples.

Chapter 5 states the main conclusions of the work, defining which goals have been achieved and which can be the next step for further developments of the technique.

All the measurements have been performed in the facilities of Bridgestone NV/SA Technical Center that is a co-financier of the PhD project. The acquisitions are performed by the Correlated Solution VIC-3D software and the post-processing is made through some Matlab scripts developed by the author to obtain the displacement or velocity spectra, the ODS or to convert the DIC data into a format file compatible with TestLab that is used to perform the modal analysis of both the tires and the tire samples.

This page intentionally left blank.

Chapter 2.

Theoretical background

2.1. Tire structure

In this short paragraph, tire structure is briefly described just to introduce the main components involved in this study. A car passenger tire must carry out several tasks such as providing the contact with the road, absorbing road irregularities and supporting vehicle load. All these tasks are demanded to sidewall and tread of the tire: the lateral surfaces of the tire are called sidewalls, while the tread or crown is the circumferential surface entering in contact with the road.
The main components of the tread area are illustrated in figure:

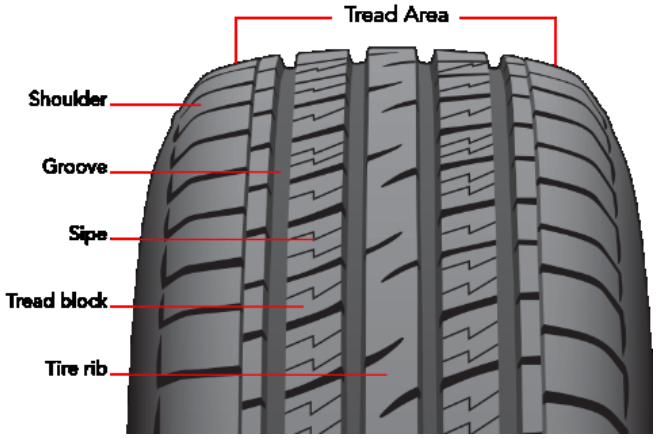

Figure 4 – Tire tread components [5]

- **grooves**: spaces between ribs needed for water evacuation;
- **sipes**: cuts in tread blocks for water evacuation and biting edges on road surface:
- **tread blocks**: their sequence and shape define the pattern design and have a strong influence on wear resistance, stability and traction;
- **ribs**: guarantee the contact of the tire with road, as well as tire shoulders;

- **shoulders**: connection point of sidewall and tread. Sometimes the shoulder tread block can have a special design for a better traction.

Tire structure is very complex because it is made of a series of layers having a well-defined function. In this work (Chapter 4) the belt package and the cap ply are considered. In Figure 5 a typical section of a radial tyre can be seen.

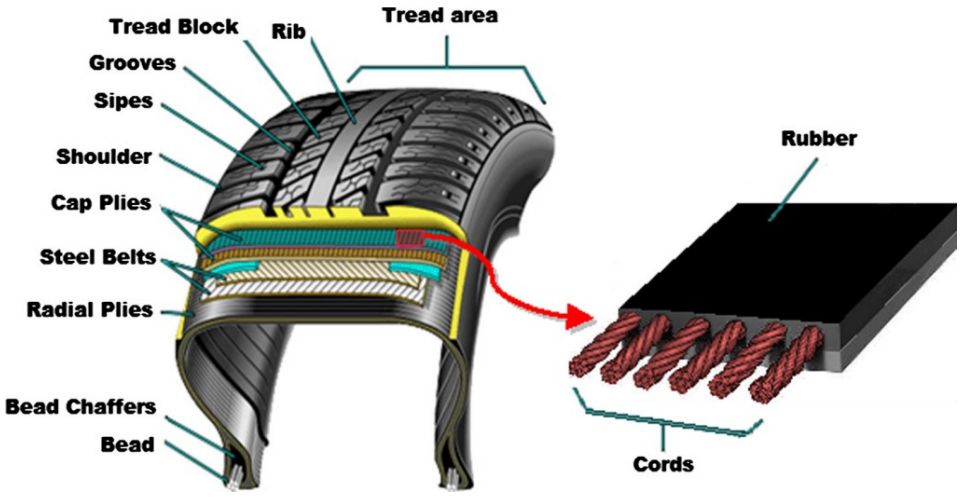

Figure 5 – Radial tire structure with a zoom on cord-rubber composite layer [6]

All the following information come from the reference book "Pneumatic Tire" [7] that can be used for further details.
Radial tires are so called because they have body ply cords that are laid radially from bead to bead, nominally at 90º to the centreline of the tread. The main components are:

- *Body ply layer.* It is made of a rubber skim coating that encapsulates the radial ply reinforcing cords. It is a calendred sandwich of two rubber layers and a reinforcing fabric. Body plies provide the strength to contain the air pressure and provide for sidewall impact resistance.
- *Cap ply layer.* It is made of rubberized parallel cords of reinforcing fabric wrapped circumferentially over the steel belts and under the tread. It is a mechanical device that restricts the amount of growth due to the centrifugal load on the tire [8].
- *Belt package.* It is made of steel cords and rubber layers. The belt skim is the rubber coating for the brass plated steel cords. The skim is calendered or extruded onto the steel cord in sheets and it is primarily formulated to resist fatigue and tear. Usually two or three belts are applied at opposite angles to one another on top of the body plies, under the tread area. They restrict expansion of the body ply cords, stabilize the tread area and provide impact resistance. Varying the belt widths and belt angles affects vehicle ride and handling characteristics.

In Figure 6 there is a sketch of body ply and cap ply layers.

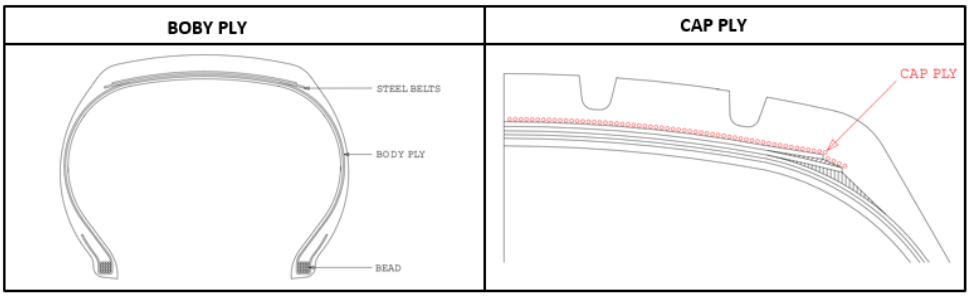

Figure 6 – Body Ply and Cap Ply sketch [8]

2.2. Noise generation mechanisms

In Figure 2 some of the main noise generation mechanisms have been introduced. In this section a brief description of them is provided. The relative importance of each mechanism is a function of several system variables, including tire characteristics, pavement surface characteristics, environmental and interfacial characteristics [9]. According to Sandberg and Ejsmont [10], independently from the frequency range, the mechanisms can be classified into two main groups, the vibrational and the air-related ones. In addition, there are also some amplification or reduction mechanisms that must be considered. During rolling, the tire is subjected to radial vibrations due to *tread impacts*: after the impact, the tread is pushed toward the tire rotational centre, it stays in this deformed configuration until the contact with the road is not released: in this moment it starts to oscillate to return to its initial position. These are the low frequency vibrations generated by the impact mechanism: it happens at the leading edge and the resulting vibrations involve the entire tire carcass. At higher frequencies the vibrations are generated by:

- *pattern impact*: impacts of tread blocks causing radial and tangential vibrations of tread blocks spreading to the sidewall;
- *stick/slip*: relative motion between tread elements and asphalt causing tangential vibrations;
- *stick/snap*: adhesive effect of tire rubber with the road giving either tangential or radial vibrations: at trailing edge each tread block is strongly deformed due to the adhesion between rubber and asphalt, so the contact release between tire and road is brutal causing blocks vibrations.

The high frequency noise is strongly influenced also by the aerodynamic mechanisms. The most important are:

- *air turbulence*: turbulence around tire due to the tire displacing air when rolling on the road and air dragged around the spinning tire [10];
- *air-pumping*: air displaced into/out of cavities in or between tire tread and road surface without necessarily being in resonance [10];

- *pipe resonance*: air displacements in grooves of tread pattern amplified by resonances [10];
- *Helmholtz resonance*: air displacement into/out of connected air cavities in the tire tread pattern and the road surface amplified by resonances [10].

As regards the amplification or reduction effects, the most important of them are the *air cavity resonance* (low frequency) and the *Horn effect* (high frequency). Between the curved tire tread and the road there is a space which forms an acoustic horn that increase the radiant efficiency [11].

All the mechanisms can be schematised according to the following chart providing an overview of the phenomenon.

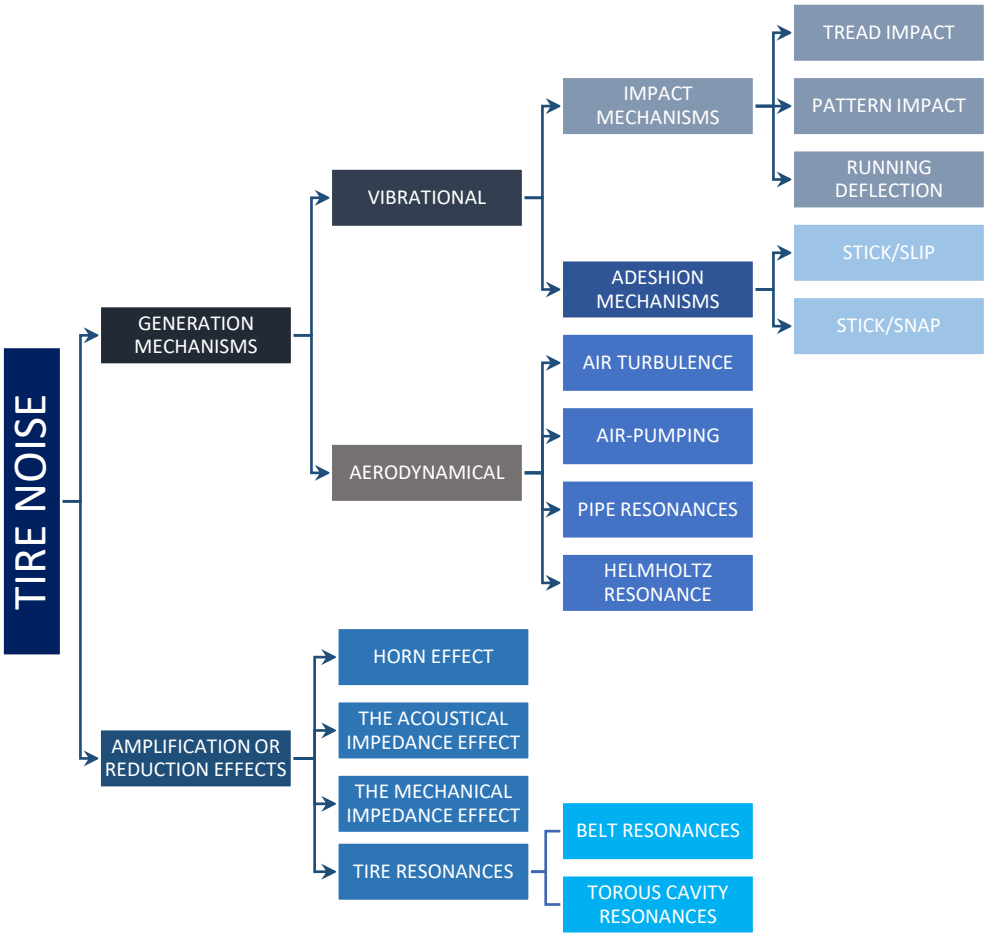

Figure 7 - Noise generation mechanisms chart

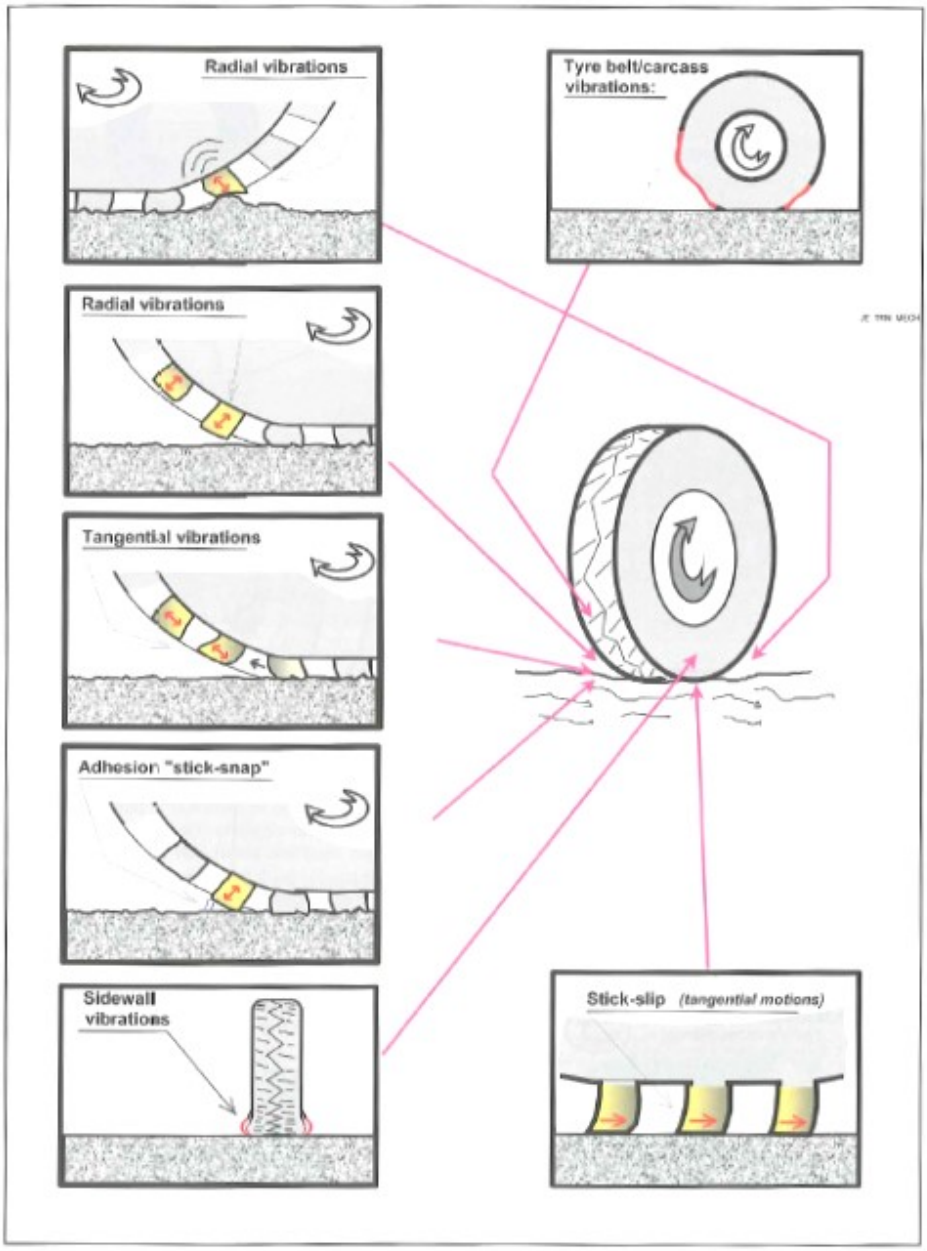

Figure 8 – Vibrational mechanisms responsible of tire noise [10]

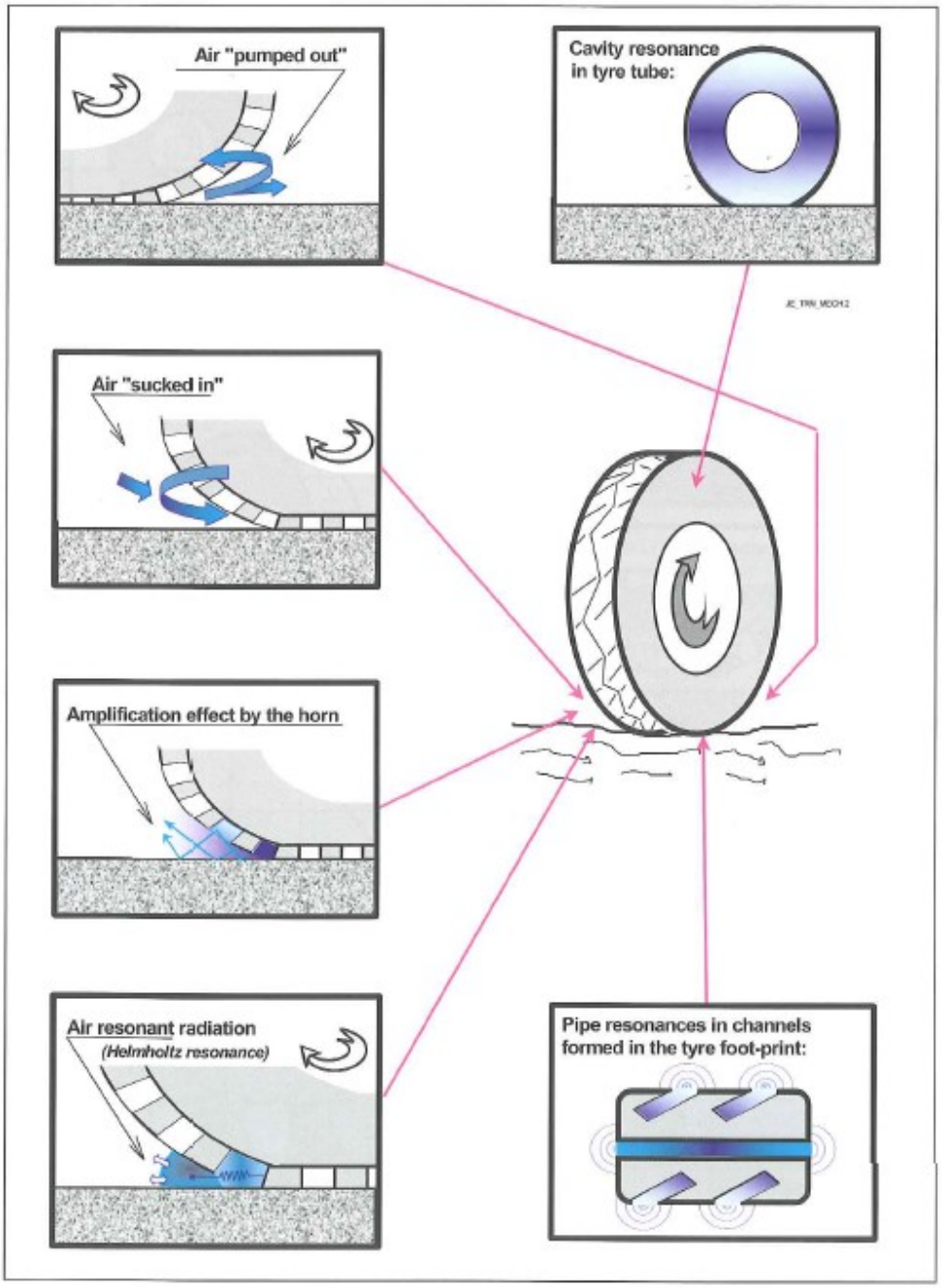

Figure 9 – Air-related mechanisms responsible of tire noise [10]

The previous figures are graphic representation of all the mechanisms previously introduced. In this work the attention is focused on the tire vibrations as main vector in noise generation.

2.3. Vibration measurement on rolling tire

Even though there are several noise generation mechanisms, the dominant one for a rolling tire below 1 kHz is the tire sidewall vibration caused by collisions between the tread blocks and the road [12], [13]. This statement is confirmed by Winroth et al.: in their work, they study the dependency of air-pumping (aerodynamic effect) and tire vibrations with speed and state that an important component of U^4 is found in measured tire/road noise on rough road surfaces where it is expected that the noise is mainly generated by tire vibrations, not air-pumping [14]. The air related phenomena are usually considered as amplification factors.

As stated in section 2.2, tire vibrations are different according to the frequency range: at low frequency (up to 250Hz) there are the carcass modes which involves the whole structure and are characterized by high amplitude displacements while in the high frequency range there are the vibrations responsible of the so-called pattern noise. In this case, the displacements are smaller and are strictly localized in the contact patch area, i.e. where there is the contact between tire and road. The impacts of tread blocks with the road cause first of all the vibrations of the blocks themselves and in turn the vibration of a small portion of the tire closer to the contact patch. The frequency depends on the rolling speed, the number of tread blocks and the pattern sequence. Tire tread pattern is made of blocks of different length to avoid the contemporary impact of the blocks with the road. The randomization of tread blocks is a common and efficient method used by tire manufacturers for reducing the tonal components in the noise. The idea is to distribute the energy over a larger frequency range, which gives a flatter sound response curve. Usually three or four different pitch lengths (the pitch length is the circumferential length of a shoulder tread blocks) are placed around the circumference of the tyre in an optimized sequence [15].

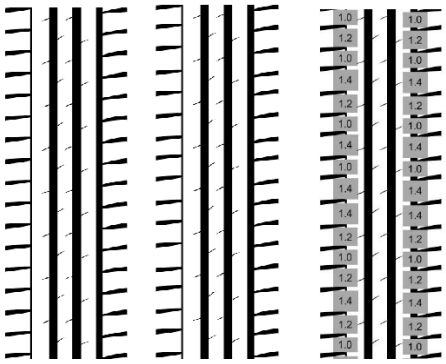

Figure 10 – Totally even pattern, no randomization (left); totally random shoulder blocks (center); optimized sequence of three pitch lengths (right). [15]

For this reason, the noise spectrum of a rolling tire does not have a peak corresponding to a certain frequency (there would be with equal length blocks) but there is a large "noisy area" with lower amplitude. In this way the overall noise level is reduced. The same happens for the vibrational spectrum. In the next figure, on the right side is presented the vibrational spectrum of a tire rolling at 80kph: the high frequency vibration is spread in a wide range (500 - 700 Hz); on the left is presented the effect of an optimized randomization (dashed line) and a mono-pitch sequence (black continues line).

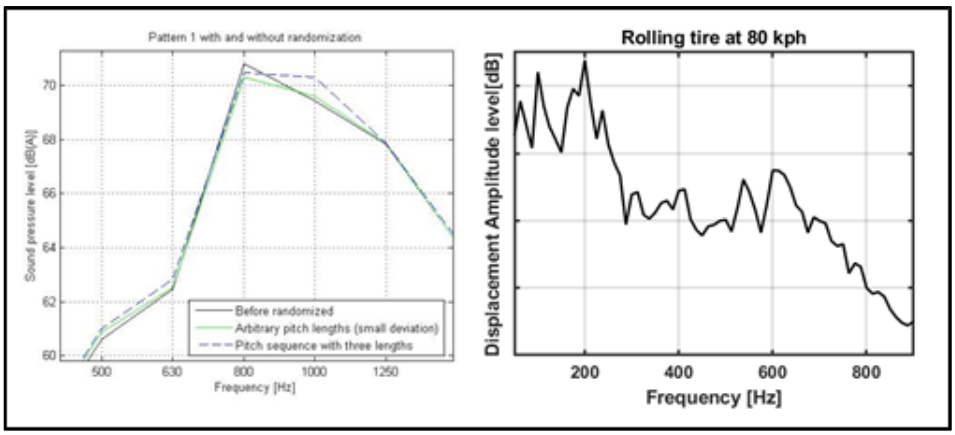

Figure 11 – Effect of pattern randomization on noise (left) [15] and vibration (right)

If the correlation between noise emission and tire vibration wants to be investigated, it is necessary to characterize the rolling tire. It should be pointed out that measurements on rolling tire are quite complex to perform for several reasons, first of all the tire itself. Tire structure is very complex, because it is made by rubber, that has a strongly non-linear behavior, and other material like nylon, steel, PET, Aramid, Kevlar, fiberglass and others whose coupling determine the global characteristic of the tire. Moreover, the measurement must be performed on a moving target and it is another complication because it reduces the number of instruments and techniques suitable for this application. For sure it is necessary to use a non-contact technique. To be honest, it is possible to develop a set-up based on the accelerometers, but it is easy to use only in static condition. Abd_Elsalam et al. [16] perform an experimental modal analysis on a non-rolling tire using a dedicated set-up suitable to vary some parameters and study their effect on the natural frequencies of the tire measuring the response of tire surface to the impact excitation using some accelerometers. In [17] the author performs the modal analysis of a loaded tire to evaluate the load effect with respect to a free-suspended tire. Yam et al. carry out a modal analysis on tire measuring the accelerations in all the directions and they were the first to obtain mode shapes in the radial, lateral and tangential direction [18]. Rocca et al. compare all the techniques defining advantages and limitations of each technique considering static and rolling measurement and they study the effect of the rolling speed on the natural frequencies comparing a static measurement made by accelerometers, with a rolling measurement in which an LDV is used [19]. Périsse uses a rotating signal transmitter to measure the acceleration of tire tread and sidewall with sensors put inside the tire to perform a vibration analysis of the rolling tire even if the number of

measurement points is very low. According to his measurement, the waves generated in the contact patch area are responsible for the noise radiation [20]. A similar work is presented in [21] where an electrodynamic shaker is used to excite a suspended tire, instead of the hammer. In rolling condition, the slip-ring could be used. A slip-ring is made of a rotor, which contains the sensors and is fixed to the rolling surface, and a static part, collecting all the cables. The biggest problem is the duration of the measurement: usually slip-ring have a small number of accelerometers, but in order to perform a significant measurement an high number of measurement points is needed, so it means that it is necessary to use a "start and stop technique", i.e. the measurement must be interrupt several times to move the accelerometers to different positions. In this situation the stationarity of measurement set-up and boundary condition is not guaranteed. Moreover, the slip-ring should be fixed to the rim, so it means that there is an addition of mass to the tire/rim system that could affect the natural frequencies of the assembly, especially in rolling condition. The first paper on this topic has been published in 1990. In this work, the time histories of sidewall accelerations measured on the sidewall of a rolling tire were analyzed in the frequency domain [22]. A system like this can be used only on the sidewall. There are few works in which micro-accelerometers are placed in the groove of the tire in order to measure the vibration of the crown: in [23] this configuration is used to perform a vibration measurement in the contact patch area to provide useful data for the experimental verification of the analytic and Finite Elements Method (FEM) models used to simulate and predict the tire tread vibrations in order to study the noise generated when the tire pass over contraction joints in Portland cement concrete pavements. In many cases the slip-ring set-up is used to perform other kind of measurements on a rolling tire and they are often mounted in the inner liner of the tire, that is, inside it. In [24] three three-axis accelerometers fixed on the inner liner of a tire are used to detect friction potential indicators on two equally smooth surfaces with different friction levels to provide a direct tire-road contact friction estimation that is essential for the autonomous cars and active safety system. Xiong and Yang in their work [25] confirm the possibility to use such set-up to obtain a lot of information about tire/road interaction by mounting it in the inner liner. This could be used also to measure vibrations, but it will be a very long procedure because the tire should be removed from the rim several times. Vercammen et al. use the accelerations measured in the inner liner of the tire to obtain the so-called dispersion diagrams, comparing experimental results with the simulated ones, in order to study the effect of rolling speed. The results show that a rotating tire is subjected to Coriolis accelerations which make the wave speed of the positive- and negative-going wave to diverge from each other. This leads to an asymmetric shape of the dispersion curves, while the dispersion curves of a non-rotating tire are symmetric with respect to the zero-wavenumber axis [26].

For sure the accelerometers are the most suitable sensors for a vibration measurement, but they have so many complications and limitations. For this reason, in literature can be found a lot of works in which this kind of measurement is performed by laser sensors and in most of the cases by means of a *Laser Doppler Vibrometer* (LDV). The LDV can be considered the state of art for this measurement for its several advantages: it is a non-contact technique, so there is no need to have a sensor placed on the measurement surface, it is possible to measure on a moving or rotating target surface and its high sensitivity allows to measure in a wide frequency range, that is probably the most important feature in accordance with the above. It has also some limitations, such as the need of a sufficiently homogeneous and optically cooperative surface, making impossible the measurement on the crown of a

patterned tire: the discontinuities generated by tread blocks and the other pattern features generate spikes in the signal when the laser spot passes through. Another potential disadvantage is related to the long measurement time, depending on the number of points to be acquired. Taking into account that the greater the number of averages, the lower the noise level, it is easy to understand that a measurement made by an LDV can be very long. For these reasons the stationarity of all the parameters influencing the measurement cannot be guaranteed when the tire is rolling: tire temperature and inflation pressure can change and an increase in tire temperature could change the response of tire materials. In literature can be found a lot of works in which the LDV is used to measure tire vibrations for several applications. Matsumoto et al. use a laser sensor installed on a wheel to measure tread displacement and evaluate the high-frequency vibrations of a tire when it passes over a cleat [27]. Rocca et al. [28] published a second paper dealing with the main experimental activities and modal analysis techniques available nowadays for characterizing the dynamic behavior of a static (unloaded and loaded tire on a fixed hub) and rotating radial tire under different boundary conditions (rolling speed, inflation pressure, preload, temperature and excitation). In the same work they identify the modes of a rolling tire using a typical test bench made of lens for LDV orientation and a cleat mounted on a rolling drum for the excitation (the set-up is presented in Figure 12). This set-up can be used to also measure the crown, but the tire is slick, i.e. it does not have the pattern, and for this reason a cleat is needed to excite the tire (more details on this topic are provided later in this paragraph). Castellini uses two different approaches to measure the sidewall vibrations: in [29] a Lagrangian approach is used because the laser spot tracks a single point along its trajectory unlike the second in which the laser spot is fixed and the tire surface flows under it (Eulerian approach) [30]. According to the approach, different phenomena can be detected: with the Eulerian approach it is possible to detect only vibrations associated with waves travelling in the laboratory reference system, while it is not possible to detect counter-rotating vibration waves that determine fixed figures and shapes [30]; with the Lagrangian approach it is possible to detect only vibrations associated with waves travelling in the rotating (synchronous with the tire) reference system. Standing waves moving with the tire cannot be detected [29]. In [31] a Scanning LDV is used to measure the vibration of the sidewall of a rolling tire mounted on a particular test bench. In [32] the LDV is used to measure the vibration of sidewall and crown of a slick tire using a tire-on-tire set-up and a cleat to excite the tire and simulating the excitation coming from road discontinuities. The data generated by an LDV measurement can be post-processed in different ways: they can be used to perform an Operational Modal Analysis (OMA) [33] on the rolling tire [19], [32]; obtain the Operational Deflection Shapes (ODS) [30]; study the correlation between tire vibration and noise in rolling condition [21]; generate the dispersion diagrams [34] in which Bolton and Kim introduce also the wavenumber domain decomposition of tire vibrations or compare the numerical and experimental dispersion diagrams [35]. Once again, the measurement is performed with LDV and a cleat is needed to excite the tire. The dispersion diagrams in rolling condition show how the effect of rolling speed is the loss of symmetry in the wave propagation due to Coriolis accelerations which make the wave speed of the waves travelling in opposite direction of the tire rotation to diverge from the speed of the waves travelling in the rotation direction [35]. This effect has been confirmed in [36] in which the authors use the LDV data to develop a model of tire based on thin cylindrical shell theory to evaluate the effect of rotation. They found that the

same shape of traveling-wave modes occurs for a rolling tire and that the excitation frequency of the forward wave is different from the backward wave.
LDV is used also to compare the vibrations levels of Trailing Edge and Leading Edge of a rolling tire by a crown measurement on a slick tire [37]. A system with mirrors is used to guarantee the perpendicularity of the laser spot with tread surface and according to the authors the Leading Edge vibration level is higher than that of Trailing Edge and tread vibration is influenced by belts. A slick tire is also used by Kindt et al in the reference paper for this kind of measurement. Using a special tire on tire test bench, with a cleat exciting the rolling slick tire and an LDV to measure tire response, in [38] the sidewall response is measured to evaluate the influence of some parameters (inflation pressure, rolling speed and cleat height). The same set-up has been used to measure both on sidewall and crown and the authors were able to identify the modes performing an OMA [39]. The same set-up is also used to perform an OMA on the rolling tire excited by the cleat to compare the data with the static case. In the same time an acoustic measurement is performed and a correlation between some acoustic peaks and vibrational modes has been found [40].

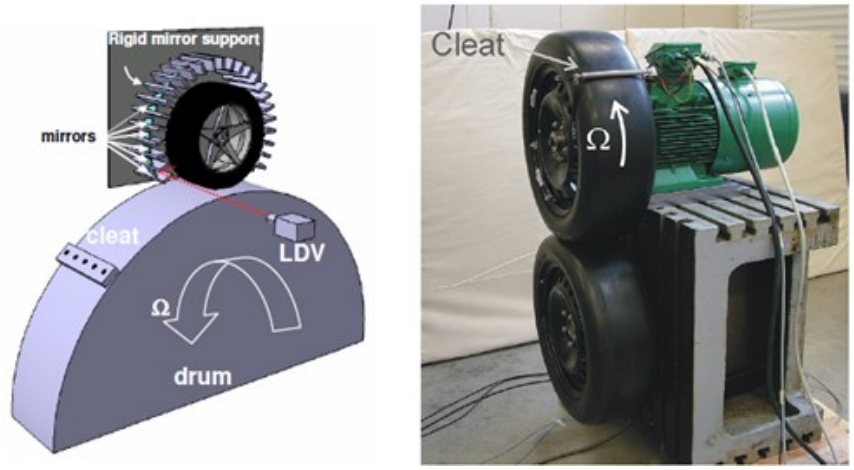

Figure 12 - Innovative test benches for measurements on rolling tires excited by cleat mounted on the drum (left) [28] and on tire-on-tire setup

Moreover, in [41] the LDV is used to perform a particular measurement: it is used in two different set-ups developed to measure the in-plane vibrations of tread blocks. The measurements allow to highlight and separate the frequency ranges related to carcass and tread blocks vibrations.

The limits of the LDV can be overcome with the Digital Image Correlation (DIC) technique. It is an optical technique, so it has all the advantages of a non-contact technique, but it is a full-field technique, so it is possible to acquire a high number of synchronous points unlike the LDV where an external sensor is always needed for the phase realignment of the signal of each point because they are acquired in different times. DIC technique is quite simple: it compares a reference image of the measurement surface with an image of the surface deformed to define the displacement of the measurement points. Since it works on displacements, it has a lower sensitivity if compared with LDV and this aspect made the

technique not suitable for a vibration measurement, especially in those cases in which there are high frequency vibrations that are characterized by very small displacements and this technique cannot detect them. The recent developments of modern fast cameras made possible to measure very small displacements, so this technique could be suitable for this kind of measurement, because it is possible to have sensor with quite high resolution and very high frame rate. Moreover, the DIC technique can be used also to measure the vibrations on the tread of a patterned tire. The confirmation of the possibility to use the DIC as a tool for vibration measurement can be found in literature: [42], [43], [44], [45], [46] are just some examples of works in which high speed DIC is used to measure vibrations of different objects and the results are compared and validated with classical techniques, such as accelerometers or LDV. The main difference with respect to the activity described here is the dimension of the target, because in the cited works the measurements are performed on simple and small objects. The target size is important because it defines the dimension of the image and in turn the resolution of the acquired images as well as the value of the smallest displacement measurable (more details in Chapter 3). A couple of DIC applications on tire can be found in literature, even if, according to author's knowledge, there were no references on vibration measurements on rolling tire performed by DIC technique when this PhD project started three years ago. In fact, the DIC technique has been used for several applications: measure the longitudinal tire slip ratio [47]; analyze stick-slip behavior of tire tread blocks [48]; measure the strain of a rubber sheet deformed by air pressure supplied below the sheet to compare these results with FEA predictions or visualize the deformation of an AGR tire, i.e. the tire of an agriculture truck [49]. Only in recent times (April 2018) a work, in which DIC is used to measure the dynamics of a racing tire of a formula SAE car in static and rolling conditions, has been published [50]. The DIC set-up is used to measure the displacement and the strain variation of the sidewall of a tire mounted on a car and rolling on a drum. The results indicate also the resonant frequencies and some operational mode shapes are shown. In [51] the DIC set-up is used to measure the vibration of a free suspended tire excited by a shaker or a hammer. The set-up is moved in different positions to measure different sections and then they are stitched to reconstruct the entire tire. The authors propose an approach to identify a uniform scaling factor that enables them to stitch the operating shapes extracted from different views. The advantage of acquiring a lot of measurement points suggests using this technique also to validate the FEM model of tire structure or materials. This is what is described in [52] where the DIC system is validated through the testing of a simple thin, rectangular rubber sample and the results are compared with the simulated ones.

One of the main advantages of the DIC technique is the possibility to work with inhomogeneous and discontinuous surfaces, the only requirement is the possibility to print the speckle pattern on it. This peculiarity made the DIC capable to measure also the crown because the pattern does not create problems unlike the laser-based techniques. This is the main innovation introduced in this thesis as regards the dynamic characterization of rolling tire. As previously described, the measurement on crown have been performed also with LDV, but only on slick tire excited by a cleat. LDV, in fact cannot measure a tire with pattern, but the excitation coming from the road it is not high enough to generate appreciable displacement on crown, so a cleat is needed. With DIC it is possible to measure a real pattern tire and the comparison these vibrations with those of sidewall provide useful information.

The importance of measuring the high frequency vibrations of a rolling tire in terms of noise emission is confirmed by Kropp et al.: they have been able to prove that there are

modes or groups of modes in the frequency range around 1 kHz that have small amplitude, but high radiation efficiency and they are mainly responsible for the noise emission [53]. Until a few years ago, the application of DIC as vibration tool was limited in terms of frequency range because the available cameras had low frame rate. The modern fast cameras have very high frame rate and a resolution such that the small displacements characterizing the high frequency vibrations can be detected.

2.4. Tire components characterization

The previous section, dealing with the state of art techniques in terms of vibration measurement on rolling tire, describes how the characterization of a rolling tire has been done in the past and briefly introduces how it is performed in this work just to highlight the main differences with respect to the current state of art. The dynamic characterization of the rolling tire will be deeply described in the next chapter. In this section, the problem of the dynamic characterization of tire components is introduced with the analysis of the available techniques and the limits of the current characterization.

2.4.1. An innovative approach to tire noise

If the understanding of noise mechanisms is complex, the evaluation of the effect of a single tire component on the overall noise is even more challenging. It depends on the complex tire structure, the coupling of the several materials used and the way in which different layers interact with each other.
One of the main difficulties in studying tire noise is the need of an experimental acoustic test on a prototype tire. In fact, there are no literature references or industrial know-how suggesting which material can be used to obtain a reduction of tire noise, so any time a variation is applied to tire structure, whatever it is, it is necessary to produce the complete tire and then test it. This procedure is too much expensive both in terms of money, because of the cost of tire testing and tire manufacturing, and time, considering the long time required to produce a tire and its testing. Moreover, the mechanism understanding of the noise generation process it is not increased and the effect of a single component cannot be evaluated because several solutions are proposed and the one giving the best result is chosen. In this way the problem is studied from a global point of view only.

In the second part of this work (Chapter 4), an innovative approach based on the dynamic characterization of tire components is proposed. The idea is to define a parameter which can be used for a preliminary selection of some materials belonging to a large group of proposals. The need for such characterization has emerged during the last couple of months of the PhD project. During this period, an activity to study the effect of different reinforcing materials on noise emission was started with the aim of finding which are the best materials for cords of cap ply and body ply. There was an evident difficulty in the choice of the

materials to be tested and as a consequence the number of tests was very high. The problem is the lack of a dynamic characterization of these components creating difficulties for material engineers which do not have adequate information to choose the materials. The available material characterization did not provide useful data since it is performed on small rubber samples (without cords) or in quasi-static conditions when sample contains also reinforcing cords: a load is applied and the deformation of the sample is measured to evaluate in-plane and out-of-plane stiffness. That's the way things are, if the effect of different materials wants to be investigated, so many tires must be produced, one for each material.
Also in the project described here this approach has been used, but, once a group of materials have been selected and the corresponding tires have been realized, in parallel some samples of cap plies and body plies made of the reinforcing materials used on the tested tires have been produced, as if they have been removed from their position inside tire structure. Unfortunately, it is impossible to cut a tire and extract each component because the layers are welded to each other, so it is necessary to produce the samples separately even if it generates some problems (as will be discussed in Chapter 4). The samples have been characterized using an electro-dynamic shaker and the 3D-DIC set-up and these results have been compared with acoustic and vibrational measurements on rolling tires.
As previously said, the aim of this activity is to find a parameter of the samples useful in predicting the effect on noise emission of the real tire. Since it is a completely new activity, there are no references in literature or industrial know-how suggesting which aspect to consider and how to define if a material is better than another in terms of noise emission. For this reason, the adopted strategy is based on the comparison of noise measurements on rolling tires, dynamic characterization of the rolling tires and dynamic characterization of the samples. The analysis of the data suggest that the mobility of the samples should be the parameter to be considered: the cases in which rolling tire noise is reduced are those in which the crown is free to vibrate and being the crown behaviour determined by cap ply and body ply layers, it can be stated that the best solutions are those giving a high crown mobility. It may seem strange that a noise reduction can be achieved increasing the mobility of a components, but this is the experimental evidence (more details will be provided in the case studies described in Paragraph 3.5). To be honest, it must be specified that the number of tested samples it is not too high, so all the results must be confirmed and validated with further tests. A dedicated project building has been realized considering a certain number of tires and tire samples, but further investigations could be performed to consolidate the outcomes of this thesis.

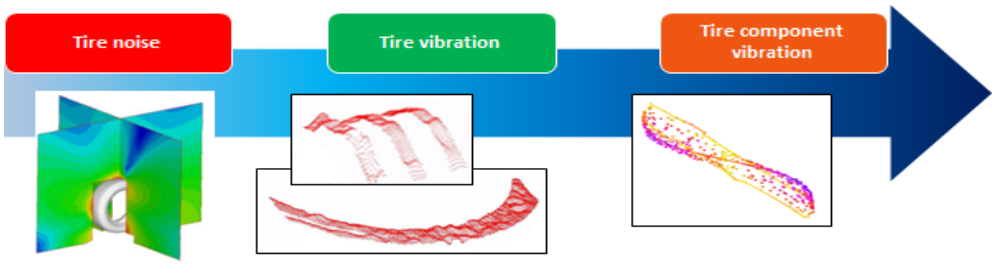

Figure 13 - Steps for noise and vibration correlation: noise [54] is related to rolling tire vibrations and then to the vibration of a single component

This new approach represents a drastic change in the way the noise is studied: in the first stage of the analysis, tire noise is related to tire behaviour through a dynamic characterization in terms of crown and sidewall vibrations; in the next step, tire vibration is related to a single component through its dynamic characterization. In this way, a significant step forward beyond the current state of art can be done increasing the level of detail of the analysis.
The current and proposed approach are compared in the following figure.

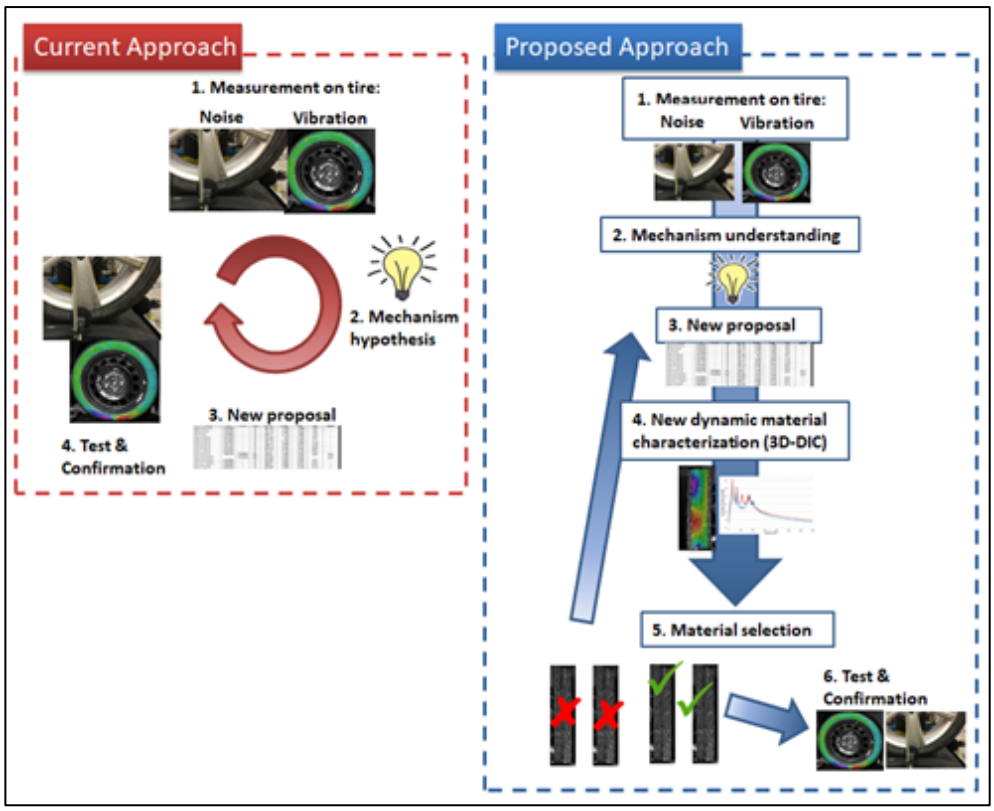

Figure 14 - Comparison of current and proposed approach for tire components characterization

Moreover, the new procedure reduces the costs of the development process as well as the devolvement times. Let's imagine having to choose the reinforcing material among a large group of materials. The current approach can be described by the following steps:

- definition of a list of materials to be tested considering only the static characterization currently available;
- production of a prototype tire for each different material selected;
- tire testing of all the prototypes;
- material selection made considering the tire that score the best results in terms of noise emission.

The approach proposed in this work is a little bit different and it is based on the dynamic characterization of tire samples. The new procedure is based on the following steps:

- definition of a list of materials considering only the static characterization currently available;
- production of tire samples using the materials previously identified;
- dynamic characterization of the samples;
- analysis of the results and selection of the materials satisfying the desired requirements;
- production of a reduced number of prototypes tire;
- test for confirmation, comparison and final selection.

The new approach can appear longer and more complex than the previous because it introduces some intermediated steps, but it has several advantages as discussed earlier. The approaches are compared in Figure 14.

2.4.2. Material characterization

The current material characterization has some limitations that should be overcome in order to increase the knowledge of material behaviour. The main problem is related to the lack of the characterization of the cord-rubber composites of which the plies are made. Rubber and cords are usually characterized separately.

As regard tire compound, i.e. the different types of available rubber, a lot of works have been done and its behaviour is very well known. Viscoelastic materials are characterized by the Dynamic Mechanical Analysis (DMA): it works by applying an oscillating force to the material and the resultant displacement of the sample is measured [55]. The deformation of the sample and the phase lag in displacement compared with the input force are measured. These data allow the calculation of damping or tan delta (δ) as well as the complex modulus [56]: the deformations are used to evaluate the complex modulus while the damping is related to phase lag. The usual outputs of DMA are Elastic (E') and Viscous (E") moduli defining the complex modulus. The ratio of the E" to the E' is the tanδ and is a measure of the energy dissipation of a material [57]. So, with this technique the samples are characterized by two parameters, tanδ and E' and they are related by the following formula

$$\tan\delta = \frac{E^{"}}{E'}$$

where E" are also called the Loss modulus and E' is the Storage modulus. The 'real' or 'storage' modulus is defined as the ratio of the in-phase stress to the strain; the 'imaginary' or 'loss' modulus is the ratio of the out-of-plane stress to strain [58]. So tanδ can be seen as the parameter which described the way in which the material absorbs and dissipates the energy.

Another important application of DMA is the measurement of the Glass Transition Temperature (Tg). It defines the temperature range in which the glassy transition occurs and it is a very important parameter for polymers because above the glass transition the material has rubbery properties instead of glassy property. It influences the material properties, because the stiffness drops dramatically with a damping increase. At the glass transition the

storage modulus decreases significantly and the loss modulus reaches the maximum. In the next figure, tanδ is plotted against temperature: the glass transition correspond to a peak since the material will absorb energy as it passes through the glass transition.

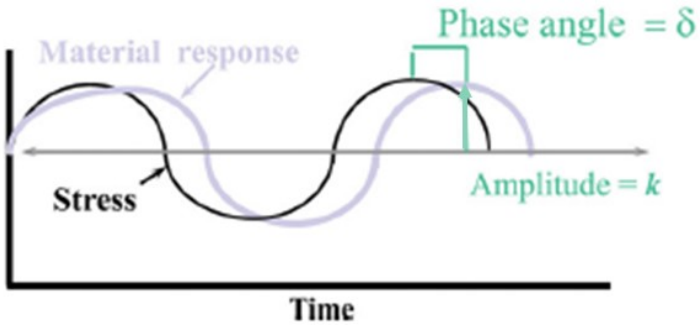

Figure 15 - Oscillating stress applied to the sample and its response [56]

In the following figure, three types of rubber taken from different areas of the same tire are considered and it is another demonstration of how complex the tire structure is because each area must perform a task.
The main problems of this technique are the frequency range and the dimension of the sample. This technique is usually used to characterized very small samples of vulcanized rubber that will be used in tire compounds, but the sample are not representative of what happen on the real tire. In the right side of Figure 16, a typical stress and strain curve is presented as well as the sample used for its evaluation. It can be seen the small dimension of the sample. The DMA, in fact, is used to evaluate the mechanical properties of the rubber, so a small sample is sufficient to get them.

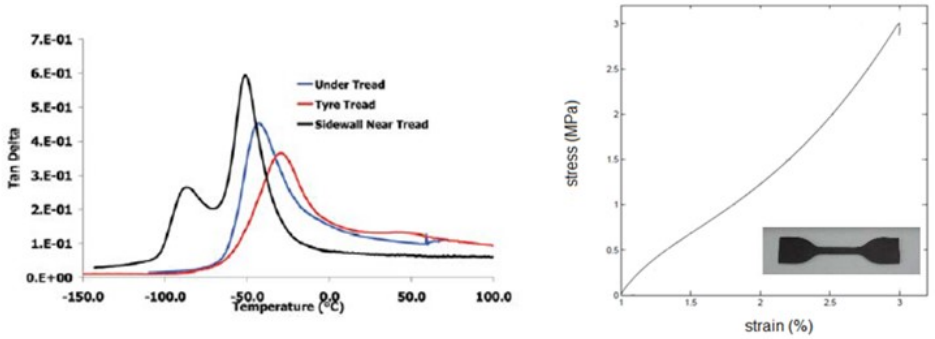

Figure 16 - Tanδ VS Temperature for different type of tire rubber [55] (left) and typical stress and strain curve of tire rubber and specimen geometry [58] (right)

As regards the reinforcing materials characterization, the main factors determining the final performance of a cord are construction and linear density. Textile corded reinforcements are complex structures made of hundreds of filaments twisted and organized into substructures [59] and a lot of efforts have been made in order to study the effects of all these parameters.

For example, Hockenberger and Koral investigated the effect of twist on the cord performance of PEN (Polyethylene Naphthalate), dimensionally stable polyester and high tenacity polyester cords [60]; the effect of combined twist with linear density has been investigated by A. Aytaç et al. on nylon 6.6 cords [61]; the adhesion of rayon, nylon, polyester and aramids has been investigated extensively [62], [63], [64] as well as the adhesion mechanisms between cord and rubber [65]. If the mechanical properties are very well known, the dynamic behaviour of cords has not been investigated.
In the same way, there is no dynamic characterization of cord-rubber composite. In [58] the available techniques for the characterization of rubber, cords and cord-rubber composites are described and an innovative investigation of mechanical response of cord-rubber composites based on a multi-scale approach is adopted in order to collect detailed data for the 3D FEM model of the cord-rubber lamina. However, everything is based on static measurements or on the DMA previously described in order to obtain the mechanical properties of the materials. Until now, indeed, there was no need for such a characterization because the effect of these components on the other tire performance does not require a dynamic characterization. A quasi-static characterization of samples with reinforcing material exist, but it is very simple and its outputs are the in-plane and the out-of-plane stiffness: the sample is placed on two supports and a vertical load is applied; the measurement of in-plane and out-of-plane deformations defines the stiffness in the two directions. As it can be easily imagined, it is very too hard to choose a material in this way because it is not possible to foresee or guess the behaviour of that material in the frequency range of pattern noise. For this reason, it is necessary to realize the complete tire and evaluate directly on tire the effect of one material compared to another one.

2.5. 3D – Digital Image Correlation

In this paragraph the DIC technique is briefly introduced. The main principles are described and the attention is focused on the different algorithms used in the case of a static measurement and in the case of a dynamic one.

2.5.1. Theory

The term “digital image correlation” refers to the class of non-contacting methods that acquire images of an object, store images in digital form and perform image analysis to extract full-field shape, deformation and/or motion measurements [66]. The measurement principle is similar to the Particle Image Velocimetry (PIV) in the fluid dynamic field.
This technique was born to perform static or quasi-static measurements of displacement to extract strain and deformation. The use of fast cameras allows to acquire images with a very high frame rate, so very small displacements can be measured and this technique can be used also to perform vibration measurements. Moreover, the use of a stereo-vision system allows

to have a 3D reconstruction of the object, so with a single acquisition the 3D response of the object is measured.

The target object must be painted defining a pattern of random points because the measurement is based on the tracking of these points between the different frames. On the images a series of subset or kernels (small interrogation area) are defined and the tracking of the subsets defines the displacement field. Since the measurement surface must be painted with a speckle pattern, each subset is characterized by an unambiguous distribution of points that define the "fingerprint" of that subset. The images are analysed frame by frame, to compare the position of these subset between a frame and the previous one: in this way the displacement is calculated for each time step. The reference and the deformed images are analysed by applying a cross-correlation in order to find the best fitting of the images and in this way the deformation and then the displacements of the measurement points are calculated.

2.5.2. Standard VS Differential algorithms

As anticipated before, the DIC technique defines the displacement from the comparison between a reference image and the deformed image. The reference image, which represents the undeformed status of the object, is divided into a certain number of smaller interrogation areas called subset. Each subset is characterized by a distribution of dots that describes it univocally and it allows the tracking in the deformed image. For each point, the displacement is calculated with respect to the central point of the subset. Point P(x,y) moves to P'(x',y') where x' = x + u and y' = y + v are the new coordinates after the deformation, u and v are the displacement components in the reference system of the cameras. The image below describes this process.

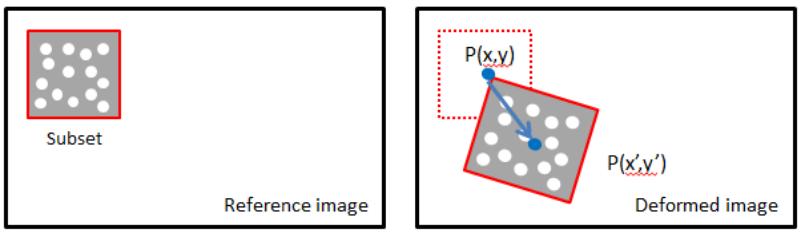

Figure 17 – Classic DIC approach

The classic DIC uses a Lagrangian approach since, frame by frame, each point is followed along its trajectory. There are cases in which this approach cannot be used, e.g. with great deformations. In these cases, a different approach is used: the Eulerian one that is described in the next subsection.

The incremental algorithm was developed for those cases in which an update of the reference image is needed in order to perform the measurement. If the object is subjected to a very high deformation, it is not possible to perform the cross correlation between the images because they differ too much, or the wide deformation could hide some measurement points or they could exit from the framed area. With this algorithm an intermediate image between

the reference and the deformed one is considered, so it's like the deformation is calculated in two times.

In this work, the incremental algorithm is used to define an Eulerian approach to study the vibrational behaviour of the rolling tire. In this case the idea it is not to follow every single point along their trajectory, but the measured area is fixed and the deformation in a certain point depends on what happens below that point of the fixed area.

With the incremental algorithm, the reference image is constantly updated: at time step t =1, the displacement is calculated comparing the deformed with the reference image, then the deformed image becomes the reference for the deformed image acquired at time step t = 2 and so on, as shown in Figure 18.

The main difference between the algorithms is that in the first case an absolute displacement is measured while a relative one is measured with the second approach. However, the possibility to use such approach gives the opportunity to measure the vibrations of a rolling tire because frame by frame the reference image is updated, so the displacement between one frame and the next is always detectable by the technique.

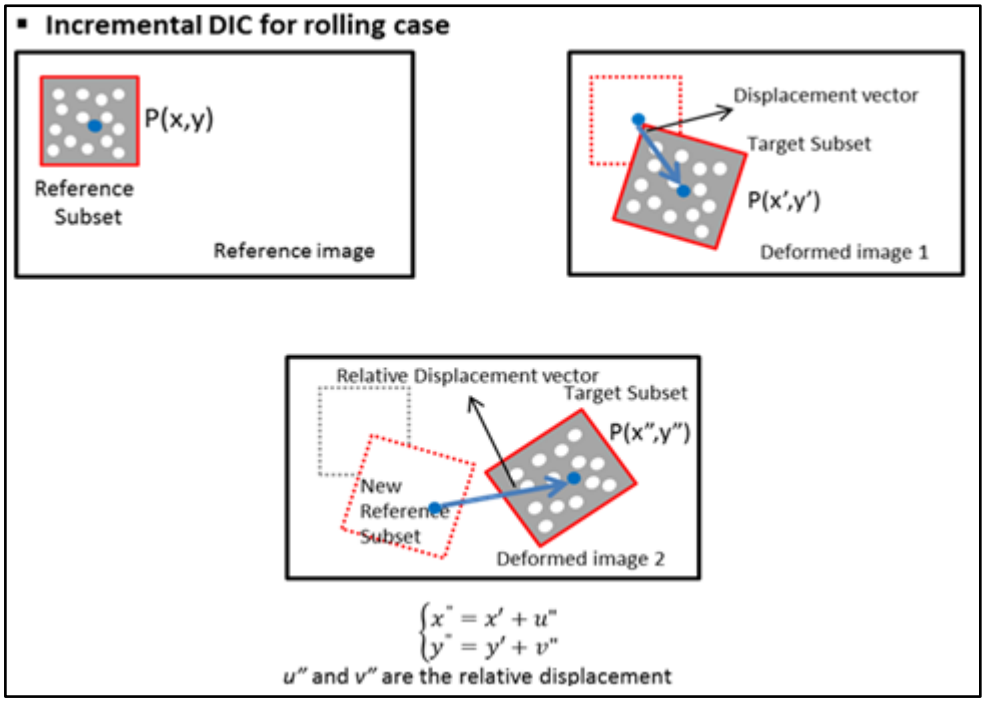

Figure 18 – DIC incremental approach

In the case of a rolling tire this is the only usable approach: every point describes a circular trajectory that is not possible to track if the reference image is kept fixed to the first acquired image, because after the first frames, the displacement will be too wide and the cross-correlation between reference and deformed image will fail (a very simple sketch of what happens is provided in the following figure).

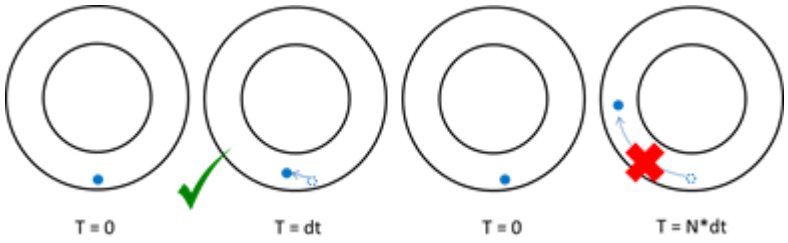

Figure 19 – Example of classic DIC algorithm applied on rolling tire: when the displacement is too wide, it cannot be used (right)

2.5.3. Speckle pattern

To perform a DIC measurement it is necessary to prepare the measurement surface with a speckle pattern in order to define the points which will be used by the correlation algorithm to define the displacements. This is a very important step, since a bad speckle pattern can compromise the measurement, or it can cause a significant error in the measurement, while a good pattern will allows the correlation to be made with high confidence and produce low noise.

For this reason, a lot of time has been spent in the definition of the best speckle finding the optimal combination of some parameters such as the ink pressure. A good pattern must have some requirements:

- high contrast: a very high contrast between speckle and surface is needed to detect the measurement points;
- percentage coverage: according to literature [67], a good speckle covers from 40 to 70% of the measurement surface, this value determines the distance between the points in the pattern;
- speckle size: speckles should be ideally 3-5 pixels in size in order to optimize spatial resolution, but the most important thing is that the speckles are consistent in size and not too small (less than 3 pixels in size is too small and can cause aliased results) [68];
- random: the pattern must be sufficiently random in order to avoid any mismatch in the correlation. If different areas of the surface have the same distribution of points the algorithm could not be able to perform the correlation or in the worst case the correlation is performed between different points;
- speckle size: it must be defined according to the distance between the camera and the object and considering the previous requirements.

The size of speckle pattern is probably the most important parameter. There is not an exact value of speckle size according to the performed measurement, it exists a wide range of size which can be used for a certain measurement. The experience guides the choice. As general rule it can be said that speckle should neither be too small nor too large: if the pattern has

points too big or too sparse, the spatial resolution will be poor; a speckle too thick will cause aliasing if the camera resolution it is not high enough to represent the geometry of the object and the resultant image will be affected by the so-called Moirè effect, i.e. the image will exhibit an interference pattern, as shown in next figure [68].

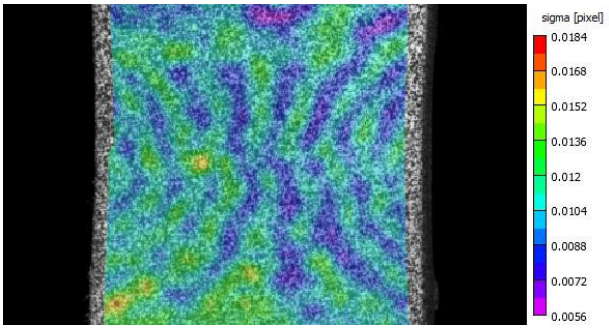

Figure 20 – Example of Moirè effect generated by a bad speckle pattern [68]

The following image contains an example of how the tire surface is prepared by means of a special printer.

Figure 21 – Example of the speckle used to measure tire vibrations

2.6 Test benches

This topic is presented in the chapter dedicated to the state of art review because the facilities have not been developed during the PhD project, but they have been provided by the tire manufacturer. Two different test benches have been used.

All the acoustic and vibrational measurement on rolling tires have been performed into a semi-anechoic chamber where the tire is mounted on a so-called tire-stand, that in a

very simple way can be considered as high mass system, with a neutral shaft and a hub to fix the tire. The tire-stand can be vertically moved to defined tire load. Under the tire there is a drum driven by an electric motor placed outside the anechoic room for insulation reasons. The electric engine defines the rolling speed of the drum and consequently of the tire. The drum can be covered by different shells according to the test to perform. Each shell has a different roughness defining different tire excitations. In this work, a replica road surface is considered since this is the surface used in the Pass-by-Noise test that is the regulated test for the measurement of the noise emission. This is the configuration most similar to the real life of the tire, so in this condition the vibrations must to be measured. Around the tire there is an array of microphones used for the noise measurement.

The measurements on tire components are performed in a different laboratory where there is a traction machine used to impose an axial load to the samples: one of the clamps is fixed while the second is movable and pull the sample.

2.7. Chapter summary

This chapter deals with a theoretical introduction to the phenomena studied in this work. In the first part tire structure is briefly described and an overview of tire noise mechanisms is provided. This short introduction has been used to explain the complexity of the phenomenon and also to justify why it is so important the measurement of rolling tire vibrations: among all the mechanisms, the most important is tire vibration. Moreover, the problem of the lack of a dynamic material characterization is introduced as well as the innovative approach proposed in this work based on the characterization of tire components.

The following paragraphs have been dedicated to the state of art overview in terms of vibration measurement on rolling tire and material characterization, describing what has been done until now and which is the innovation introduced during the PhD project.

This page intentionally left blank.

Chapter 3.

Tire characterization

In this chapter, the optimization of the DIC measurement set-up on rolling tire is described considering some of the parameters that mostly influence the measurement or the image processing such as the camera resolution, the distance from the object, the framed area and so on. Static and dynamic measurements require different optimizations. In the first part the results of an impact test are presented, while the second part is dedicated to the dynamic optimization. Both the set-up configurations are validated through LDV comparison. In the final section, two case studies are presented to describe one of the main outcomes of this project in terms of noise reduction trough tire vibration control.

3.1. Set-up optimization and validation in static condition

This section deals with the static characterization of a reference tire based on the classic impact test to define the optimal set-up configuration for this test case and to test the DIC capabilities with a simple case. The same measurement is performed with the LDV and both the data are used for the Experimental Modal Analysis and the results are compared for the static validation of the DIC system.

3.1.1. Static tire characterization

DIC capabilities as vibration measurement tool have been tested in the simple static case of the classic impact test.

3D-DIC set-up is made of two cameras to measure displacements and deformations in three directions. The cameras must be placed at the same distance from the target object and they must have the same angle in order to have a correct 3D reconstruction. The distance between the cameras and the object depends on the size of the target but also on the resolution needed to measure the desired phenomenon which in turns depends on the excitation, as will be discuss later. The set-up is made of two synchronized fast cameras characterized by a maximum frame rate of 4000 fps at the maximum resolution of 1024 x 1024 pixels and an internal storage of 8GB which defines the number of acquired frames (5400) and accordingly the measurement time that is very short (1.35 seconds): the images are stored into the internal memory of the cameras and then they are transferred to the PC through a LAN cable connection. This operation requires about 10 minutes. The illumination of the scene is

provided by 2 LED lamps of 175 W each. A DAQ unit complete the system: it is used to acquire the load cell used during post-processing for the calculation of the FRFs and it is triggered with the master camera. The cameras must be oriented according to Figure 23.

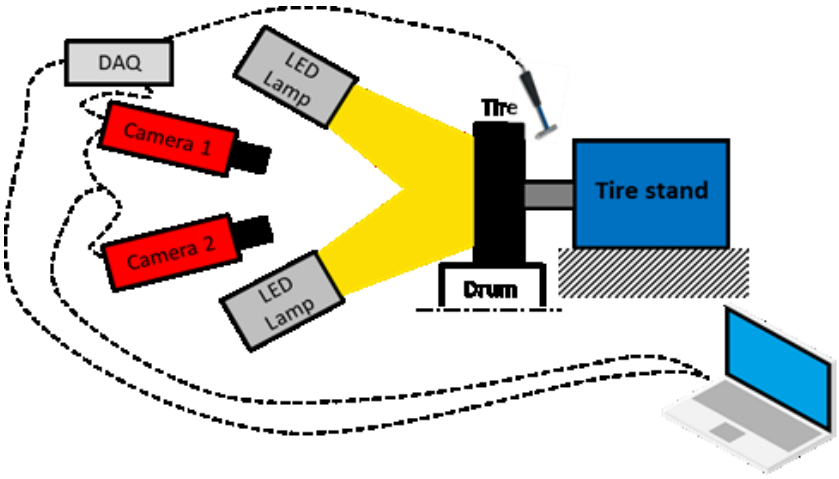

Figure 22 – 3D-DC measurement set-up for static measurement

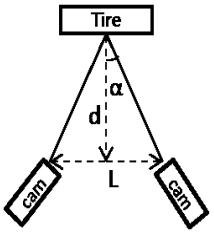

$$\sin \alpha = \frac{L/2}{d} \cong 0.25$$

Figure 23 – Cameras configuration

All the images are processed with Correlated Solution VIC-3D software in order to perform the correlation and obtain the displacement field. In static condition this operation requires less than 30 minutes.

After this step, all the data are exported into Matlab format files and post-processed with a script which select a median circumference of 80 points like LDV (DIC defines a displacement field of thousands of points), convert the displacement into velocity time histories (to perform the comparison with LDV data the displacements are differentiated obtaining the velocities: this is the reason why the abscissa of all the following plots refers to a velocity instead of a displacement) and generate a Test.Lab format file in order to use this software to perform the modal analysis. This file simulates the synchronous acquisition of 81 channels: the hammer and 80 velocity signals.

For the static characterization the tire is mounted on the rim, the inflation pressure is the same at which the tire is subjected in rolling condition and it is loaded. Several tests have been done to find the best impact point. Since the focus is the measurement of the out-of-plane vibrations of the sidewall, it is very important to define the optimal hammering conditions because the excitation in that direction must be high enough to generate appreciable velocity or displacement in the measurement direction. The optimal solution in terms of high excitation and low noise is hitting the so-called opposite serial side (OSS) that is the sidewall opposite to the measured one. In this way the hammer does not cover the measurement surface and the saturation of DIC system is avoided: the displacements in the impact area are too much higher than those of the other points, so the range to be measured would be too wide and the smallest displacement could not be correctly measured. The average FRFs obtained along the three directions with the static test are reported in Figure 24.

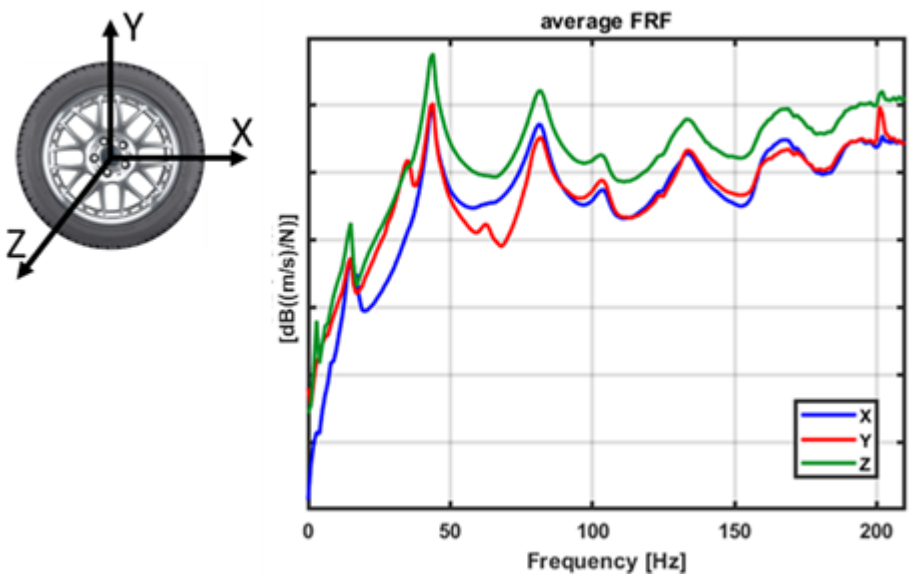

Figure 24 – FRFs along X (lateral), Y (vertical) and Z (out-of-plane) direction of a loaded tire-rim assembly with fixed hub and the reference system (on the left)

In the figure the average FRFs obtained for the 3 directions are presented: X and Y axis define the plane of the sidewall, while Z axis define the out-of-plane direction. It must be pointed out that the excitation was mainly in the Z direction since the focus is the measurement of the out-of-plane vibrations which are supposed to be the most influencing the noise emission and also because the Z direction is the only direction measured by the available LDV used for the validation. For this reason, the mobility level of the out-plane-direction (green line) is higher than the others. As anticipated, the LDV comparison is the reason why on the y axis there is the velocity-force ratio (mobility) instead of the displacement-force one (receptance). Despite the out-of-plane excitation, the system can measure in all the directions and it is interesting to see how the cavity resonance peak around 200 Hz is detected in the vertical direction as expected.

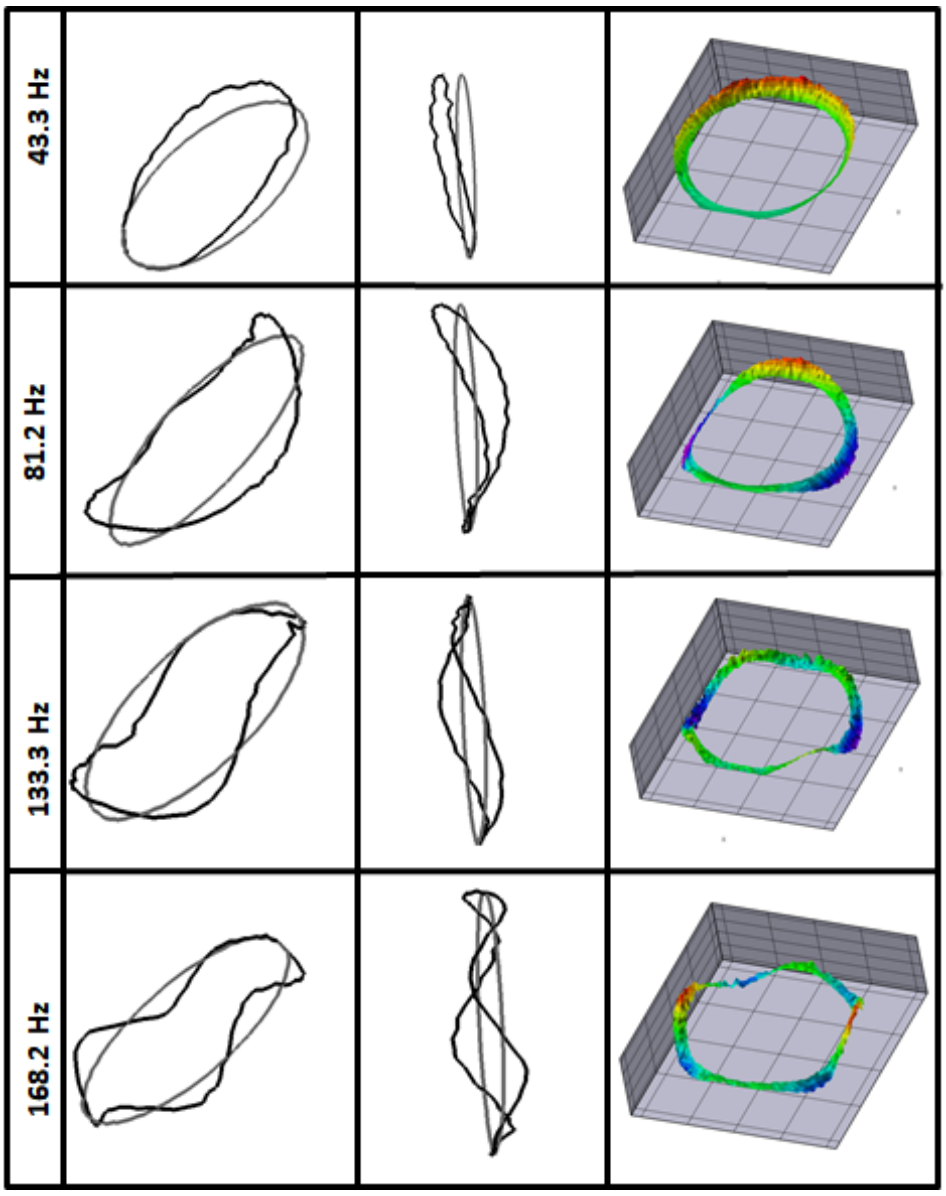

Figure 25 – Out-of-plane modes of static tire: 2 different views of the mode shapes obtained with TestLab (on the left) and 3D visualization of the same mode shapes using the software of image processing (third column)

The air inside the tire, in fact, resonates at specific frequencies, depending of the air volume enclosed between tire and rim, generating a rigid vertical displacement of the tire structure. The resonance frequencies are aligned for all the directions because of the excitation

magnifying the out-of-plane displacements. In Figure 25 the mode shapes are presented considering only a circumference instead of all the points measured by DIC in order to consider the same points measured by the Scanning LDV, because this is the way in which the comparison between the techniques is made. For this reason, only the radial modes are detected and the out-of-planes mode shapes are visualized. In the last column there is the 3D visualization of the mode shapes considering all the DIC points. In Figure 25 the grey line represents the undeformed circumference extracted from the DIC data, while the black line shows the mode shape.

3.1.2. Static validation

The Scanning LDV set-up for static measurement is shown in Figure 26: the tire is mounted on the tire-stand and the laser head is placed in front of the tire sidewall. LDV and hammer's load cell are connected to the data acquisition system (LMS SCADAS Mobile). The laser spot is moved by a LabView VI controlling the rotation of two small glasses needed to move the laser spot through the points of the measurement circumference defined on the sidewall. All the data are processed in LMS TestLab and mode shape and the modal parameters are obtained by means of the Polymax algorithm.
In the figure there is also an accelerometer: it is used in rolling condition as phase reference sensor. In rolling condition, in fact, the measurement setup is the same, the only differences are the excitation and the reference sensor: hammer impact with load cell in static condition, rolling tire with accelerometer fixed on the tire-stand for the dynamic case.

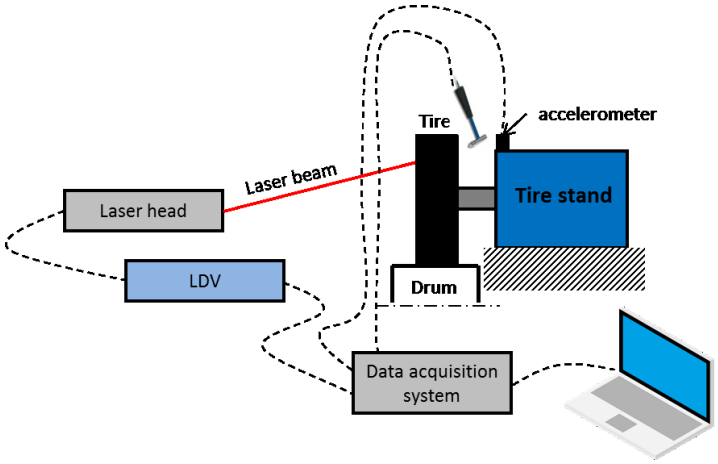

Figure 26 – LDV measurement set-up for static and dynamic measurement

The DIC set-up has been previously described.

Figure 27 shows the average FRFs obtained for the two systems considering a circumference of 80 points and in the same conditions of load and inflation pressure. There

is a good correlation between LDV and DIC both in terms of amplitude and frequency. There is a small frequency shift for some modes and a difference in terms of amplitude, but this could be related to the number of averages: the FRF obtained by LDV is the results of the average of 5 impacts instead of the DIC's FRF which is the results of a single measurement. As expected the hammer can excite tire structure up to about 200Hz, where there is the biggest difference of the curves: due to its higher sensitivity, the LDV is capable to detect the cavity mode (the peak at 200 Hz) instead of DIC where the peak is scarcely visible. However, it must be remembered that the cavity is well detected by DIC in the vertical direction, in fact the spectrum of displacement presents a clear peak at 200 Hz, but it is not reported here since the comparison is made on the out-of-plane component. Moreover, there is a small frequency shift, but it could be related to a higher noise level which characterizes the DIC technique if compared with the LDV. The results are summarized below.

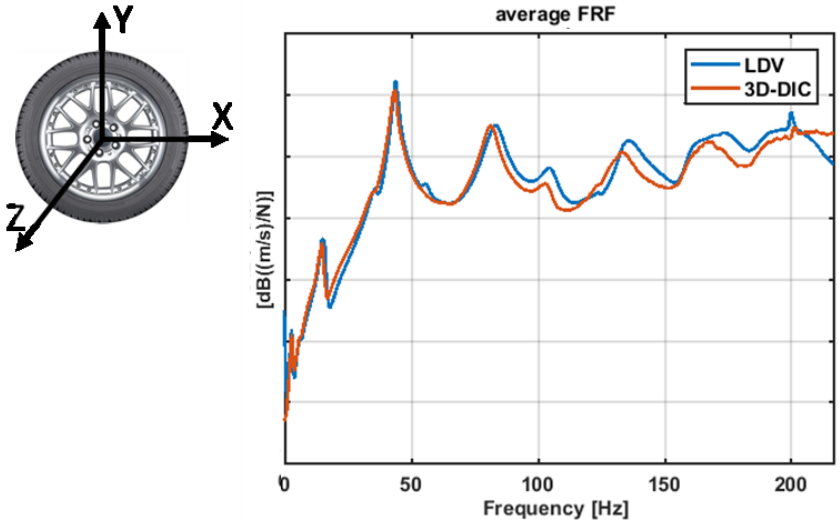

Figure 27 – Comparison of the average FRFs considering a circumference of 80 points both for LDV and 3D-DIC

	LDV	**3D-DIC**
	Frequency [Hz]	Frequency [Hz]
Mode 1	15.1	14.9
Mode 2	43.2	42.9
Mode 3	78.9	78.3
Mode 4	103.2	102.3
Mode 5	129.6	129.3
Mode 6	156.3	156.1

Table 1 – Frequency comparison between DIC and LDV in static condition

The frequency axis is truncated above 210 Hz since at higher frequency there are no significant information because of the damping of the tire making impossible to excite the

structure at higher frequency in static conditions. In the next figure the mode shapes obtained with the two systems are compared showing is a good correlation (except for the 4th mode).

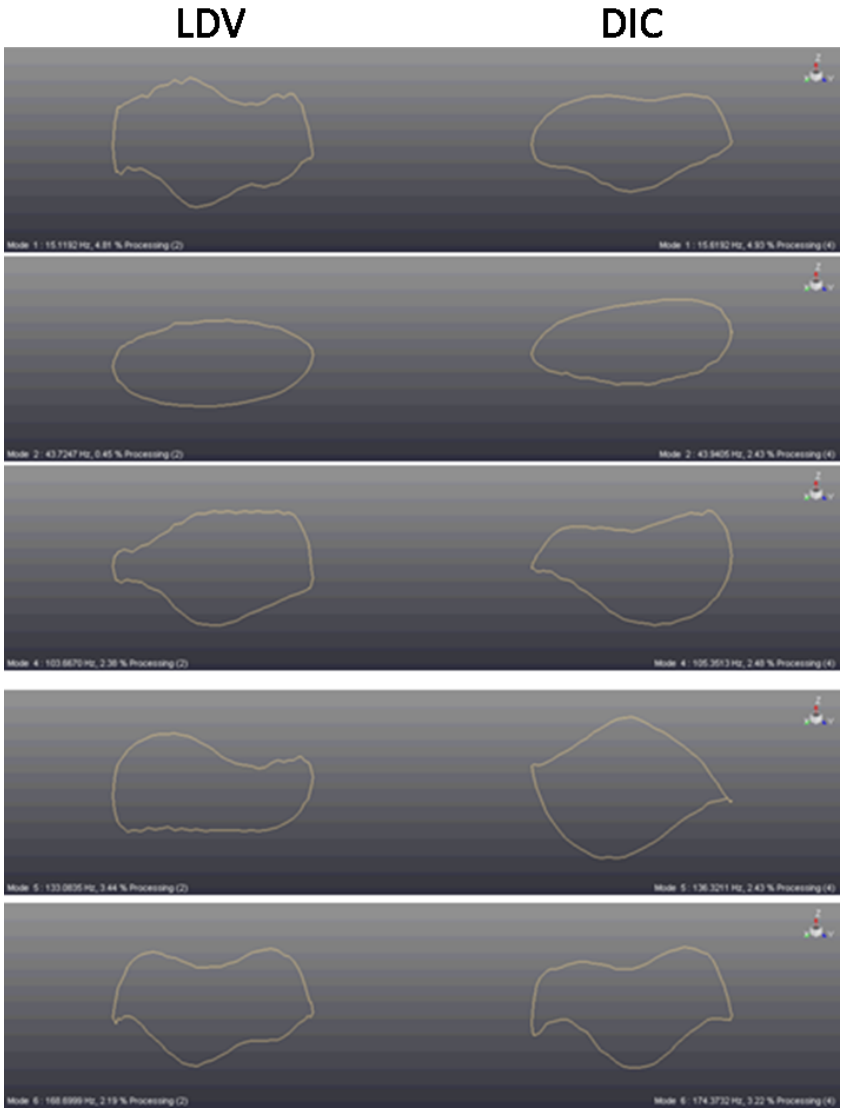

Figure 28 - Mode shapes comparison: LDV on the left side and DIC on the right side

In some points, the LDV mode shapes are noisier than DIC ones because of the sidewall curvature and the embossed lettering on the sidewall causing disturbance to the laser.

3.2. Dynamic measurement

Moving from static to dynamic case, the main differences are the excitation and the frequency range of interest. The correct measurement of the high frequency vibrations requires a dedicated set-up optimization. In the next paragraphs the main differences between static and dynamic excitation and the most important parameters that can influence the measurement are analysed.

3.2.1. Excitation

In static condition the attention is focused on the low frequency carcass modes involving the entire sidewall. They are characterized by high amplitude displacements and all the structure is strongly excited by the energy coming from the impact of the hammer with the tire. In these conditions, the global tire framing, i.e. a configuration where the entire sidewall is measured, is suitable to perform a correct vibration measurement, as demonstrated in the previous paragraph, since the sensitivity and the spatial resolution are high enough to detect the levels of the analysed displacements. When the tire is rolling, the energy coming from the road generates the high frequency vibrations responsible of the so-called "pattern noise" in addition to the low frequency carcass vibrations. The high frequency vibrations are characterized by very small displacements localized in the area closer to the contact patch. The next figure shows the different excitation and the difference in the excitation localization passing from the static condition (left side of the figure) to the dynamic one (right side).

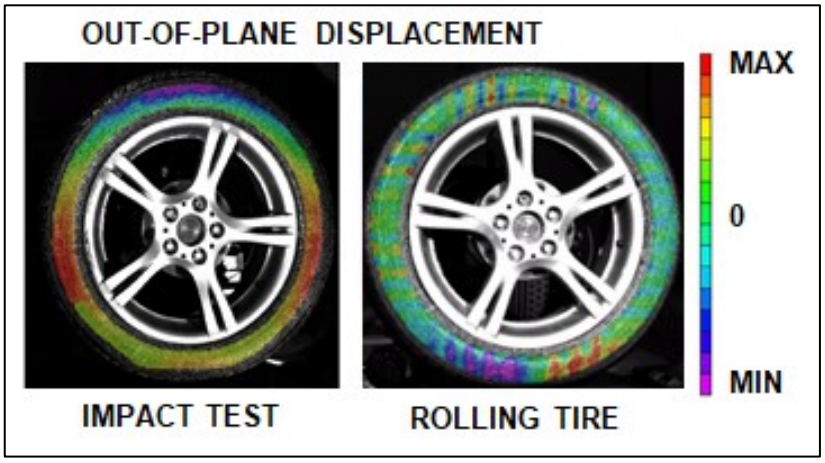

Figure 29 – Static VS Rolling excitation

In the case of the rolling tire the high frequency vibrations coming from the road are localized in the area around the contact patch, but the resolution of the measurement system with full-tire frame can only measure the low frequency vibrations because the sensitivity of the system is not high enough to detect the very small displacements generated by tread blocks impacts. This is related both to the pixel number of the sensor and to the size of the rolling object. When the frame is focused on the entire tire, the pixels are distributed over a large surface, so the spatial resolution is low and a lot of pixels are "unused" since they are focused out of the tire surface. Cameras with a much higher resolution could measure the high frequency vibrations with a full-tire frame. However, high frequency vibrations require a high frame rate: currently there is a technological limitation that does not allow to have sensors with a higher resolution and a high frame rate. The high frequency measurement requires a different framing.

3.2.2. Optimal framing

In this section, the effect of different framings is analysed according to the distance between the object and the cameras. It is needed to demonstrate how the sensitivity of DIC set-up can be increased reducing the distance from the target. To demonstrate this dependency, the same tire rolling at the same speed was tested in the different set-up configurations reported in Figure 30. The analysis is based on three steps: starting from a framing on the entire sidewall, the cameras are progressively moved closer to the tire and focus is moved on the contact patch area.

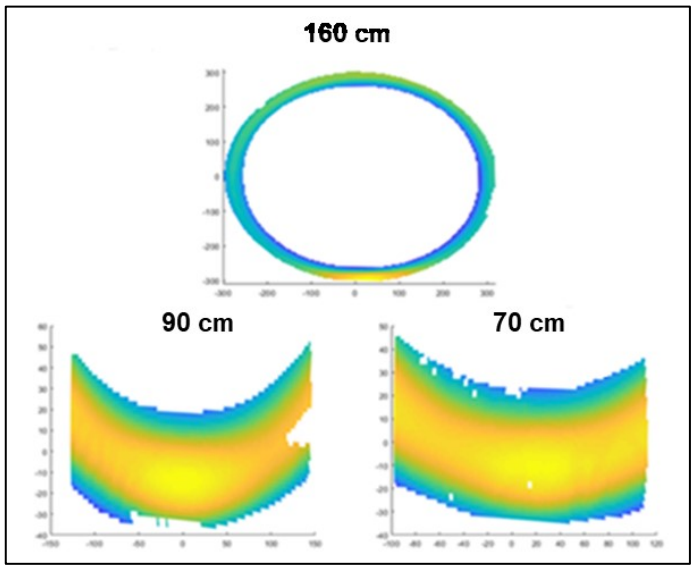

Figure 30 – Comparison of measurement areas for three different distances between cameras and tire sidewall

Three different distances between the cameras and the sidewall have been considered: in the case of a full-field view the tire-cameras distance is 160 cm, with a distance of 90 cm the cameras are focused on the contact patch and if the distance is reduced up to 70 cm the framed region is further reduced keeping the focus on the contact patch area.

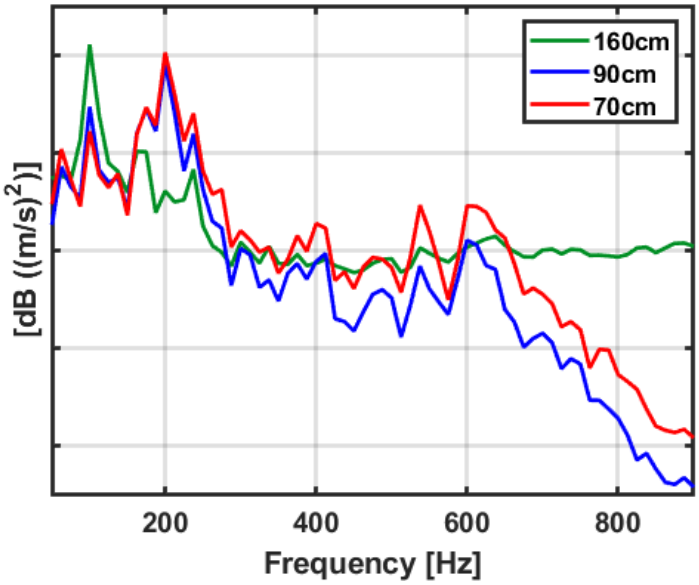

Figure 31 – Comparison of the average out-of-plane velocity Autopowers: effect of the measurement distance

A Matlab reconstruction of the different measurement areas can be seen in Figure 30, while the Figure 31 shows how the system resolution is progressively increased moving the cameras towards the tire: the closer the cameras are to the object, the smaller is the distance between two consecutive points because the pixels of the sensors are focused on a smaller area, so the spatial resolution is increased and the measurement system is able to detect smaller displacement. The disadvantage is the progressive reduction of the measurement area, so it is necessary to define the minimum distance beyond which the system resolution is no longer increased. This distance can be defined performing several measurements identifying the distance beyond which there is no significant change of the spectra or comparing the results with an LDV measurement. This second strategy has been adopted: during the validation process the distance has been identified, so all the following measurements have been performed using this distance.
The spectra analysis highlights how:

- the global frame (green line) cannot be used to measure the high frequency vibrations since the spectrum is flat above about 250 Hz and the vibrations level is comparable with the noise one; moreover, the accuracy in the cavity noise area (around 200Hz) is low if compared with the other measurements, because the system sensitivity it is not high enough to measure a phenomena which have the main component in the vertical direction;

- the closer views are suitable for the high frequency vibration measurement and the lower the distance from the object, the higher the accuracy and the resolution. In this configuration, also the cavity resonance is detected, but the low frequency vibration is underestimated due to a saturation of the measurement system. It can be stated that this set-up is suitable to measure the too wide displacement range of a rolling tire, but with the appropriate set-up variations according to the frequency range of interest.

To measure the high frequency vibration, in fact, a closer view is needed: if a full-field sidewall measurement is performed and only the points localized in the contact patch area are considered during post-processing, it is not possible to extract correct high frequency results. Figure 33 presents the average spectra referring to the different framings or different processing areas described by Figure 32.

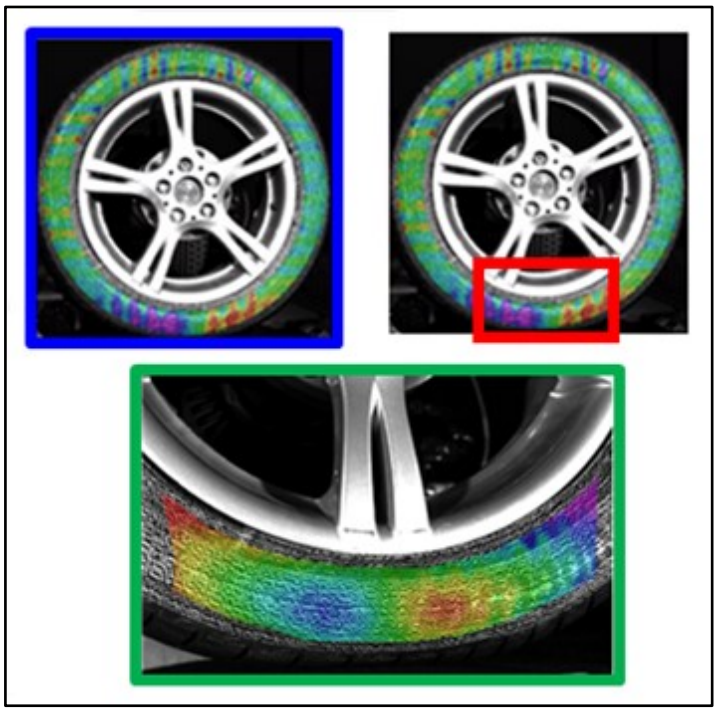

Figure 32 – Regions of interest comparison

The colour of each spectrum is related to the colour of the contour lines used to specify the areas in Figure 32: the blue is used for the average velocity Autopowers obtained with full-view frame, the red for the average velocity Autopowers obtained processing only the points localized in the contact patch (CP) area of the full-view measurement and the average velocity Autopowers of a closer view measurement is the green one. The comparison between blue and red line confirms the previous statement, i.e. the need to focus the cameras on the contact patch because, if the points localized in the contact patch are extracted from a full-tire frame acquisition, the measurement has no high frequency contents because the

resolution of DIC set-up in this configuration is not high enough to measure the smaller displacements. The high frequency vibrations can be measured only with the closer view (green line) even if the low frequency cannot be correctly measured because the peaks are well detected in terms of frequency, but the amplitude is underestimated with respect to the full-view frame.

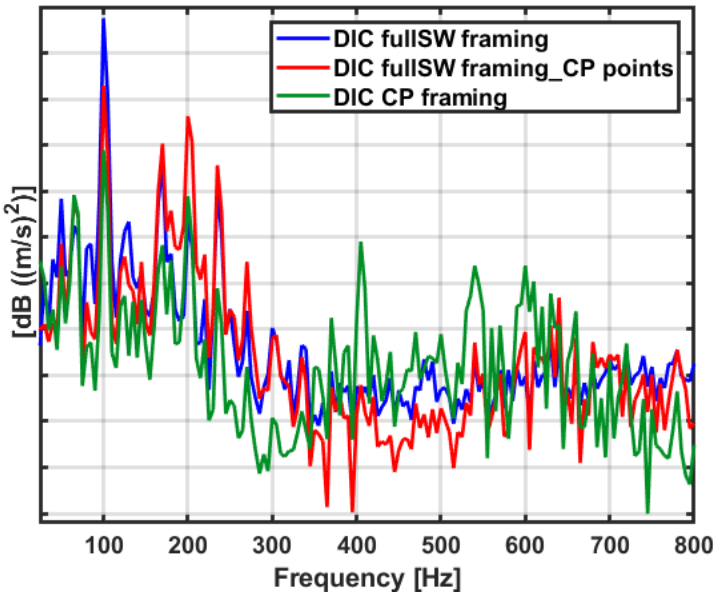

Figure 33 – Comparisons of the average out-of-plane velocity Autopowers obtained processing different areas or with different framings

In conclusion it can be stated that the DIC technique can be used to measure the whole frequency range of interest, but the frame size must be chosen according to the frequency range of interest: the closer view is suitable for the measurement in the high frequency range responsible for the Airborne noise, while the full-view is suitable for a Structureborne noise study. In this way each of these configurations has a good correlation with the LDV as will be demonstrated in the last paragraph of this section. However, although the closer view is suitable to measure about a quarter of the sidewall surface, this is not a limitation because the measurement is performed on the most representative area, indeed tire vibration response is concentrated around a third of the tire closer to the excitation location [69]. It will be demonstrated in the next paragraph.

3.2.3. Sidewall components

In this section the different contributions coming from different sidewall areas are analysed to define if the measurement on the contact patch area can be considered

representative of tire vibrational behaviour. The same reference tire has been tested four times at the same rolling speed and, keeping the same distance from the tire, the set-up has been moved several times in order to measure:

- the contact patch area (CP);
- the portion of sidewall closer to the trailing edge (T.E.);
- the top of the sidewall (TOP);
- the portion of sidewall closer to the leading edge (L.E.).

The same parameters have been used in the acquisitions and during data processing. An accelerometer fixed on the tire-stand has been used as phase reference sensor for the realignment of the DIC signals of the measurements: under the hypothesis of stationarity phenomenon (reasonable considering the very short acquisition time), this allows us to align in time all the measured signals and avoid errors due to time delays related to not simultaneous acquisitions [70]. The measurement areas are those plotted in the next figure with different colours. Moreover, the room temperature, the inflation pressure and the tire temperature have been controlled before starting each test to guarantee the same boundary conditions for all the measurements.

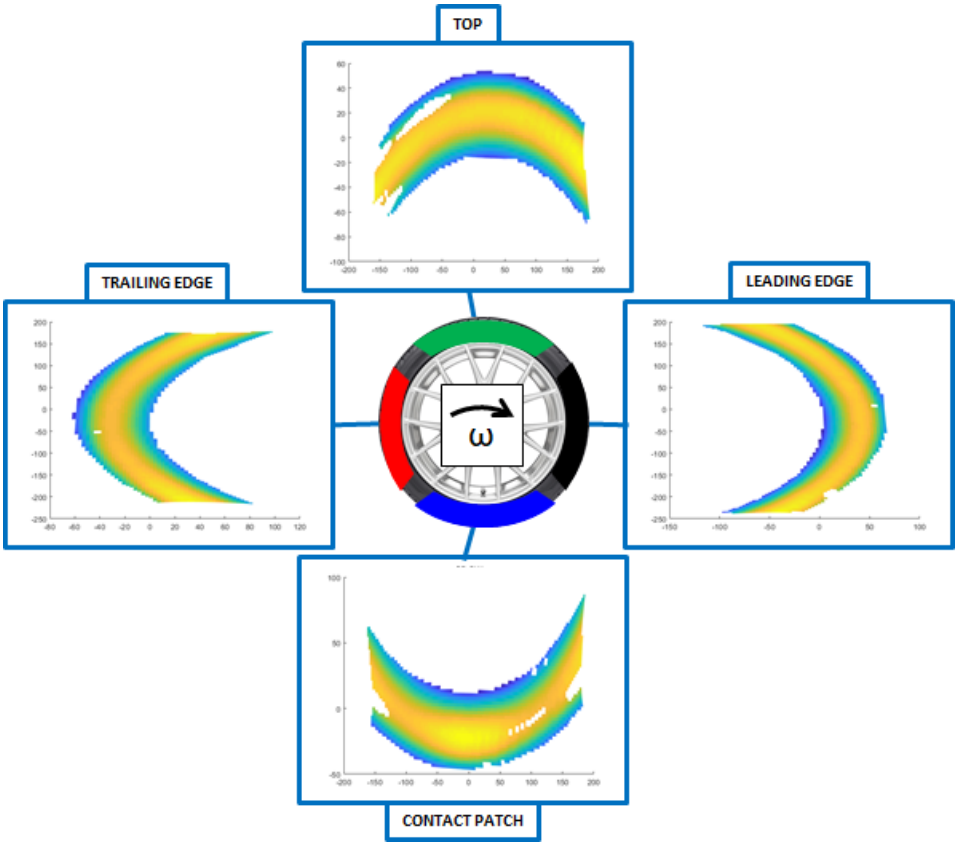

Figure 34 – Visualization of the measurement regions defined on tire sidewall

The main contribution to sidewall vibration in the high frequency range comes from the contact patch, then there are the portions of sidewall placed at the trailing and leading edge while the top region has a very low contribution. It must be specified there is not a general rule regarding the ranking of sidewall's lateral regions (T.E. and L.E.), sometimes the vibration levels are comparable, sometimes one level is too much higher than the other one, it depends on the tire construction. At leading edge, the vibrations are generated from the impact with the road, while at the trailing edge the excitation is given by the so-called stick-slip and stick-snap effects causing a sudden contact release: the rubber in contact with the road is strongly deformed due to adhesion forces that guarantee the traction of the tire and, when the tread blocks are leaving the contact patch, they continue to deform themselves because they try to keep the contact with the road, until the adhesion is abruptly lost and the blocks start to vibrate. This is one of the reasons why this effect is strictly localized in the contact patch area: the effect of tread blocks vibration tends to decay rapidly. All these effects are strictly related to tire structure and compound, so for this reason a general rule cannot be defined in terms of vibration ranking. The results strongly depend on the tread compound because the excitation coming to the sidewall is filtered by the crown itself, so if a high damped tread construction is used, a big part of the excitation is dissipated in the contact area and the trailing edge of the sidewall is not strongly excited.

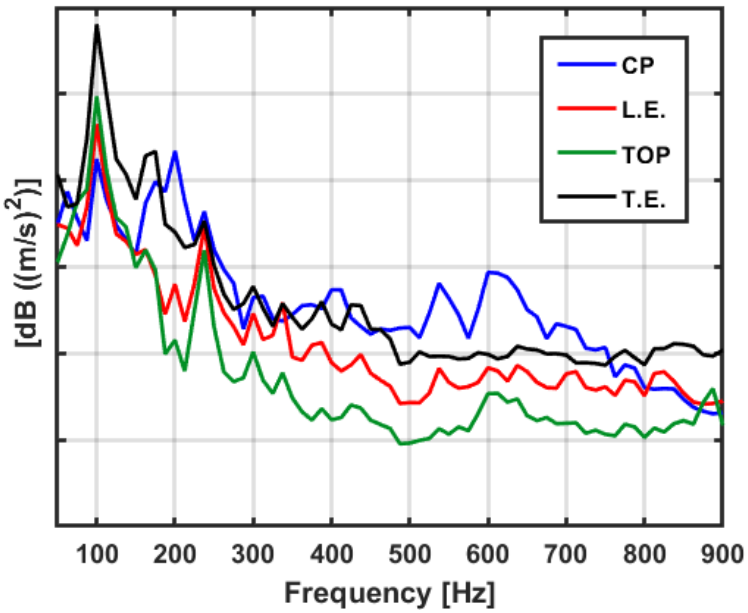

Figure 35 – Comparison of the average out-of-plane velocity Autopowers: contributions of different sidewall regions (DIC case)

Beyond this, the aim of this measurement was to demonstrate that the reduction of the measurement area and the decision of focusing the camera on the contact patch is correct since the main contribution comes from that sidewall's region. To confirm this statement, the same processing was performed using the data of an LDV measurement.

More details about the LDV set-up will be provided in the paragraph dedicated to the validation of the DIC set-up. Briefly, it can be said that the main difference between DIC and LDV are the measurement grid and the acquisition time: DIC measurement is an instantaneous acquisition of thousands of points overall the framed surface, while the scanning LDV acquire along a user-defined grid (in this case a circular grid of 80 points is used) and the acquisition is much longer. In order to extract the contribution of each region, during data processing, the points are divided into 4 groups of 20 points each so four areas are defined as well as the DIC case. The colours used are the same of the previous case, as shown in Figure 36. In this figure, the scanning grid is superimposed on the tire image and the sidewall appears white because it is painted with a high reflecting paint to increase the level of LDV signal.

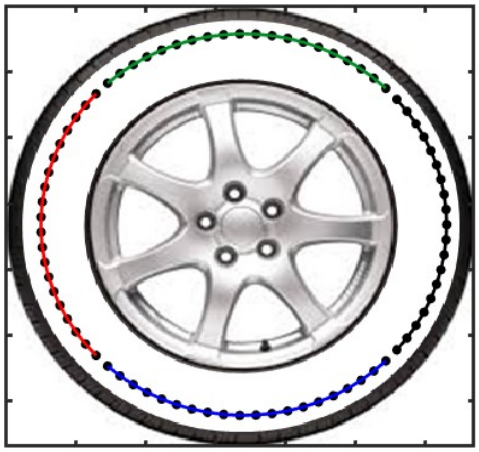

Figure 36 – Division of the LDV measurement grid in sectors to compare the DIC measurement on different sidewall's regions

The LDV measurement confirms how the contribution of contact patch is higher than other areas and that the top region has a very low contribution as expected. The ranking between trailing and leading area is confirmed even if their vibration levels are different from the DIC measurement and the difference between the two areas is amplified with respect to DIC results. The LDV results can be considered more accurate than the DIC's ones: the excitation in these regions is lower than that of the contact patch and the higher sensitivity of the LDV is suitable to correctly measure the smaller displacements of trailing and leading edge with respect to the DIC technique. The DIC accuracy in these regions could be increased reducing the measurement distance, but it is not the scope of this investigation. The aim of this measurement was just to demonstrate that the contact patch is the most representative region of the global tire behaviour. For this reason, the distance used for the acquisitions is not the one needed to obtain the same vibration level of the LDV, but it has been defined ideally dividing the tire surface in four equal areas. The optimal distance, that is the one providing the same vibration level measured by the LDV, as previously stated, will be defined in the paragraph dedicated to the validation of the DIC system in rolling condition.

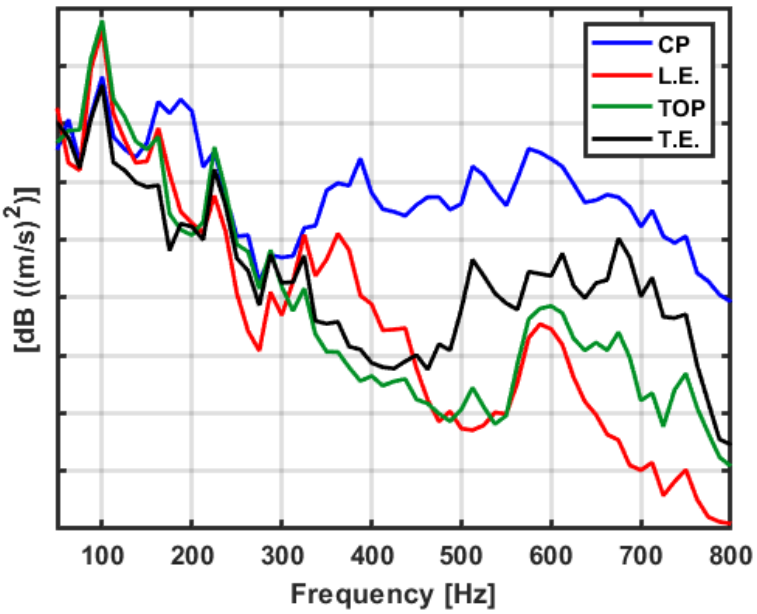

Figure 37 – Comparison of the average out-of-plane velocity Autopowers: contributions of different sidewall regions (LDV case)

Moreover, it must be specified that a direct comparison between DIC and LDV measurements cannot be performed since the LDV data are obtained averaging 20 points for each sector, while the DIC spectra are the average of thousands of points for each region. To perform a direct comparison a group of 20 points should be extracted from each DIC region, but this was not the topic of this test. The comparison considering the same number of measurement points will be done in the paragraph dedicated to the validation of the DIC set-up.
This test has been performed also for the development of a measurement procedure that can be used to validate the FEM models simulating the vibrations of a complete sidewall of a rolling tire: the measurement of several areas and their combination provides a set of accurate data with an high spatial resolution providing the displacement time histories of a number of points comparable to the number of nodes of a detailed FEM model. Of course, this procedure is needed if the high frequency vibrations must be validated; if the focus is the validation of the model in the low frequency range, for example in the case of a tire passing over a cleat, a measurement on the entire sidewall of the rolling tire is enough since the carcass modes up to 200 Hz are correctly measured and the number of points is high enough.

3.2.4. Effect of subset size

To perform the image correlation, it is necessary to define the size of the subset or kernel, i.e. the size of the interrogation areas in which the images are divided to evaluate the displacement of measurement points as described in paragraph 2.5.2. The subset size defines

the length of the side of the squared interrogation area expressed in pixels and it defines the number of measurement points because the smaller the subset, the higher the number of points. However, small subsets significantly increase the noise level of the measurement. This effect has been observed processing the same acquisition with different subset. The first case refers to a measurement on tire rolling at 80kph and the image correlation has been performed with four different subset sizes. The results are plotted in the next figure and the subset sizes are indicated in the legend.

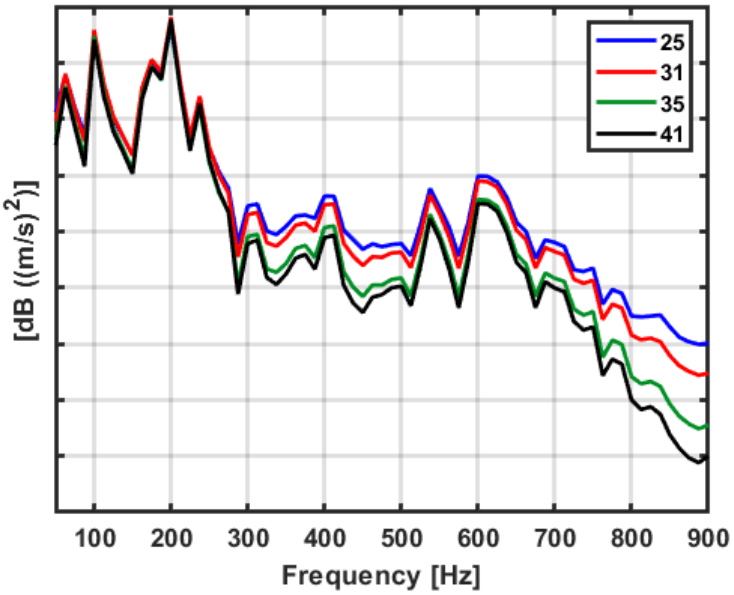

Figure 38 – Comparison of the average out-of-plane velocity Autopowers: effect of subset size (dynamic case)

The vibrational level is strongly influenced by the subset size. This variation depends on the number of averages: each subset measures the displacement for its central point and the value of the displacement assigned to the point is the average of the displacements of the points contained in that subset, so the bigger the subset, the higher the number of points and consequently the number of averages. With big subsets, the displacement value is more accurate because the main effect of subset size is the variation of the noise level: where the displacements are higher, i.e. at the resonance frequencies, there is no significant variation of the measured displacement (at low frequency where there are the carcass modes below 200 Hz the spectra are the same), but where the excitation is lower, the dependency to the subset is very strong, both for the typical frequencies of the pattern noise modes, where the displacement value is more accurate with big subset, and the area in which there are no information, because of noise reduction (the curves are shifted downwards). The same effect can be seen also in the static case.

For the static case, the same dependency is observed as regard the noise level, but in correspondence of the peaks there is no effect, because of the strong excitation generating high amplitude displacements.

A bigger subset must be preferred even if the number of measurement points is reduced, because the accuracy of the measured displacement is increased. Due to this strong dependency to the subset size, it is important to process all the data with the same subset if a comparison of several tires must be performed. It exists a lower limit above which there is no significative variation of the spectra as can be seen from the Figure 38; the optimal value of the subset can be defined comparing the DIC measurement with the LDV's one.

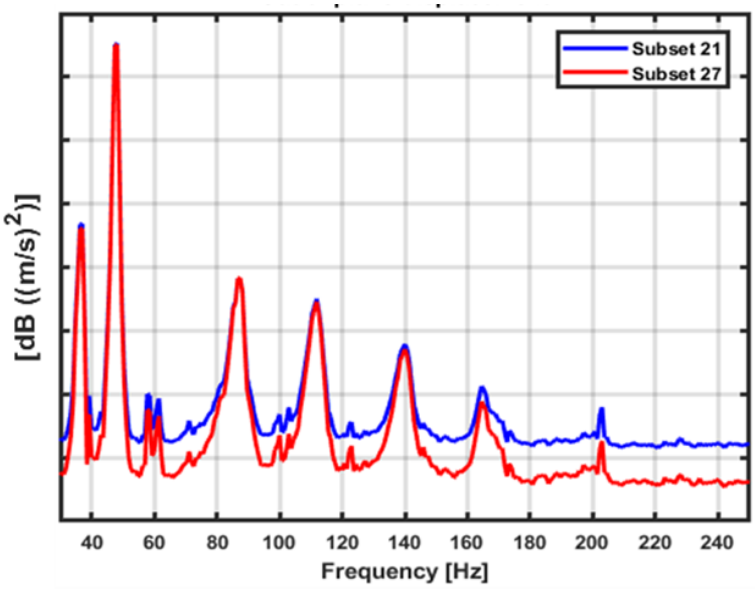

Figure 39 - Comparison of the average out-of-plane velocity Autopowers: effect of subset size (static case)

3.2.5. Effect of frames number

One of the main problems of the DIC technique as vibration measurement tool is the short acquisition time. It depends on the size of the memory of fast cameras that, combined with image size, defines the number of images acquired and consequently the duration of the acquisition. The memory installed onboard the cameras is limited and the image size is quite big: their combination results in very fast acquisitions. The increasing of acquisition length could have positive effects on the results in terms of noise reduction and accuracy increase. The expectation is an effect similar to that of the subset size previously described.

In order to study the effect of the acquisition time, the camera resolution and consequently the image size have been reduced: in this way the dimension of each image file is reduced and, keeping the frame rate constant, it is possible to increase the number of frames acquired

and the acquisition time. For the considered case, working with the maximum cameras resolution, the available system can acquire 5400 frames at the maximum frame rate of 4000 fps, but if the resolution is reduced the number of frames is increased up to 7200, passing from an acquisition time of 1.35 seconds to 1.8 seconds and as expected the effect is a noise reduction (the acquisition time is increased by 30%).

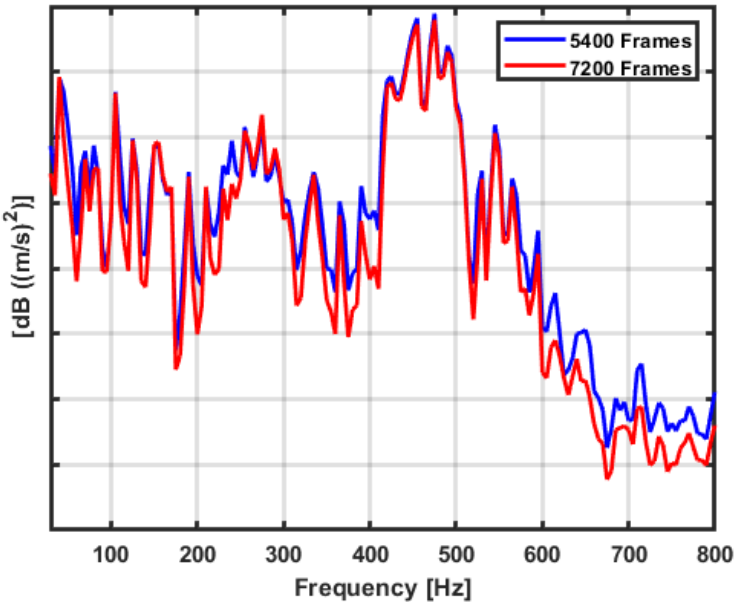

Figure 40 – Comparison of the average out-of-plane velocity Autopowers: effect of time histories length

The spectra reported here refers to two different processing of the same test: in one case the usual time history length is used (the first 5400 frames of the longer acquisition) while in the second case all the frames have been considered (7200 frames). This strategy has been adopted in order to evaluate the effect of a longer acquisition time avoiding the introduction of other factors that could influence the comparison, such as different framing, different boundary conditions, different calibration and son on. In this way the framing is the same as well as the resolution of system, the field of view and the points considered. The blue line is the average spectra obtained working with the truncated time histories while the red one refers to the longer acquisition time. As expected, the effect of a longer acquisition time is similar to that of the subset size: a reduction of the noise level and the values of the resonances are slightly adjusted. The curves, in fact, have the same shape, the peaks are almost unchanged, but the red one is shifted downwards in those areas in which there are no information. This is the consequence of the higher number of averages.
The image size cannot be reduced as your liking, but it must be considered the dimension of the calibration target to be used. It depends on the distance between the cameras and the object. Before performing a measurement, it is necessary to calibrate all the measurement system in order to define all the intrinsic and extrinsic parameters needed to perform a good

measurement and a correct 3D reconstruction. The calibration is done moving a reference target in different positions and acquiring an image for each position. The calibration target is a high reflective white plate with black dots placed in known position and the analysis of the calibration images defines all the calibration parameters comparing the real position of black dots in the acquired images with their ideal positions. Each target, indeed, has three characteristic points used by the software to automatically recognize the target used. In this way, the software knows a priori the positions of all the dots of the target and can compare them with the positions of the dots in the acquired calibration images. The comparison defines the positions of the cameras with respect to the object. The size of the calibration target defines the image size, i.e. the resolution of the cameras: in the cases presented here, the number of frames cannot be higher than 7200 considering the smallest target available. The different configurations are presented in the next figure.

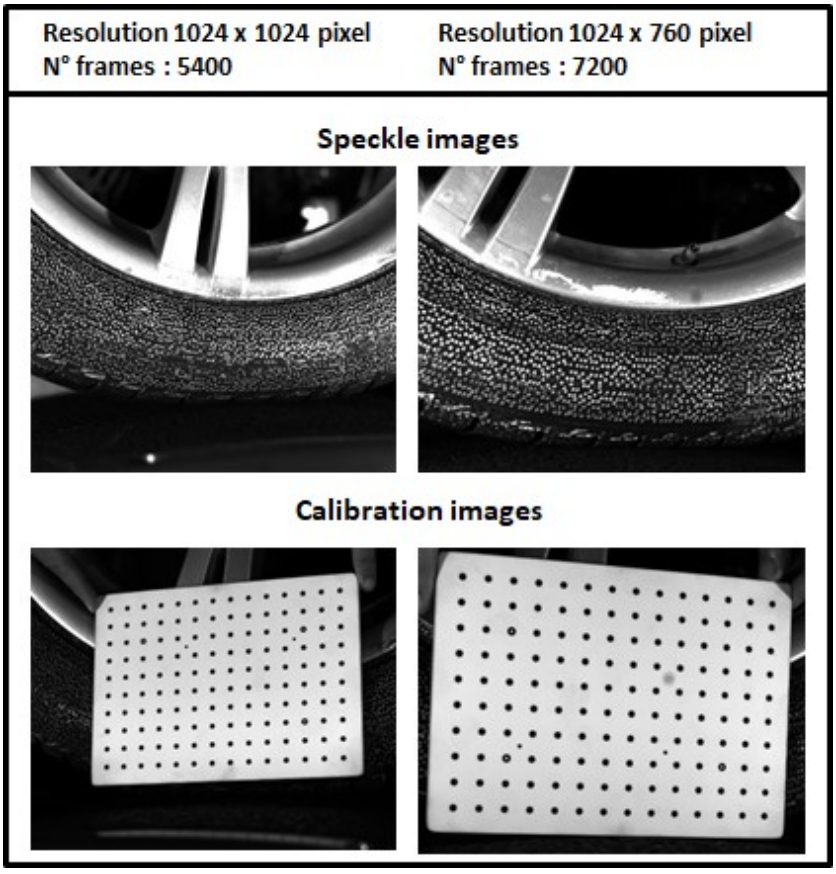

Figure 41 – Framing optimization to increase the number of acquired frames

The upper images show the difference in terms of framed area: it is almost the same since the width of the images is the same, while the height is reduced. Of course, in this way the

cameras can be placed a little bit closer to the tire, so the area is slightly reduced. The lower pictures show how much the resolution can be reduced: as anticipated, the image size must be comparable to that of the calibration target. From this figure it is evident how can be convenient to reduce the image size avoiding the acquisition of no relevant points and increasing the acquisition time.

As well as the subset size, to compare two different tire it is necessary to acquire the same number of frames. In conclusion it can be stated that in order to perform an accurate measurement it is necessary to acquire as many images as possible considering the dimension of the target and processing the data with a big subset size.

3.2.6. Measurement on tread area

The measurement on crown is very complex to perform and a lot of time has been spent to find the optimal set-up configuration. The main problem is represented by the presence of tire lugs and sipes that generate discontinuities on the surface and shadows that made impossible the image correlation since some points are hidden to the cameras and it is not possible to measure the displacements of several points because the correlation algorithm cannot track some subsets. Another problem is represented by the excitation: the sidewall is stiffer than the tread made of a highly damped compound, so the excitation coming from the road has the possibility to propagate on this surface and a wide region is strongly excited as demonstrated in paragraph 3.1.2.3. On the crown the situation is completely different since tread compound is softer than sidewall's one because the tire must be deformable to have the biggest contact patch possible and to absorb the road irregularities. For these reasons tread compound has a high damping causing the dissipation of the energy coming from the road, so only the region closer to the contact patch, both for the leading and the trailing edge, are characterized by high amplitude vibrations. It must be considered when choosing the area to be measured. As well as for the sidewall, a measurement on the entire leading or trailing edge crown area cannot be performed: the distance of the cameras from the object would be too high and the sensitivity of DIC set-up would be very low. It is the same problem described when speaking about the measurement on the sidewall. The only way to measure the crown vibration is working with a closer view and focusing the cameras on the area closer to the contact patch. When the closer view is used, the size of the sipes and most of all the lugs is increased and they generate shadows that hide some points of the speckle pattern causing the tracking failure. In order to define the displacement of a measurement point, the DIC algorithm needs to track the subsets between two consecutive frames: the deformation of the surface is evaluated and then the displacements of the measurement points. It can be done only if the algorithm can recognize the subset by its fingerprint that is represented by the unique set of dots of the speckle pattern characterizing each subset. If some of these points are not clearly visible in a frame, the tracking fails and the result is a zero in the time history of the points associated with the unmatched subsets. It should be avoided because it can cause significant errors when performing the FFT, even more so considering that it generally happens for several frames and for many points. In this condition the measurement cannot be performed. In Figure 42 there is a simple sketch of what happens on the tread area during

rolling. A small portion of the tread area is zoomed in. The rolling direction is indicated by the ω vector and the grey line represents a slot, i.e. a sipe or a lug, and in green is indicated the considered subset. At the instant of time t, all the characteristic points of the subset are clearly visible, but when the slot enters in the subset area, too many points of the speckle disappear and when the cross-correlation is performed, no matching subset in the reference image is found. The result, as mentioned before, is a zero in the time history. Moreover, if the number of uncorrelated subsets is too high, the effect will be an "empty frame", indeed a zero in the time histories of all the points for the corresponding time instant. However, exploiting the fact of working with the incremental algorithm that constantly update the reference image, it is possible to process the "empty frames" with a self-made manual procedure in which the tracking is done manually for one subset and then the software is able to perform automatically the correlation on the other subsets of the same frame. With this procedure the subset is manually deformed by manually matching only the visible points.

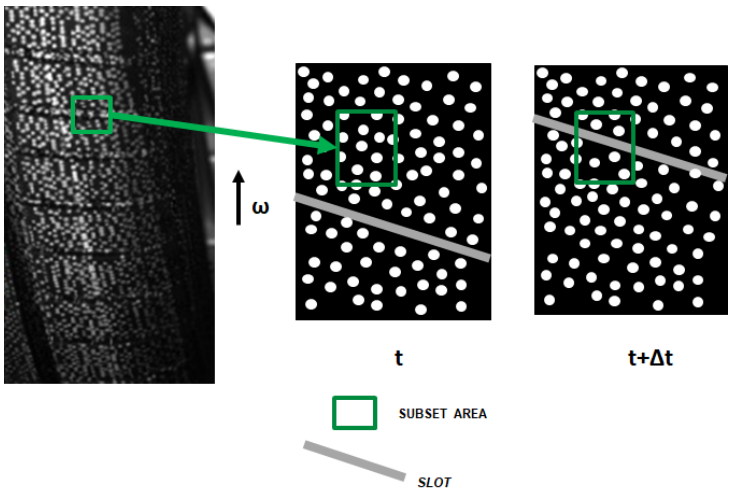

Figure 42 – Sketch of voids effect on tracking in the crown area

This procedure can be very long, but it is necessary to correctly pass from the time to the frequency domain. In fact, the missing frame cannot be removed since the acquisition system works with a constant time step defined by the frame rate of the cameras, so, if a zero value is removed from the time history and it is replaced with the displacement value of the following frame, an error is introduced since a displacement calculated on a double step time is considered as if it was calculated on a single time step. Moreover, the length of time history would be reduced. The importance of recovery the empty frames is described in Figure 43. The blue line is the average velocity Autopower obtained with a measurement with no empty frames, while the red line refers to the same measurement in which 200 random frames are removed simulating a measurement with a realistic number of empty frames. In order to avoid errors due to different lengths of the time histories, only the first 5000 frames are considered for the case with no empty frames. In the second curve, the same number of images are considered, but 200 random frames are eliminated and replaced with the following. It is clear how important is to recover the empty frames since the error introduced is not negligible both

in terms of curve shape and frequency peaks. The number of empty frames is strictly related to the rolling speed (when the tire rolls slowly the subset tracking is easier and the number of empty frames is generally very low, just a couple of frames) but most of all it depends on the quality of the speckle and the position of the LED lamps: the illumination must be homogenous as much as possible and the reflections should be avoided, but sometimes it is not possible and it can generate errors during the image correlation. The optimization of these two parameters can drastically reduce the number of frames to be calculated with the manual procedure. However, if the number of frames to be recalculated is very low it is possible to interpolate the zeros in the time histories introducing a negligible error.

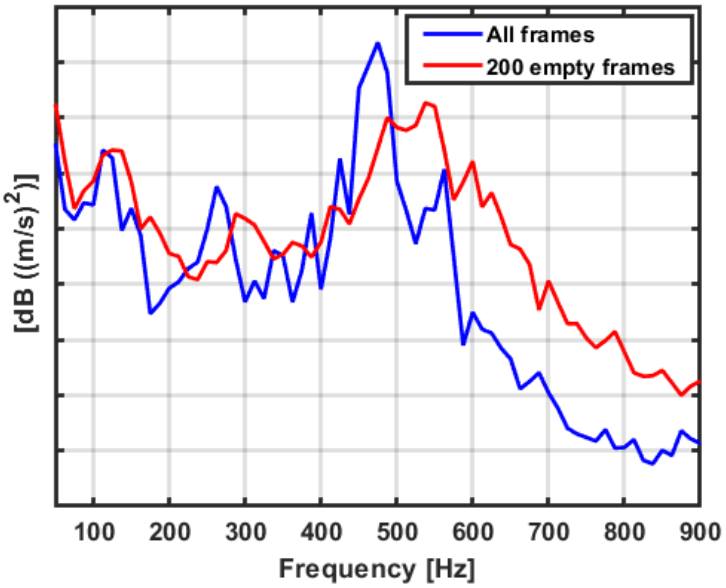

Figure 43 – Comparison of the average out-of-plane velocity Autopowers: effect of uncorrelated frames

Nevertheless, if the measurement on the central ribs is always possible, the measurement on the external ribs is strictly related to tire size: with small tires it is almost impossible because the size of the lugs generates too big voids compared to the shoulder rib's width and the number of missing frames is very high. The only way to process these data would be to use the manual procedure frame by frame, but it is a very long procedure and it does not make sense to perform a measurement in this way. For tire of big size and with a large tread, it is possible to measure also on the lateral ribs, even if the number of uncorrelated frames to be manually recovered is quite high.

After a series of optimization step, the final set-up for the measurement on crown has been found. With the current configuration it is possible to measure the central ribs and the great advantage is the possibility to define a ROI for each rib, so it is possible to know the vibration level of each rib. However, in this work, the attention is focused on the global behaviour of tread compared to the sidewall to evaluate the overall effect of some construction changes, so the ribs are not considered separately.

The height of the measurement area is about 25 cm closer to the contact patch in order to detect the excitation coming from the road that is subjected to rapid decay due to the high damping of tread compound. Moreover, it is almost the same position in which the measurement on the sidewall is performed, so it makes more sense the comparison between sidewall and average crown vibration.
The measurement area is the one described in the next figure.

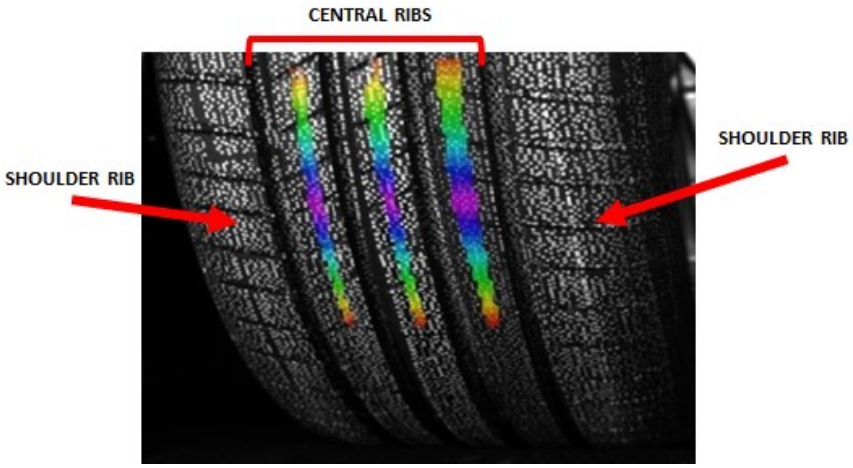

Figure 44 – Measurement area on tire crown

In order to define a standard measurement procedure, it is necessary to decide in which region of tire crown the measurement must be performed, i.e. if it is more representative the trailing or the leading edge, considering that when the tire is rolling the friction between tire and road delete the speckle pattern and after some tire revolutions it is difficult to measure because of the speckle deletion, so usually it is not possible to measure both the sides. For this reason, it is generally very difficult to perform a measurement for both the sides. To identify the most representative region, some tires have been testes both on trailing and leading edge and the typical situation is reported in the next figure. For simplicity of visualization only three tires are considered. Even if they are characterized by different constructions, it is evident how it is more interesting to characterize the crown measuring the trailing rather than the leading edge area because the vibration level is higher (the exact displacement values on the Y axis cannot be reported for confidentiality) and the major contribution in the frequency range of pattern noise is localized in that area. The leading edge velocity Autopowers show a strong decay due to the damping of the tread compound which absorb the impacts with the road avoiding the wave propagation. Moreover, the high frequency vibrations are mainly related to the vibrations of tread blocks that are not related to the impacts only, but also to stick-slip and stick-snap phenomena previously described that are localized at the trailing edge. Maybe, if it was possible to put the cameras closer to the contact patch area on the leading edge side, the high frequency vibrations would be measured, but it is a limit of the current set-up and the configuration of the facility used to performed the measurements. It is very difficult to measure near the contact patch because of the shadows generated by the tire and it is almost impossible to have a good illumination of the scene in the area between the drum and the tire.

This test confirms that the trailing edge is more excited and here there is the major contribution in terms of crown vibration. Moreover, according to what explained in the previous paragraphs, the crown's data are analysed using the same value of subset size.

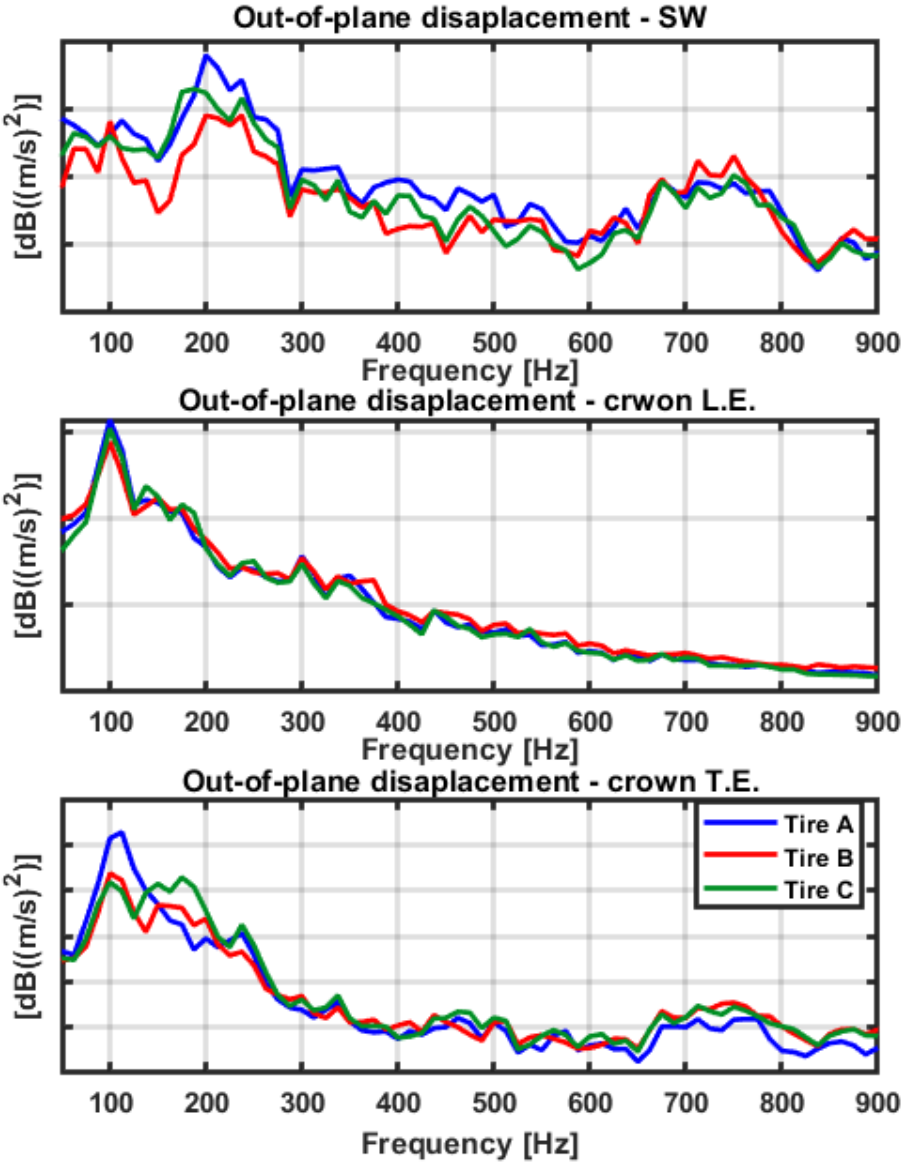

Figure 45 – Comparison of the contributions of tire TE, LE and Sidewall in terms of out-of-plane velocity Autopowers

3.2.7. Background noise

The evaluation of the noise level of DIC set-up has been done performing an acquisition in the final configuration before starting an acquisition. The system has been calibrated and the acquisition has been performed with the still tire.

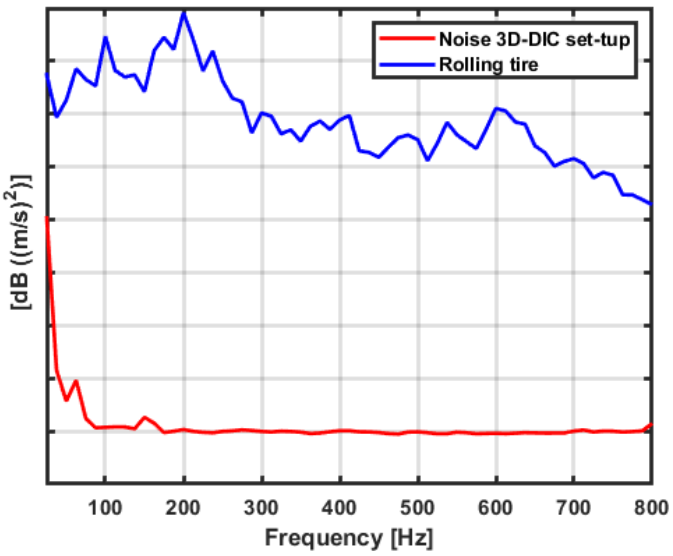

Figure 46 – Average out-of-plane velocity Autopowers of a rolling tire and background noise

As shown in the figure, the background noise level is very low compared with the vibration level, so it does not affect the measurement. There are just a couple of peaks that can influence the measurement, but they are out of the frequency range analysed in rolling conditions. The peaks are localized at 50 and 150 Hz, so it is not something related to set-up itself, but it seems to be an electric disturbance that can be eliminated with a better insulation of the cable and the connectors.

3.3. Dynamic validation

This paragraph presents the comparison of the measurement performed with the two techniques to evaluate the effective capabilities of DIC technique as innovative tool for vibration measurement and to validate the new set-up.
Figure 47 shows the comparison of the Scanning LDV with the DIC measurement performed with a the full-sidewall view. The LDV curve is the average of the out-of-plane velocity Autopowers of 80 points defining the measurement circumference. A circumference of 80

points is extracted from the thousands of measurement points of the DIC acquisition in order to perform the comparison considering the same points. As previously stated, this comparison confirms that the full field view cannot be used to measure in the whole range of interest: the vibrations in the frequency range of pattern noise (500 – 700 Hz in this case for the considered rolling speed) are not correctly evaluated, but the low frequency vibrations are well detected. There is an amplitude shift in the whole measurement range, but this could be related to the number of averages: as repeatedly said, DIC measurement is very fast (1.35 sec) so it is intrinsically affected by a higher noise level with respect to LDV technique (the longer acquisition allows to reduce the measurement noise). In the DIC case the noise could be reduced by performing several measurements and averaging them or using a bigger subset dimension during image processing according to the previous paragraphs.
If the measurements performed on the contact patch are compared, the correlation is good. The comparison is made considering a grid of 40 equally spaced points on the contact patch. The results of this comparison are presented in Figure 48, where the two average spectra are plotted using the original sampling frequency that is slightly different for the two set-ups in order to compare in detail the Autopowers and avoiding the introduction of possible errors due to the resampling processing. In all the previous images, the data have been plotted after a resampling in order to have a lower frequency resolution but clearer data. If the resolution given by the sampling frequency is used, the spectra are very noisy because they contain all the peaks related to the cyclical excitation given by the impact of the tire with road, in fact they are equally spaced with a Δf depending on the rolling speed. The comparison in the final configuration of DIC set-up is reported in Figure 48 and the data are presented using the frequency resolution given by the acquisition parameters of each set-up in order to avoid any mistakes related to data manipulations.

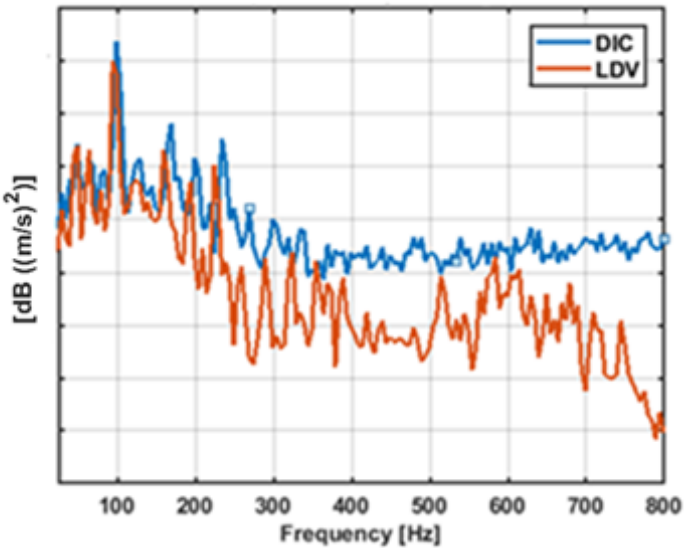

Figure 47 – Comparison of the average out-of-plane velocity Autopowers between DIC and LDV with full-view framing

When the cameras are focused on the contact patch of the tire, there is a good correlation between LDV and the 3D-DIC measurements. The shape of the average velocity Autopowers is almost the same, the amplitude levels are comparable in the high frequency region (above 500 Hz) and the noise level of the DIC signal is significantly reduced with respect to the previous case. The resolution increase of DIC set-up due to closer framing allows to correctly measure the high frequency vibration even if there is a small overestimation of the displacements measured by DIC.

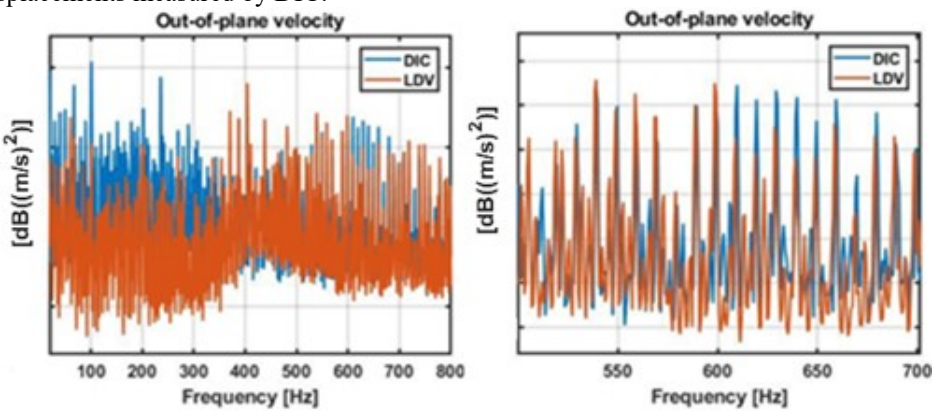

Figure 48 – Comparison between DIC and LDV in terms of average out-of-plane velocity Autopowers after set-up optimization; the right-side figure is a zoom in the frequency range of interest

The main difference is visible in the low frequency range, where the DIC cannot be used with this configuration, as said several times. The right-side of Figure 48 is a zoom in the frequency range of the pattern noise. In this area the good correlation between the two systems can be seen, even if there is a very slight difference in terms of amplitude level. The DIC set-up could be further optimized to reduce the small gap, but for the moment the main topic was the development of a tool for the comparison of different tires in rolling condition giving correct information and this result has been obtained. If a further analysis will be focused on the measurement on the exact values of the displacements it will be necessary to improve this aspect.

3.4. Operational Modal Analysis on rolling tire

The same tire tested in static condition has been tested in rolling condition in order to evaluate the effect of rolling speed on tire carcass modes. The data are compared with those of the static measurement, so the full-tire view is used also for the dynamic measurement and the comparison is limited only to the low frequency range.

In the case of static measurement both the Experimental Modal Analysis (EMA) and the Operational Modal Analysis (OMA) approach can be used: in the first case the FRFs can

be calculated considering the out-of-plane response of tire points and the signal of hammer's load cell; if the OMA is performed one of the measurement points will be considered as phase reference. In dynamic condition there is a unique possibility: the OMA because the input force cannot be calculated and the only way to perform a modal analysis is the OMA. Since the acquisition of all the point is synchronous, one of them can be considered as phase reference sensor or an external sensor can be used, for example an accelerometer fixed on the tire stand. In this work the first approach is used.

In order to compare the two cases, the OMA approach has been used also for the static case. First of all, the two algorithms have been compared in the case of impact test to verify the possibility of using the OMA. The results are summarized in the following table.

	EMA	**OMA**
Mode 1	43.3 Hz	43.3 Hz
Mode 2	81.1 Hz	81.2 Hz
Mode 3	133.1 Hz	133.3 Hz
Mode 4	168.1 Hz	168.2 Hz
1st cavity mode	202.3 Hz	202.3 Hz

Table 2 – EMA VS OMA in the case of impact test

There is a good correspondence between the two methods. So, the comparison of the average velocity Autopower of static and dynamic case can be done and it is reported in Figure 49, while in Figure 50 the mode shapes obtained in the two cases are compared, considering only the first four modes. The cavity mode is omitted because, even if it is detected, in the out-of-plane direction it is buried into the noise since its main contribution is in the vertical in-plane direction.

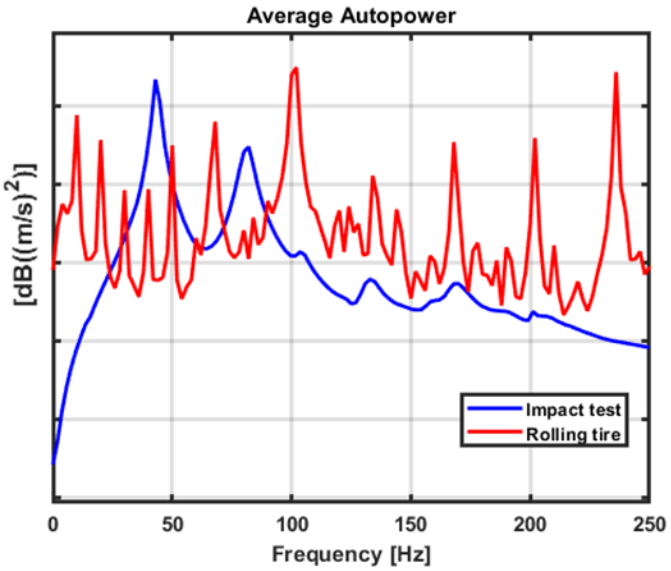

Figure 49 - Average Autopower of the comparison between impact test and rolling tire

The comparison of the average Autopower highlights the effect of rolling speed that is not homogenous in the all frequency range because some peaks are slightly moved backward, as expected, but above 100 Hz the effect seems to disappear. It could be related to a not perfect calculation of the rolling speed during the image processing.

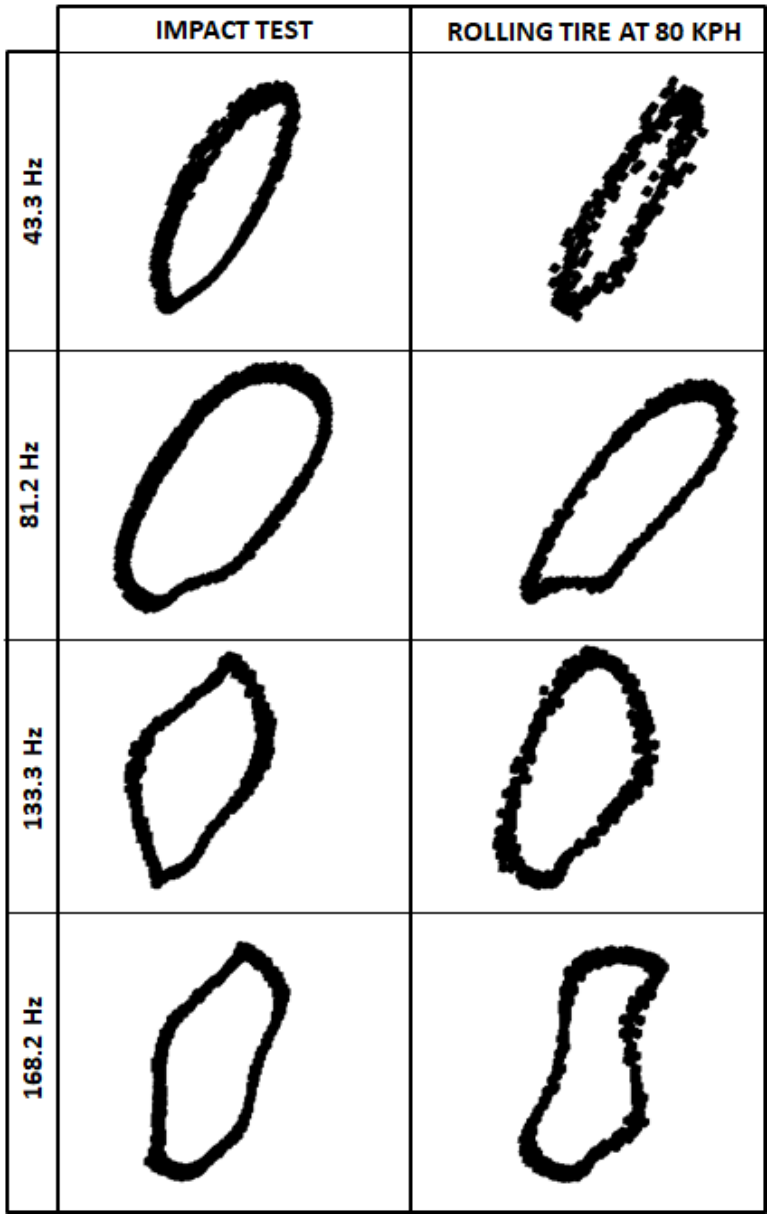

Figure 50 - Comparison of mode shape of the same tire tested in static and rolling condition

This effect can be seen also in the mode shapes: the shapes are perfectly detected, but there is always a portion of the tire with a lobe moved from the expected position. The animation of the mode shapes shows a wave propagation that is not physical but could be related to an error in the correlation algorithm. The mode shapes show a good correlation, except for the first mode that in rolling conditions seems to be noisier.

3.5. Case studies

After the development, the optimization and the validation of measurement set-up, measurement procedure and post-processing algorithms, the 3D-DIC set-up has been used to evaluate its capability to detect differences between tires with different constructions and to analyse how the vibrations of a rolling tire depends on tire constructions. The DIC measurement results have been finally correlated to acoustic measurements to assess the effect of tire vibration on noise emission. The aim of these measurements is to deepen the knowledge as regard the understanding of noise generation mechanism related to tire vibrations and the definition of a trendline which could suggest some guidelines for tire designer and developer, especially exploiting the new info coming from the measurement on crown, not available until today.

Several comparisons have been considered and the analysis of the results suggests that tire noise is strictly related to the vibration level of the sidewall, so the guideline to be followed when designing a silent tire is to limit as much as possible the vibrations of the sidewall. In the case studies presented here, this effect is obtained controlling two different parameters:

- *Sidewall stiffness.* Tire with low noise emission are characterized by low sidewall mobility, so a possible countermeasure for noise reduction is to use a tire with a stiff sidewall even if it can cause a slight increase of crown's mobility. Moreover, the sidewall influences also the shape of tire footprint, i.e. the contact area between tire and road, and the noise emission is strictly related to the footprint.
- *Dissipation of the excitation coming from the road.* A noise-oriented tire structure can be obtained with a high damped crown in order to reduce the energy coming from the road and consequently the excitation transferred to the sidewall.

These are two different strategies useful to reduce noise and they can be obtained in different ways. In the next two paragraphs two examples are described: the paragraph 3.5.1 deals with a change in sidewall construction while paragraph 3.5.2 deals with a change in crown structure. Whatever the technical solution adopted, it is important to reduce the mobility of the sidewall since it acts as a loudspeaker and it is the major noise source. It should be noted the importance of the DIC measurements for the identification of these guidelines, because for the first time it is possible to compare experimental data of sidewall and crown of real patterned tire. In literature can be found so many works in which sidewall and crown vibrations are compared, but in most cases the results refer to simulations or slick tire excited by a cleat that are not realistic because they are completely different from a patterned tire because of the lack of the excitation responsible of the pattern noise.

In the next sections two case studies are presented: in the first case two tires with significant difference in terms of sidewall construction are considered; in the second one the comparison regards two tires with standard and high damped treads.
The results presented do not depend on the tire size. In fact, different sizes have been considered and the main outcomes are not related on the size, at most the size can emphasize or attenuate the effect of the solution considered. For each case study, it will not be provided too many details as regard construction or tire specifications, but the construction will be briefly described providing only the information needed for the explanation of the results. Moreover, for confidentiality reasons, in both the cases the tires are identified as Tire A and Tire B: Tire A is always the reference tire, i.e. a normal production tire or a tire with a "standard" construction, while Tire B is a prototype or a "special" construction tire.

3.5.1. Case study 1: sidewall construction

The first case study deals with the comparison of two passenger tires with different sidewall construction: the main difference between the two tires is the increase of sidewall stiffness of Tire B; there are no changes in terms of tread compound, stiffness or material, so both the tires should receive almost the same excitation when rolling at the same speed since the characteristics of the test surface and the portion of tire that enters in contact with the road are unchanged. Wanting to be strict, the excitation is not exactly the same because every change in crown or sidewall construction influences the shape of tire footprint, i.e. the tire-road interface, and the way in which they interact. The footprint of Tire B is a little bit rounder than the other one with two advantages:

- a rounder footprint is better in terms of noise emission (tire industry know-how);
- the pressure distribution reduces moving toward the shoulders, so the sidewall excitation is reduced.

The increase of sidewall stiffness is obtained by adding a layer of stiff material to the structure of Tire A, but also another rubber layer since all the materials must be coupled with rubber, so beside the stiffness increase there is also a damping increase of sidewall and a mass increase due to the additional rubber. The effect of this solution is described in the next two figures where the average displacements Autopowers for sidewall and crown (trailing edge side) are plotted.
Figure 51 represents the comparison between the two tires considered in terms of sidewall vibrations level. Each curve is the average of the displacement Autopower of all the measurement points. It is evident how Tire B (red line), the one with the stiffer sidewall, has lower vibration level if compared to Tire A almost in the all frequency range of interest, but especially in the pattern noise zone. The tested tires have the same tread pattern design, the same sequence of tread blocks as well as the same size. The combination of these parameters with the rolling speed (80 kph) define the pattern noise zone that is localized in the range 500 – 800 Hz and this is the zone in which there are the biggest differences. The Autopowers have a similar global shape, the same resonance frequencies but the vibration level is significantly reduced by sidewall stiffness, but also by the damping of the additive rubber

layer. It is interesting to see what happens on the crown. The results are presented in Figure 52 in which the average displacement Autopowers of the crowns, measured at the trailing edges of the tires, are plotted.

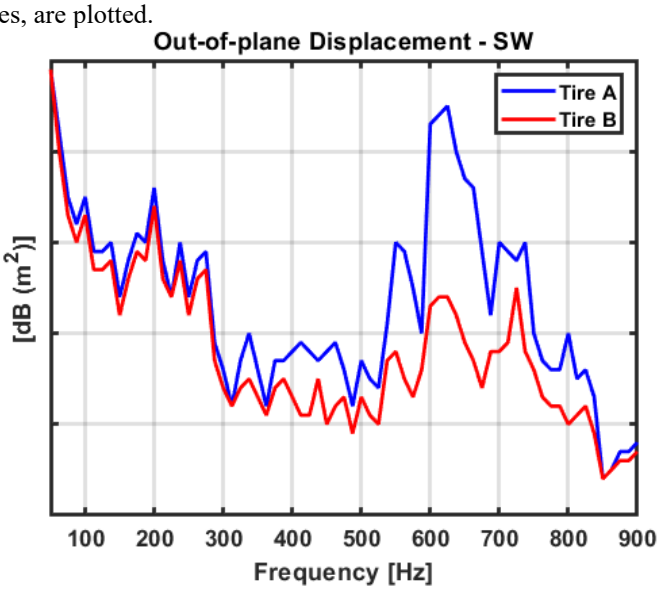

Figure 51 – Effect of stiffer sidewall on the average Autopowers of the out-of-plane displacement of the sidewall

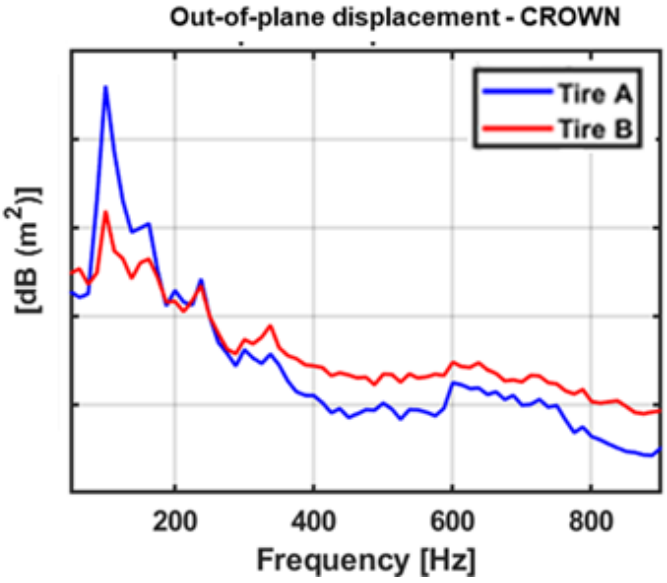

Figure 52 – Effect of stiffer sidewall on the average Autopowers of the out-of-plane displacement of tread area

The figure shows that the change in sidewall construction, has an effect also on the crown since there is a ranking inversion because, in the frequency range of pattern noise, the crown of Tire B has a higher vibration level. This effect is connected to tire construction: if the sidewall stiffness is increased, the energy transferred to the sidewall is reduced at it is driven to the tread area.
From this case study, it is clear that a change in terms of construction has an effect not only in the modified component, but in the whole structure. As a consequence, the tire/road interaction changes and consequently also the excitation of the rolling tire. These results are reasonable because if a structure is made by two connected parts, when one of them is forced to have a lower mobility due to an increase of its stiffness, being the excitation the same, the energy is forced to move towards the less stiff components which increase its mobility. This is what happen with Tire B: the excitation coming from the road is almost the same but, being the sidewall stiffness increased, the energy is partially transferred to the crown and partially dissipated, so the crown vibration level will be increased. Moreover, it must be considered the changes in terms of footprint: Tire B has a footprint a little bit rounder, it means a reduction of the contact zone in shoulders area and therefore of the sidewall. In this way, the excitation is transferred to the high damped component, the tread area, and it is good in terms of overall noise emission. The increase of vibration for tread of Tire B is very low and the gain in terms of sidewall vibration reduction is more important. In the next figure the comparison of mode shapes for the peak at 600 Hz are plotted both for sidewall and crown. They are a frame took from a Matlab animation of the mode shapes. The colours used are in accordance with the colours used for the Autopowers.

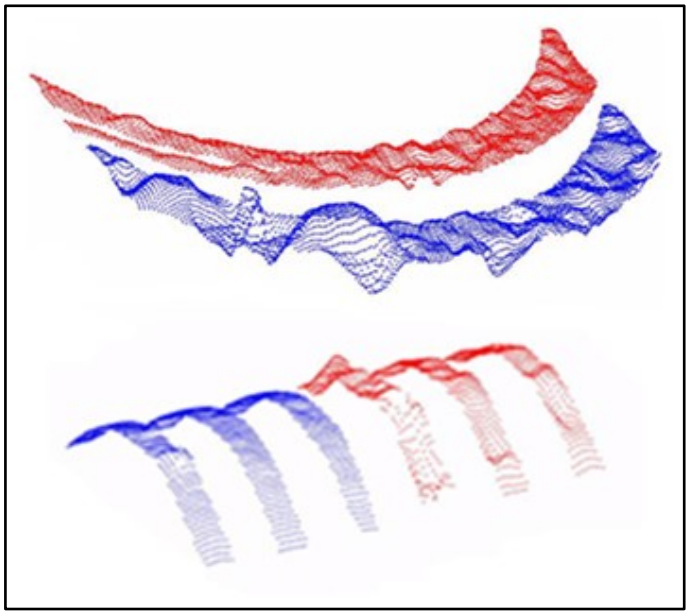

Figure 53 - Comparison of sidewall and crown mode shape at 600 Hz to visualize the difference in terms of displacement amplitude

In the upper part of Figure 53, the difference in terms of vibration amplitude is clearly visible for the sidewall, a little bit less for the crown (lower part of the same figure). It depends on the combination of two factors: the amplitude of crown displacements is lower than the sidewall and, in the mode shape animations, the same amplification factor has been used for both the cases to conserve the ranking. For this reason, the displacements of the crown are not too visible (in the animation it is clearer).

The tires were tested into a semi-anechoic chamber where there is an array of microphones used to simulate the Pass-by-Noise test and it is interesting to highlight two aspects:

- Tire A is noisier than Tire B, in fact a reduction of 0.8 dB for Tire B is measured;
- The analysis of directivity shows that the major differences are localized in the Trailing Edge, despite the only construction change was done on the sidewall and the difference in terms of vibrations is localized in that area.

The next figure represents the overall directivity of tire noise. In this graph, for each position of the microphones, represented by a certain angle, the overall value in dB(A) of the corresponding microphone is reported (each microphone is indicated with a circle in the plot). Three main outcomes come from the graph:

1. There are no significant differences at Leading Edge.
2. There is a ranking inversion between sidewall and Trailing Edge. In the sidewall area, Tire B is a little bit noisier than Tire A, but the reduction of Tire B noise at TE is greater than the increase at the sidewall, so the overall is a reduction of noise emitted by Tire B.
3. The major differences in terms of noise emission are localized in the TE area.

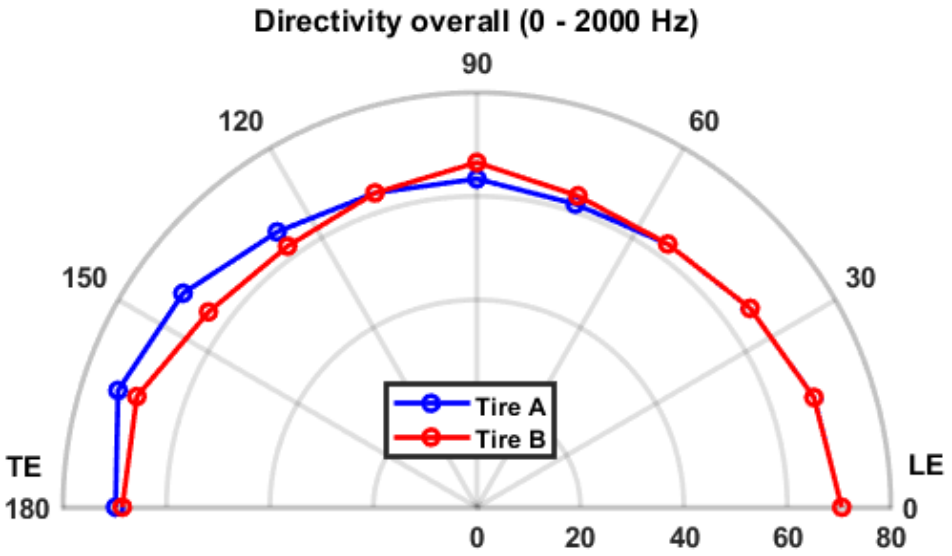

Figure 54 – Directivity of tested tires

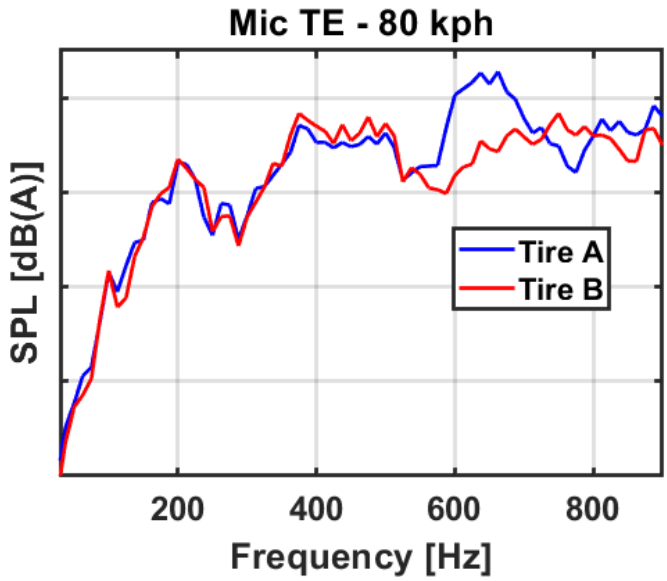

Figure 55 – Effect of stiffer sidewall on noise emission for the microphone in which there is the main difference

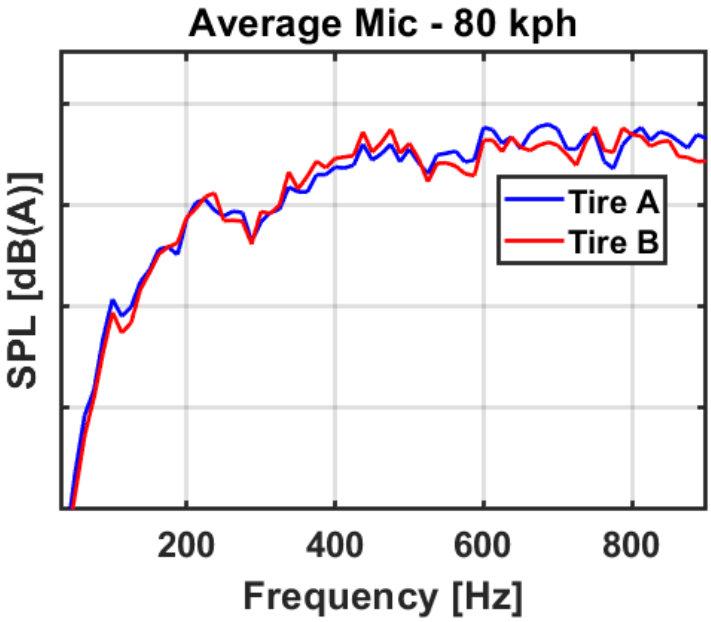

Figure 56 – Effect of stiffer sidewall on the average of all the microphones of the array

It can be interesting to analyse what happen in the TE zone. They are plotted in Figure 55. Up to about 350 Hz they are identical, there is a small range in which Tire B is a little bit

noisier than Tire A, but, in the frequency range of pattern noise, Tire B reduces significantly the noise emission. It is not easy to find a direct correspondence between vibrational and acoustic peaks, but it can be stated that there is a good correspondence in terms of ranking and spectra shapes: effectively where the vibration level of sidewall is higher, the noise levels are higher. Since both the tires show a directivity having the maximum noise emission in the TE, in this area the microphone signals have the biggest difference and a big difference in terms of noise is expected. However, it must be considered also what happens in the other directions. In fact, if the average of all the microphones that make up the array are considered, the spectra change and the differences between the tires are less pronounced: they justify the reduction of 0.8 dB(A) measured with the standard test used to evaluate the noise emission of a rolling tire.

From this test case, it is evident that the high frequency vibrations are very important in terms of noise emission, instead of several works in which it is stated that the aero-acoustic effects are predominant. In this case, the tires have the same size, the same pattern, same grooves dimension and so on, so the contribution of the aero-acoustic effects, like pipe, horn effect, air pumping is the same for both tires because they mainly depends on geometry parameters (for example pipe noise depends on the length and the cross section of the tube created by the grooves with the road, the horn effect depends mainly on the diameter of the tire). What changes is the way in which the structure receives the excitation coming from the impact of tread blocks with the road and how tire vibrates.

Combining noise data with the vibrational ones, it can be said that the main effect of a stiffer sidewall is the increase of crown vibration amplitude in the TE area with a noise reduction. Being the crown structure the same for both the tires, it is reasonable to hypothesize that they receive almost the same excitation, but the stiffer sidewall has mode shapes characterized by lower amplitude and a different phase distribution that results in a more silent tire.

3.5.2. Case study 2: crown construction

In this paragraph, the effect of a change in crown construction is analysed. Two tires are compared: Tire A is the reference and Tire B has a highly damped tread. The idea is to leave the crown free to vibrate and dissipate the excitation coming from the road and evaluate the effect of this kind of tread on noise emission. In particular, it must be evaluated if a more damped tread can reduce the energy transferred to the sidewall as well as the previous case, but with a different solution. The average displacement Autopowers of sidewall and crown are plotted in Figure 57 and Figure 58. As expected, the damping increase in crown has a positive effect on sidewall vibration level that is lower for Tire B, but also the crown vibration is reduced due to the increased damping. In this case the measurements were performed at 50 kph, to evaluate also the effect of this solution with different rolling speeds, so the pattern noise is shifted in the frequency range 400 – 550 Hz. It can be seen that the higher damping has a strong positive effect above 150 Hz on the sidewall, while the vibration level of the crown is reduced in the frequency range of the pattern noise only. The effect on the crown can be justified by changing the way the tire interacts with the road: the contact is softer and smoother than the standard tire, in fact the average Autopower of Tire B is flatter in the

pattern noise. A strong positive effect is registered also in terms of sidewall vibration level: there is a reduction in terms of amplitude, but there is also a change in the shape of the Autopower because the double peak between 400 and 500 Hz became a single peak at about 450 Hz.

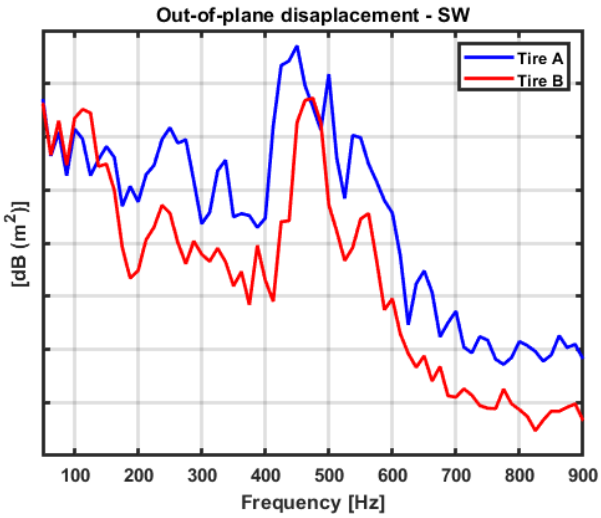

Figure 57 – Effect of tread change in terms of sidewall vibrations: comparison of the average displacement Autopowers

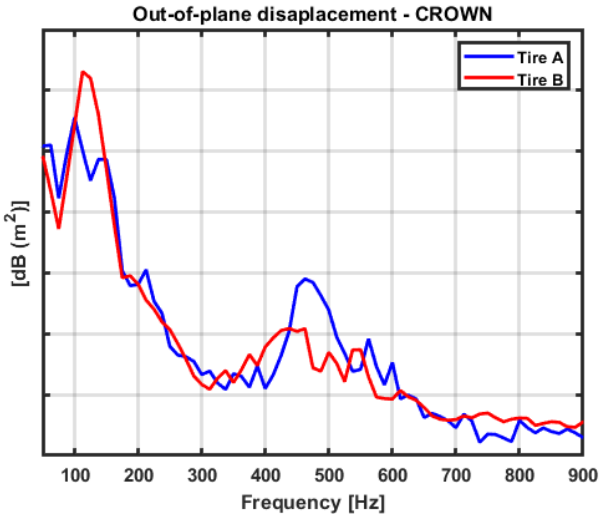

Figure 58 – Effect of tread change in terms of crown vibrations: comparison of the average displacement Autopowers

Moreover, the effect of damped tread is not localized only in this frequency range, but there is a global reduction of the vibrational level. In terms of noise emission, there is a reduction

of about 1 dB(A) passing from Tire A to Tire B estimated according to the standard Pass-by-Noise test. In Figure 59 the average of the microphones is plotted.

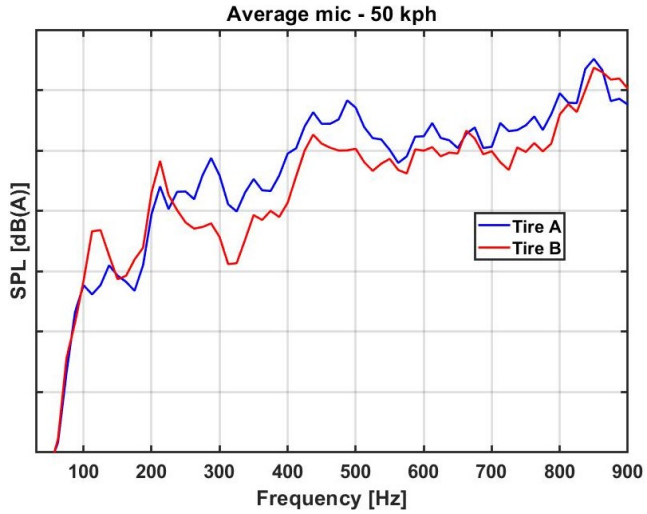

Figure 59 – Effect of tread change in terms of noise emission: average of all the microphones of the array

The analysis of the average microphone spectrum highlights that Tire A is noisier than Tire B almost in the whole frequency range, except for the region below 200 Hz. It is interesting to notice how there is a good correlation between sidewall vibrational spectra and acoustic spectra: Tire A has two main peaks between 400 and 500 Hz as well as the microphone, while Tire B has a single vibrational peak and the acoustic spectra is quite flat in that region.

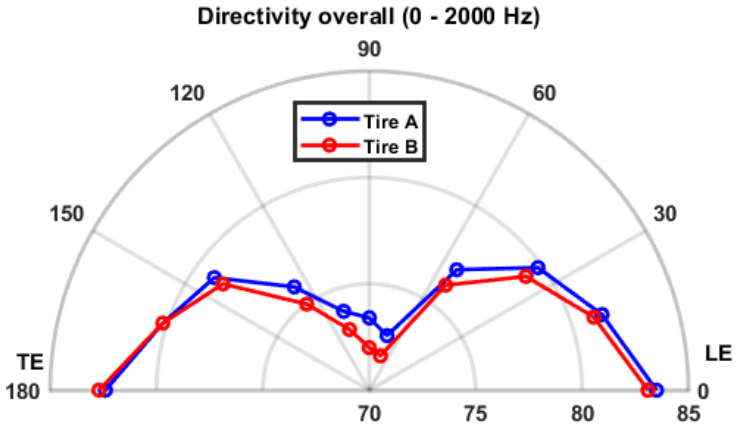

Figure 60 – Directivity comparison for the tested tires in the frequency range 0 - 2000 Hz

In this second case study, the directivity of the noise emission is completely shifted towards the L.E., but some differences can be seen also on the sidewall. This difference with respect

to the previous case is related to the different crown construction that results in a change of the way in which tire and road interact. The high damping of Tire B reduces the mobility of the crown because of a more rapid decay of the excitation that influences mainly the leading edge, but also the energy transferred to the sidewall is reduced because of the smoother impact of tread blocks with the road and its absorption by the leading edge. In this way, the characteristics of the excitation reaching the sidewall change and the result is a difference also in terms of resonances that was not registered in the previous case. It can be also related to a different sequence of tread block impacts depending on a different deformation of the tire.
The damped crown modifies also the vibrations in the vertical direction, as reported in the next figure where the average vertical displacement Autopowers are compared. The curve shapes are similar to the out-of-plane component, but the levels are different and it is important to analyse how the Autopower of damped crown changes. The average vibration level can be considered the same for both the tires, but in the contact patch area there is a significative change: in Tire A three main peaks can be identified, while on Tire B there is only one big peak. In this frequency range is localized the effect of damping material.

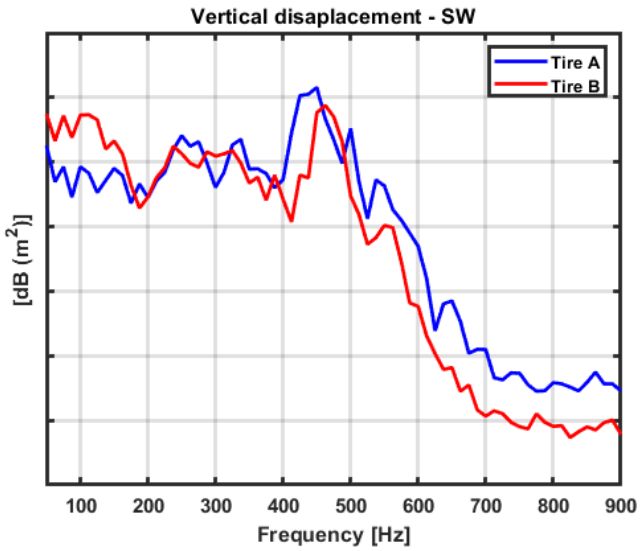

Figure 61 – Average Autopowers of vertical in-plane displacement

3.6. Chapter summary

This is the chapter dedicated to the measurement of rolling tire vibrations. It is divided into two main parts: the first one deals with the optimization of the set-up and its

validation both in static and dynamic condition; the second one contains two case studies in which the technique is used to evaluate two different technical solution giving a noise reduction.

The first part describes what has been done in order to make the DIC set-up suitable to measure tire vibrations in a wide frequency range, both on sidewall and crown: in static condition the characteristic of DIC of being a full-field technique can be exploited to perform the measurement and it is quite easy; in rolling conditions it is necessary to modify the framing according to the frequency range of interest: the full-field view can be used if the low frequency vibrations want to be studied, the closer view on the contact patch must be adopted if the analysis is focused on the high frequency vibrations. It depends on the type of vibrations characterizing the different frequency range and the amplitude of the displacements that changes significantly moving from low frequency carcass modes to high frequency pattern noise. It has been demonstrated that the contact patch is the most representative region for high frequency vibrations and all the parameters influencing the measurement have been analysed. Summarizing, it can be said that in order to perform a good and accurate measurement it is necessary to reduce as much as possible the size of the acquired images to increase the resolution of the system and the acquisition time at the maximum frame rate and a big subset size must be used in order to reduce the measurement noise and increase the measurement accuracy. The background noise level has been evaluated and it is very low. The set-up can be used also to perform measurements on the crown and it represents the main innovation of this work in terms of vibration measurement, even if the current set-up can be used only on the central ribs. The shadows and the irregularities generated by shoulder sipes and lugs made impossible the measurement on the shoulder ribs. The system has been validated both in static and dynamic condition through the comparison with the Scanning LDV showing a good correlation in both the cases.

In the second part, two case studies are presented. The first one deals with a sidewall construction change: a standard tire with one with stiffer sidewall are compared to analyse which are the effects of such solution in terms of sidewall and crown vibration. In this case the noise reduction is related to a reduction of sidewall vibration even if that of crown is slightly increased. In the second case, a higher noise reduction has been obtained using a high damped tread. The noise reduction is higher because has been increased the damping of the area entering in contact with the road, so there is a reduction of vibrations both for sidewall and crown area.

This page intentionally left blank.

Chapter 4.

Tire components characterization

This chapter deals with the description of the innovative tire components dynamic characterization, describing all the optimization process and in the second section a case study is presented to demonstrate how this method works and the main outcomes. As anticipated in the introduction, the idea is to characterize the body ply and the cap ply layers, defining which are the best materials for a noise-oriented tire structure.

4.1. Set-up optimization

The definition of the optimal set-up configuration, the identification of the best measurement conditions as well as the geometry and the construction of the samples required a lot of time and tests. Being a completely new activity, there are no literary references or industrial background suggesting how to realize the samples, so it is important to illustrate all the optimization steps done to find the configuration that best represents what happens on the real tire. The main problems are related to the difficulty to excite the sample at high frequency (above 500 Hz) because of the high damping of the rubber and the clamping of the samples that have a certain curvature due to manufacturing.

4.1.1. Measurement set-up

The measurement set-up is made of:

- 2 fast-cameras with CCD sensors, a frame rate of 4000 fps with the maximum resolution of 1024 x 1024 pixels (the frame rate can be increased reducing the image size and consequently the resolution);
- 2 LED lamps of 175 W each in order to provide a good illumination of the scene avoiding optical interferences;
- a shaker with load cell for the acquisition of the excitation signal;
- the shaker's amplifier connected to LMS TestLab in order to control the excitation signal;
- a DAQ unit connected to the cameras for the synchronization of the load cell with the cameras: it receives the trigger from the master camera and starts the acquisition of the load cell signal;
- the traction machine to apply a vertical load to the sample.

In the next figure there is a sketch of the experimental set-up.

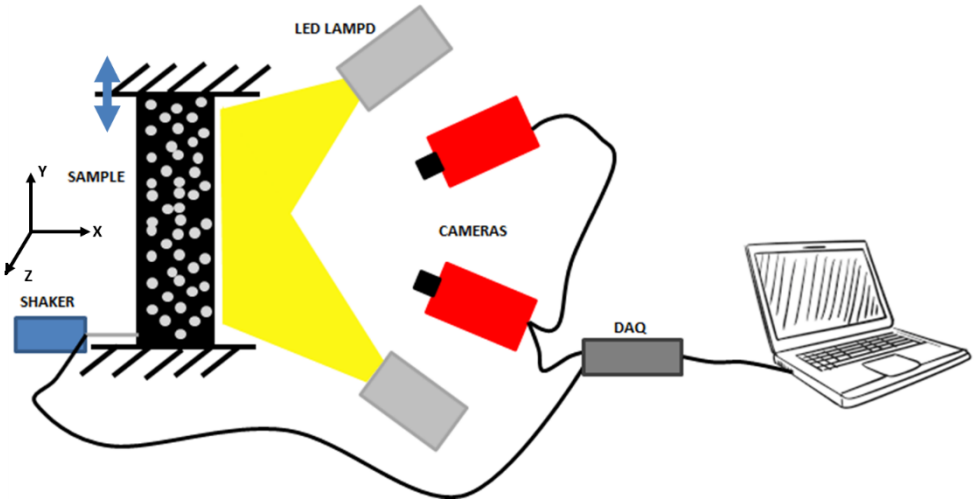

Figure 62 – Sketch of the experimental set-up for the characterization of tire samples

The measurement procedure is made of the following steps:

- The sample is clamped into the traction machine at both the edges. The lower clamp is fixed, while the other one is fixed to a moving crosshead and is free to move up and down to impose the desired axial load to the sample. The imposed load has been appropriately calculated so that it is similar to that the tire component is subjected on a real tire in operating conditions.
- Once the sample is clamped and the load is applied, the shaker can be fixed on it. Since the focus is the measurement of the out-of-plane displacements, to evaluate the out-of-plane mobility of the slabs, the shaker is fixed in order to excite the Z direction according to the reference system reported in Figure 62: the X and Y axis defines the in-plane directions, while the Z axis identifies the out-of-plane direction.
- The acquisition is made by the 3D-DIC system in order to measure the vibrations of the slabs. The resolution is significantly reduced with respect to the measurement on tire to reduce the image size and increase the number acquired images: the length of the time history is increased and the final signal is characterized by a lower noise level, as demonstrated in paragraph 3.1.2.5.
- The images are processed with Correlated Solution VIC3D software to perform the image correlation and a self-made Matlab script is used to extract the time histories of a representative number of points, generating a throughput file compatible with TestLab that is used to calculate the FRFs and perform the modal analysis obtaining the modal parameters and the mode shapes of the tested slabs.

The procedure is summarized in the next scheme.

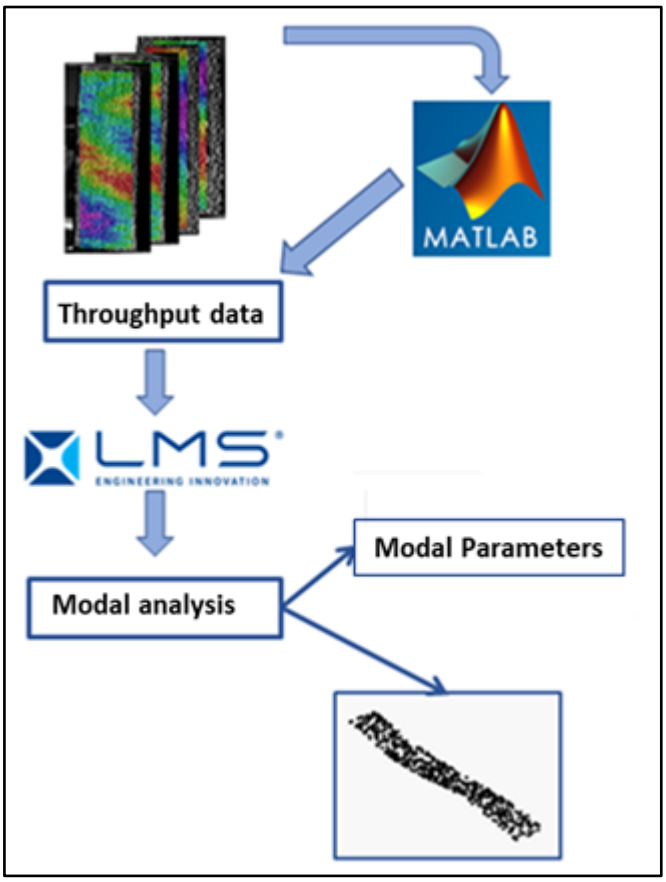

Figure 63 – Post-processing flow

4.1.2. Excitation

Several coupling systems between the stinger and the sample have been analysed and the optimal solution is the direct connection of the edge of the stinger to the sample, making sure that the connection is tight. This is the best practice because the mass of the sample is very low, so every fixing system could represent a significant addiction of a concentrated mass and it acts as an additional constraint to the slab. Even the stinger itself represents an additional constraint as demonstrated by the following figure.

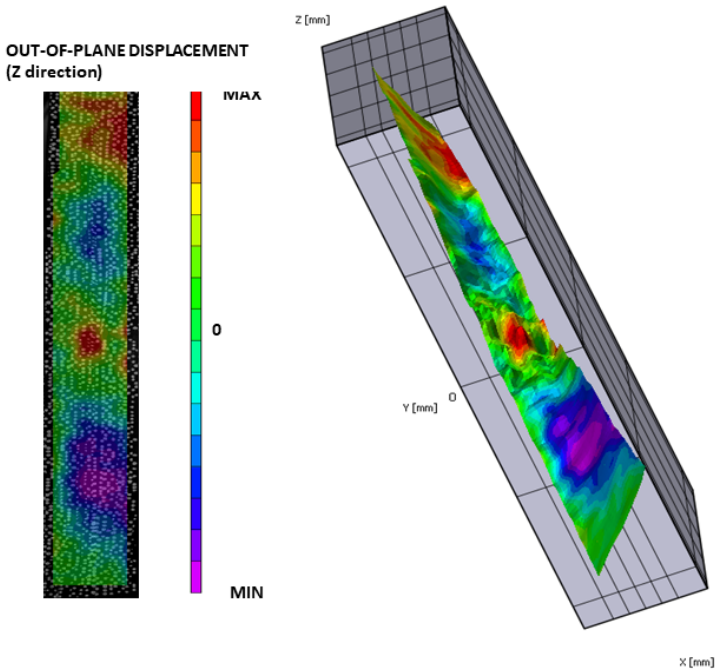

Figure 64 – 2D displacement map of tested samples (left); on the right there is the 3D visualization of the same sample to highlight the not flat shape of the sample and localization of the excitation

On the left side of the figure there is an instantaneous map of the out-of-plane displacements measured by 3D-DIC. It refers to the first tests where the shaker was placed at the centre of the slab. This is not the best configuration because the stinger represents a constraint: the excitation is strictly localized in a central point of the slab that is in phase opposition with the surrounding points so there is no symmetry in the propagation of the waves generated by the shaker and introduces a phase shift not related to the analysed phenomenon. The right side of the figure contains a 3D-picture of the same displacement map and it highlights how the stinger, placed in the middle of the slab, introduces a discontinuity of the slab, like if there was a support beyond the two joints. Effectively, considering the very small mass of the sample, the stinger represents another constraint with 1 degree of freedom (the displacement in the out-of-plane direction): the point integral with the stinger and a small surrounding area move faithfully following the movements of the stinger, generating a zone in which the displacements are not coherent with those of the other points of the slab. The central region, as shown in the right side of Figure 64, is characterized by a drastic displacement variation that is not physical, but it is related to the presence of the stinger. The best practice is fixing the shaker closer to one of the joints to reduce as much as possible the influence of stinger itself because it is placed near a node of the structure that is stiff and where the displacements are almost null, in this way the influence of the stinger is mitigated.

Moreover, the stinger should be placed in a central position to excite the bending modes only. The right side of Figure 64, in fact, allows to introduce another drawback of some tested slabs: in most cases, the samples are not perfectly flat due to residual internal

stresses deriving from the manufacturing process generating a torsional effect that is preserved even after the load application. The result is a twist of the slab visible in Figure 64 in which a displacement map of the out-of-plane displacement is superimposed to the 3D geometry of the sample (right side). The slab is not flat, but it appears torsionally deformed and it creates a torsional effect affecting the bending modes up to completely cover them. Since the bending modes are the most important in terms of noise emission, the excitation point must be chosen in order to reduce as much as possible the excitation of the torsional modes, so the stinger must be placed on the centreline. Moreover, the not flat samples create so many problems during the measurement, mainly in terms of illumination because they generate strong reflections of the LED lights used to illuminate the scene that generate localized saturation areas in the acquired images introducing an error in the measurement.

4.1.3. Samples optimization

The dimensions and how the samples are realized are very important for the correct characterization of the reinforcing layers. The first tests, in fact, were conducted on samples of cap ply (CP) and body ply (BP) only: they are calendered slabs made of vulcanized rubber and some cords of reinforcing materials. The manufacturing process is very complex and difficult and it generates very thin and lightweight samples with the residual stress giving a not perfectly flat shape.

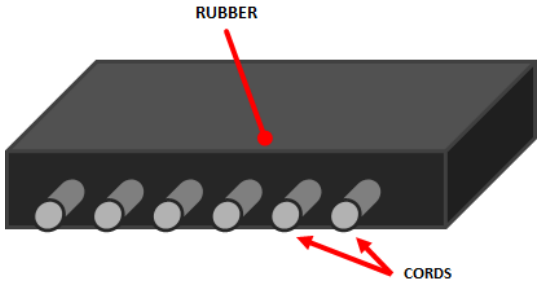

Figure 65 – Sketch of sample structure

Just from the analysis of the first results, it is clear that this kind of sample are not correctly designed because they are strongly influenced by the mass and the thickness of the slabs. In Table 3, it is described an example of one of the test cases analysed. The exact values of the features considered, the reinforcing materials tested as well as the dimensions, the masses of the sample and all the other sensible data are omitted for confidentiality reasons. However, in terms of mechanism understanding, it is not important to know the exact values of the features, but it is more interesting and useful to consider the variation of each parameter with respect to the reference sample.
In the first case study, the effect of the reinforcing material modulus wants to be studied, so four different samples have been realised. They have the same rubber layers, but the cords are made of different reinforcing fabrics. The structure of the sample is quite simple because it is made of a certain number of cords drowned between two layers of rubber as described

in Figure 65. In Table 3, the main features of the samples tested in the first test case are indicated. The sample "A" is assumed to be the reference, so the characteristics of the other samples are expressed as a percentage of increase or reduction compared to it.

	Sample A	Sample B	Sample C	Sample D
Modulus	1	1.14	0.96	5
Mass fabric	1	0.8	0.65	1.2
Rubber mass	1	0.8	0.73	1.19
Total mass	1	0.8	0.59	1.18
Total gauge	1	0.8	0.7	1.3

Table 3 – Features of the samples used in the first case study

The value of each feature is supposed to be 1 for the reference, so a value higher than 1 means an increment, a value lower than 1 means a reduction (for example the mass of Sample B is 0.8, hence the mass is reduced by 20% with respect to the mass of the reference slab). The parameters described in the table are the most important for the explanation of the results. The modulus can be seen as the Young modulus of the cord material, the mass is the total mass of the sample (rubber and cords) and the total gauge is the thickness of the sample, i.e. the sum of cord diameter and the layers of rubber.

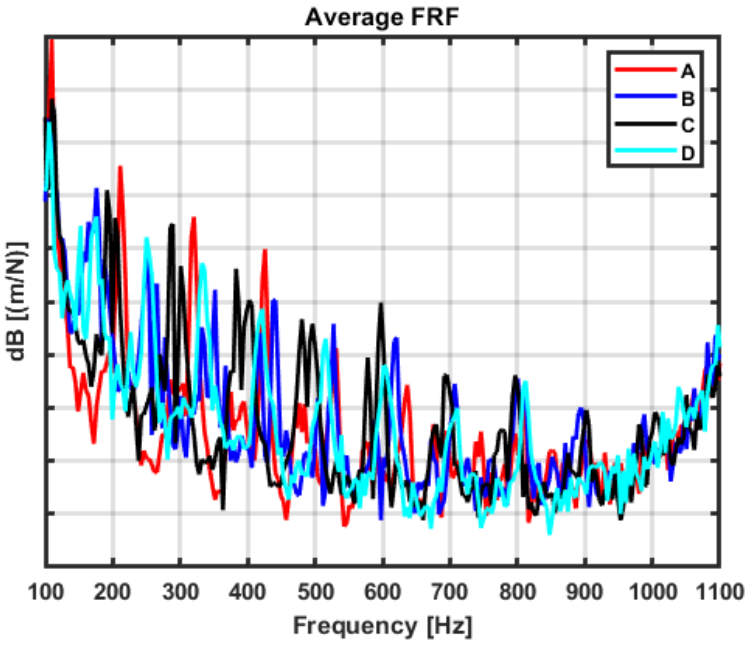

Figure 66 – Average FRFs of the tested samples

The reinforcing materials have been chosen taking into account only the modulus in order to have two materials stiffer and one less stiff than the reference, considering materials

commonly used in real tires. Moreover, the thickness of samples B and C is lower than the reference as well as the mass, while Sample D is heavier and thicker. The mass variations are mainly related to the cord diameter, but also to the mass of the rubber layers since a cord with higher diameter requires a thicker rubber layer. The average FRFs are reported in Figure 66. In the frequency range of interest, all the natural modes of the samples are detected and the material changes produce appreciable variations in terms of both amplitude and frequency. However, even if all the modes and the modal parameters can be extracted using the PolyMax modal parameters estimation method, these FRFs are not clearly readable and easy to analyse. The reason why the FRFs are noisy can be understood looking at Figure 67 in which the second bending mode for one of the samples is presented, but these considerations can be extended to all the modes and all the samples. The dots represent the points in which the sample has been discretized (they are a subset of all the thousands of measurement points) while the external and central lines have been added just to facilitate the visualization of the mode shapes. The lines considered are the centreline and the border lines.

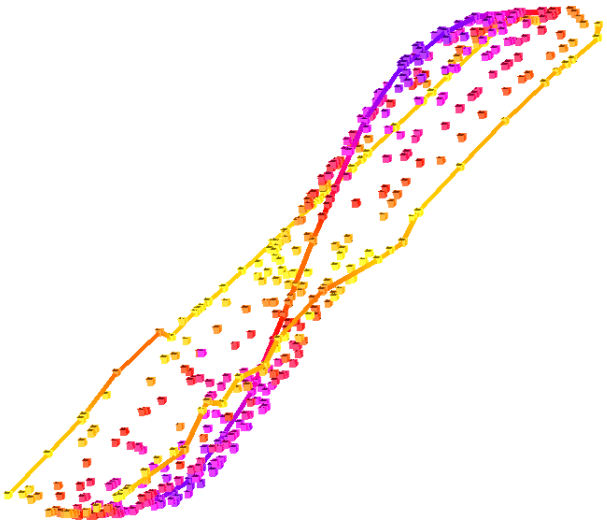

Figure 67 – 2nd bending mode visualization

Even if the shape of the second bending mode is correctly reconstructed by PolyMax algorithm, the points are not excited in the same way, but there is a strong displacement gradient moving from the centreline towards the borders that are completely still or moving in phase opposition with respect to the centreline. The displacement gradient is visualized using a colormap: moving from yellow to purple there is an increase of displacement amplitude (from zero to the maximum displacement whose value depends on the sample considered). Looking at the picture, it can be seen how only the centreline as the typical shape of a second bending mode, because there is a vertical displacement gradient (Y direction), but there is a gradient also in the horizontal direction (X). This effect is due to technological limits in the sample manufacturing. The samples, in fact, are realized in the same way they can be found on the real tire, but on a smaller scale and this process introduces all the

problems discussed in the previous section. Maybe the best solution would be the extraction of a sample from a real tire, but unfortunately it is almost impossible because it would be necessary to separate different rubber layers welded on each other. From the figure, it is partially visible another drawback of the samples. Looking at the upper and the lower edges, the points have not null displacement meaning that the clamping is not perfect, since these points should be motionless. It could be related to the small thickness of the samples related to the available clamping system.
The shape of the bending modes depends on the structure of the samples. As described in Figure 65, they are made of cords covered by two rubber layers, but the external borders are made of rubber because it is required by processing. It generates a different excitation level along the section: the excitation is lower in the areas where there is mainly rubber, due to the high damping, while the central area is stiffer because it contains the cords that allow the propagation of the excitation and the frequency range of the sample response is wiser because of the lower damping. This theory is confirmed by the analysis of the out-of-plane displacement Autopowers of three points of the same slab laying on different positions of the same section: point 1 and 3 are on the border lines, while point 2 is placed in the middle of the section. The results are plotted in Figure 68.

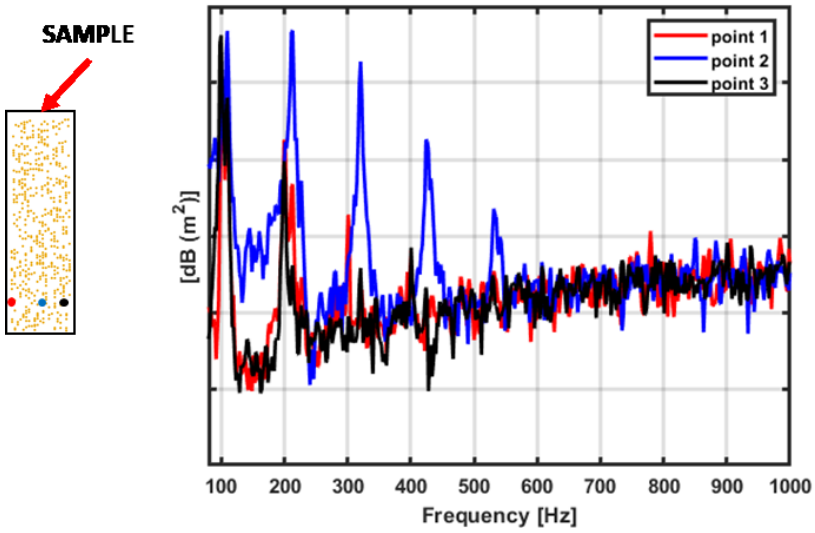

Figure 68 – Out-of-plane displacement Autopowers of three points of the reference sample

On the left side there is a miniature of the sample and the points in which it has been discretized; on the right there are the Autopowers of the three points. The blue line refers to the point on the centreline, while the red and the black lines are the points on the borders. For the central point, the resonance peaks are clearly visible with respect to the other curves that are noisier and highly damped, in fact above about 250 Hz their contribution is negligible. When the FRF sum is considered to perform the modal analysis, the resulting curves will not be smooth and the peaks of the modes are not easy to detect.

Moreover, the blue line does not present the double peaks visible in the FRFs. Once again, the reason must be found in the shape of the sample: the residual stress generates a buckling of the sample magnifying torsional modes and introducing a torsional effect also on the bending modes. So, every bending peaks in the FRFs seems to be split, but they are bending and torsional modes that have similar frequencies, so they appear as if they were coupled modes.
The previous figure suggests considering the Autopowers of the displacements to compare the samples instead of the FRFs. It can be done only if the excitation is the same for the samples and this is the case, because the signals of the load cell for all the slabs of the test case 1 are the same. The excitation used is white signal in the frequency range 100 – 1000 Hz and the excitation point is almost the same for each slab. It is not exactly the same because the stinger is glued manually to the sample, so there is a slight variability on its exact position. Despite all, the excitation is the same for all the measurement as described by Figure 69 representing the Autopowers of each load cell signal. This result was expected since the stinger is placed in the middle of the sample to maximize the excitation of the bending modes. Moreover, this figure suggests that the analysis of Autopowers can be performed to compare the samples.

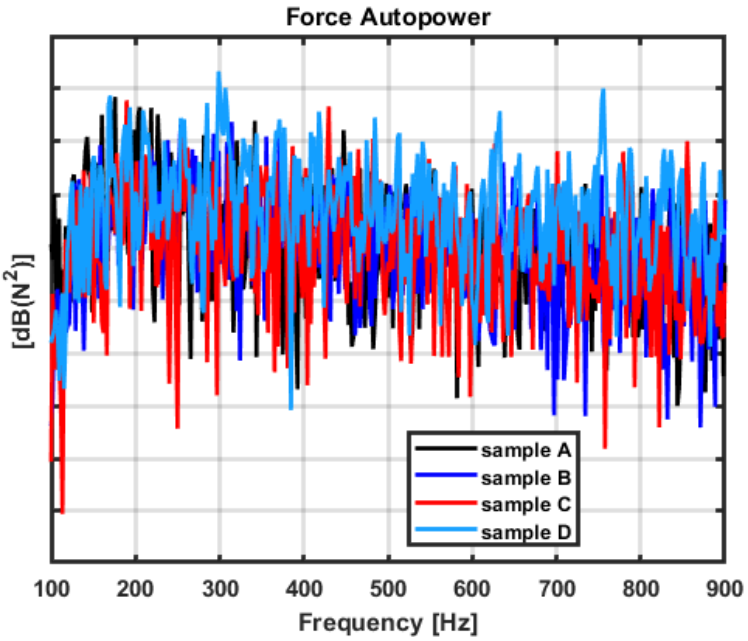

Figure 69 – Comparison of load cell signals

The data presented in Figure 70 are the average out-of-plane displacement Autopowers obtained considering only the points on the centreline of each sample: in this way the displacement gradients are neglected as well as the torsional effects. The results are truncated at 700 Hz because an anti-aliasing filter has been used and 2/3 of the frequency range has been considered. However, the results are not the expected: there is a frequency shift, but it

does not depend on the stiffness of the cords, but it seems to be related to the mass of the samples.

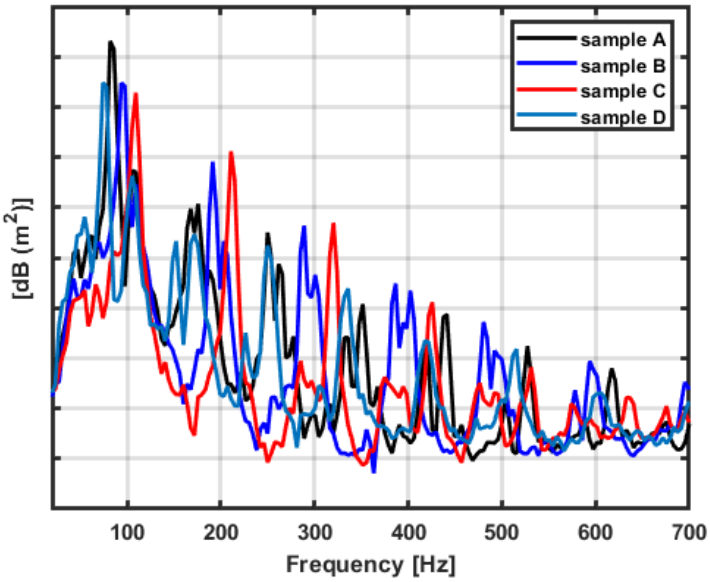

Figure 70 – Comparison of displacement Autopowers obtained considering only the centreline of each slab

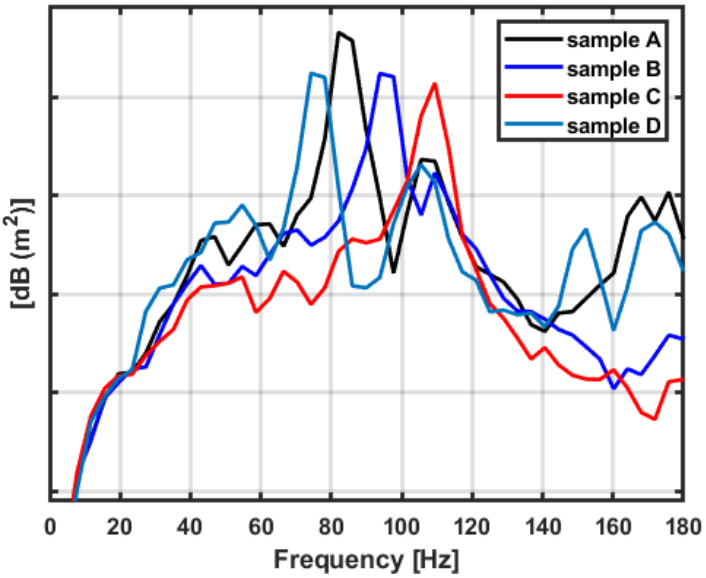

Figure 71 – Focus on the first resonance

A zoom on the first resonance (see Figure 71) can show it better. The samples D and B have a modulus higher than the reference but the peak of the first one is shifted backward, while the second one is shifted forward with respect to the reference sample A; moreover, the frequency of Sample C is shifted ahead of the Sample B even if it has the lowest stiffness. It is clear that there is no relationship with the modulus. Looking at the features of the samples, the experimental evidence is that the frequency variations seems to be related to mass and total gauge variations: the samples B and C have lower mass and lower total gauge than the reference and their frequencies are shifted forward, instead of the Sample D which is heavier and thicker than the reference and it is moved backward. However, these evidences are not supported by the numerical results because the frequencies obtained considering the formulas for a beam fixed at both the edges are in contrast with the experimental observations. It could be related to the samples that are particular sandwiches because they are not made of several layers of different materials, but there are two layers with some embedded cords and in this configuration the mass effect seems to be predominant with respect to the material changes. These results are confirmed by the second test campaign analysed. The samples used are similar to the previous ones, but different rubbers are used for the upper and the lower layer.

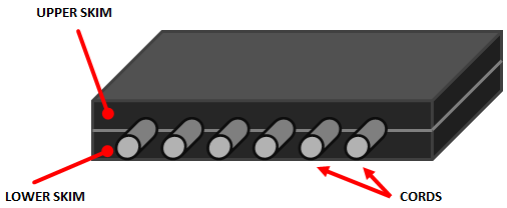

Figure 72 – Sketch of the samples used in the second case study where are indicated the components considered in the table

In this case different types of rubber, reinforcing materials and thicknesses are combined according to the following table:

	SKIM				CORD	TOTAL GAUGE
	LOWER		UPPER			
	Type	Gauge	Type	Gauge	Type	
Sample A	S1	1	S1	1	C1	1
Sample B	S1	1	S2	1	C1	1
Sample C	S2	1	S2	1	C1	1
Sample D	S3	1	S3	1	C2	1.05
Sample E	S3	1.1	S3	1.1	C2	1.2
Sample F	S3	1	S3	1	C3	0.98

Table 4 – Features of samples tested in the 2nd case study

In the table are described the main features of the samples tested during the second test campaign. The samples are realized taking into account the combination of three different parameters: the type and the gauge of the upper skim, the type and the gauge of the lower skim and cord type (that means different material and different diameter). Three different

skim types have been considered and they are indicated as S1, S2 or S3 as well as the three different cord types are indicated as C1, C2 and C3. As regard the gauge value, the real value of the sample A is taken as reference and the other values are defined in relative terms with respect to the reference (a value higher than 1 indicates an increment, a value lower than 1 means a reduction with respect to the reference). In the next figure a sketch of the slab's structure is presented and all the components studied in this case study are indicated.
The sample are excited in the same way of the previous case and, according to what previously explained, the analysis of the results is made considering only the points on the centreline of the samples.

The spectra must be analysed considering three different comparisons, because each of them studies the effect of a specific feature. The first one deals with skims material change; the second studies the effect of skims thickness and the last one compares two samples with same skims and different cords. These tests confirm how the results are not affected by material changes. For every comparison are presented the average Autopower of the out-of-plane displacement and the main features of the samples considered to facilitate the reader. The data must be analysed in this way:

- *Sample A VS Sample B VS Sample C:*

	SKIM				CORD	TOTAL GAUGE
	LOWER		UPPER			
	Type	Gauge	Type	Gauge	Type	
Sample A	S1	1	S1	1	C1	1
Sample B	S1	1	S2	1	C1	1
Sample C	S2	1	S2	1	C1	1

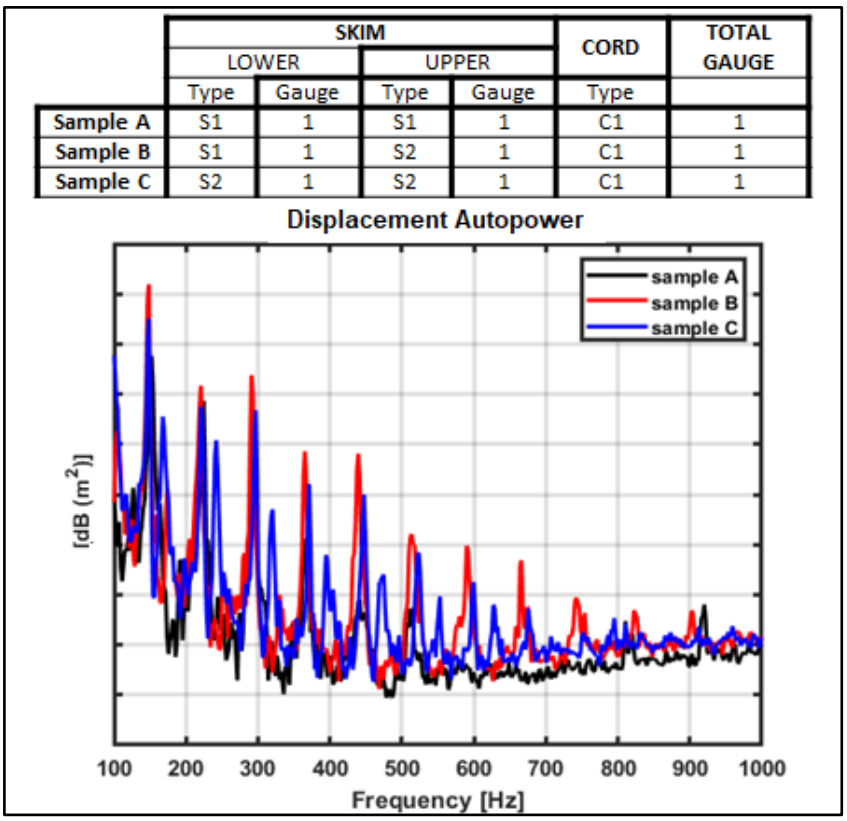

Figure 73 – Effect of skim change: out-of-plane displacement Autopower comparison

In this first comparison, the value of the total gauge is the same for all the sample because they have the same cord type (therefore the cord diameter is the same) and the two rubber layers have the same thickness. The samples differ from each other for the skim type: the samples A and C have different type of rubber but the lower and the upper ones are the same for each sample, instead of Sample B in which the two types are mixed. The frequencies of the first bending modes are not affected by the material of the skim and the variations are negligible up to about 400 Hz. The main effect of material change is the reduction of the amplitude of the out-of-plane displacement Autopowers for Sample C due to a higher damping of the S2 material.

- *Sample D VS Sample E:*

	SKIM				CORD	TOTAL GAUGE
	LOWER		UPPER			
	Type	Gauge	Type	Gauge	Type	Gauge
Sample D	S3	1	S3	1	C2	1.05
Sample E	S3	1.1	S3	1.1	C2	1.2

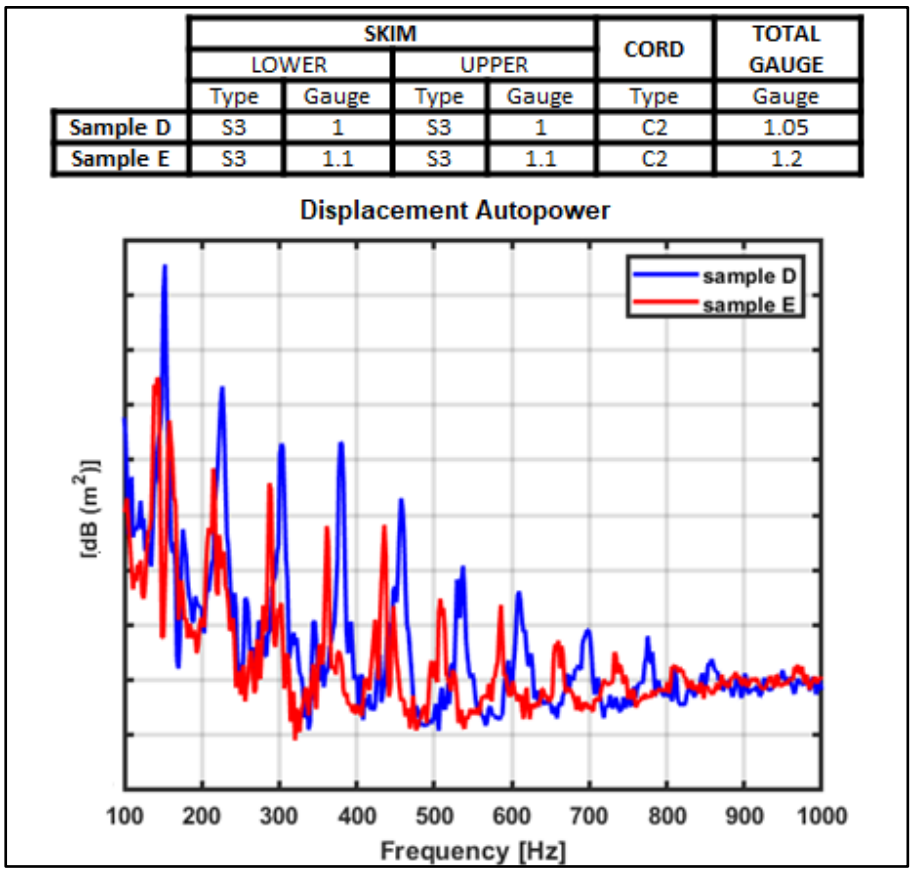

Figure 74 – Effect of cord change: out-of-plane displacement Autopower comparison

The samples of this group are compared in order to evaluate the effect of the skim gauge. The samples have the same cords and the same skim types, but the thickness of the skim of the sample E is the 10% higher and the total gauge is the 15% higher. This comparison

confirms the influence of the skim gauges on the results. Since there are no variations in terms of materials, the frequency shift of the resonance peaks can be only related to the variation of the thickness and consequently to the mass of the samples remaining the other dimensions of the sample unchanged. Once again, an amplitude reduction with the increase of the thickness of the slabs can be observed and it is related to the increase of the quantity of damping material.

- *Sample A VS Sample D VS Sample F:*

	SKIM				CORD	TOTAL GAUGE
	LOWER		UPPER			
	Type	Gauge	Type	Gauge	Type	
Sample A	S1	1	S1	1	C1	1
Sample E	S3	1.1	S3	1.1	C2	1.2
Sample F	S3	1	S3	1	C3	0.98

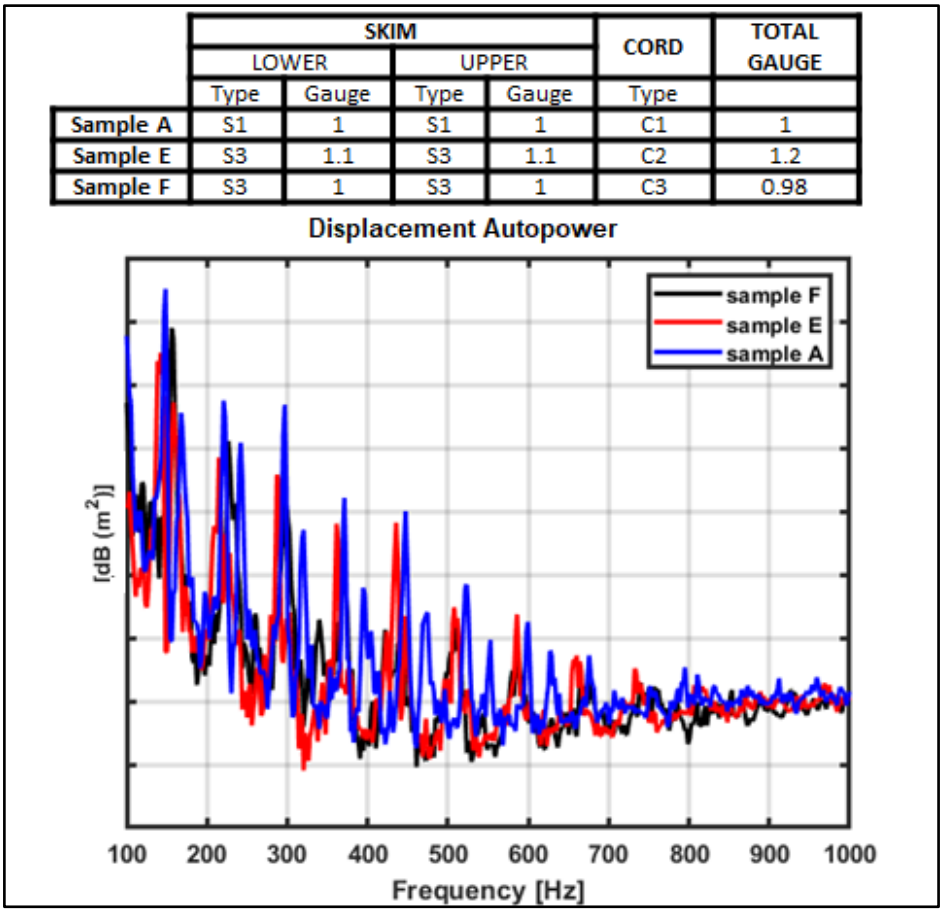

Figure 75 – Effect of mixed skim and cord change: out-of-plane displacement Autopower comparison

The last comparison is made in order to evaluate the effect of a cord change. It is similar to the first case study, but the rubber layers and the cords taken into account are different from that configuration, because they refer to another tire component (Body Ply instead of Cap Ply). This test has been made just to confirm if the frequency shift depends on mass and thickness of the samples and that it is not a consequence of a material change. In fact, the results are similar to those presented in the previous plots.

All the measurements confirm the previous results: the frequency shift is related to the total gauge and it is not important if the increase is due to the thickness of the rubber layer or to the cord diameter. In fact, if a cord with high diameter is considered, the thickness of the rubber needed to produce the samples is higher and the mass of the samples is very sensitive to rubber variation, being the mass of the cords significantly lower than the rubber mass. The cord package is quite different since the cord material of C2 and C3 is the same, but it changes the rubber they are vulcanized with: the effect is a slight reduction of the total gauge of the final sample, but also in this case the frequency shift of the first bending mode is related to the variation of the total gauge.

Summarizing, a lot of samples have been produced and tested (more than those presented in this work) to define the optimal measurement conditions, the geometry of the sample and most of all their structure. The most important and influencing features of the slabs have been considered and mixed in order to evaluate their contribution. The results reported here suggest that a slab made only of cords and two rubber layers is not feasible for the dynamic characterization of the cord-rubber composites. The final sample is made of a layer of reinforcing material, as described here, fixed to the belt package, according the position that CP or BP have in the real tire structure. More details in the next paragraph.

4.2 Dynamic characterization

The final samples are made of reinforcing layer (for example the cap ply) fixed to the belt package: in this way the reinforcing layer is connected to a stiffer and heavier component. Consequently, the samples have almost the same mass since the variation due to a reinforcing material change is negligible being the mass of belts much higher and the stiffness of the samples is determined by the properties belt package.

The results presented in this section, refers to two different groups of samples in which the effect of three different cap ply layers is studied considering two different belt packages. A sketch of how it is made the final sample to be tested is described in the next figure.

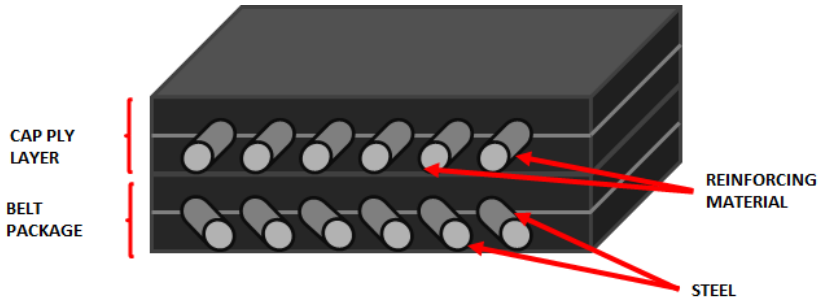

Figure 76 – Sketch of final samples with belt layer

In the sketch the structure of the samples can be seen. Two main components can be distinguished:

- the lower part is the belt package. It is a calendered sheet of rubber layers and one or more layers of steel cords with a certain angle to give strength, resistance and flexibility to the tire at the same time;
- the upper part is the cap ply layer described in the previous paragraph.

The fabric materials of the cap ply layers are those indicated as Sample A, Sample B and Sample C in Table 3 to evaluate how different the results are in this new configuration. In this new testing campaign, the Sample A can be considered as the reference for the first type of belt package considered, as well as the Sample D is the reference for the second group, in fact it has the same cap ply of A but a different belt layer. The same strategy has been adopted also for samples B - E and C – F: they have the same reinforcing layer but different belts. As regard the belt packages, they differ mainly for the number of filaments making up each cord and the configuration of the cords. For this reason, the mass of belt B2 (i.e. that of samples D, E and F) is 15% higher, due to an increase of rubber and steel: the different configuration of the filaments increases the diameter of the cords and in turn the thickness of the rubber layer necessary for calendering. The effect is an increase in terms of in-plane stiffness. The following tables briefly summarize the information.

In Table 5, the configuration of the tested samples is described. As previously said, the three cap ply layers are tested on the two belts. Table 6 describes the differences between the two belts: they only differ for the number of filaments therefore the belt B2 is a little bit heavier due to the configuration of the cords that requires more steel and more rubber. In Table 7, the three samples having the belt B1 are compared. From the values it is clear what explained before: the effect of the cap ply change is negligible in terms of samples features since the values relative to the upper layer are 1 or 2 orders of magnitude less than the belt package. In this way no significant frequency shifts are expected but only variations in terms of samples mobility deriving from the coupling of the different layers. In this first stage of the material characterization, the attention is focused on the mobility of the samples in the same way as for the rolling tire because for the mechanism understanding it is important to evaluate if it is better to have high or low mobility of the samples. In a second time, an analysis in terms of frequency resonance shift can be done, i.e. it can be studied how to shift forward or backward a mode giving a high peak in the noise spectrum.

The new optimized measurement set-up has been used to characterize the slabs described in Table 5 and the results obtained for the two groups are presented in Figure 77 where the Autopowers of the out-plane displacement are plotted considering only the points on the centreline as described in the previous paragraph, so the comparison of the results is made considering the same points. The results are divided into two groups based on belt type, but the same colours have been used for the same cap ply layers described in Figure 71 so the Sample C is black because it contains the Sample A of the cited figure, Sample A and B are blue and red respectively because they have the reinforcing layer B and C of the same test.

As expected, there are no significant frequency shift, except for the red line of Belt B2 group in which the small shift, visible in the first group, seems to be magnified passing from Belt B1 to B2. In these testes, the cap ply layer affects only the amplitude of the displacements. In terms of ranking, it can be said that up to about 300 Hz it is conserved for both the belts, in fact the amplitude of samples B and C is higher than the reference as well as E and F

compared with D. Moreover, the red lines, have generally a little bit higher level than the others even if at around 300 Hz the ranking between the red and the black lines is inverted for both the cases.

	BELT		CAP PLY		
	B1	**B2**	**C1**	**C2**	**C3**
SAMPLE A	X		X		
SAMPLE B	X			X	
SAMPLEC	X				X
SAMPLE D		X	X		
SAMPLE E		X		X	
SAMPLE F		X			X

Table 5 - Final samples configuration

	BELT B1	**BELT B2**
Rubber mass	1	1.10
Steel mass	1	1.24
Total mass	1	1.14
Density of steel cords	1	1.25

Table 6 – Belt packages comparison

	Sample A	**Sample B**	**Sample C**
Mass of belt package	1	0.99	1.02
Mass of reinforcing layer	1	0.6	1.16
Total Mass	1	0.98	1.02
Cap Ply Fabric Modulus	1	1.02	0.95
Belt package gauge	1	0.97	1.05
Reinforcing material gauge	1	0.8	0.7
Total gauge	1	0.98	0.99

Table 7 – Main features of the samples with B1 belt

The main difference between the two test cases is the dispersion of the results: in the first one, the differences between the curves are lower than the second group and for certain it requires a further investigation to confirm the results. This effect could be related to the different belts: the configuration of the steel cords in the second belt increases the in-plane stiffness, so the out-of-plane excitation could be magnified as well as the displacements in this direction because of the reduction of the in-plane mobility. Despite the excitation is the same used for the samples without belts, the response of the new samples is limited up to 300 – 350 Hz: it depends on the different characteristics of the belted samples that have lower natural frequencies if compared with non-belted samples and the higher damping due to the increase of rubber layer. However, if the results presented in the paragraph dedicated to the

static characterization of the tire and the validation of the DIC set-up are recalled, the frequency of the resonances obtained here are comparable with those of a real tire. It is related to the new structure of the samples that is closer to that of the final tire. In the same way, the static measurement on the tire proves that it is not possible to excite the tire structure at the frequency typical of the rolling conditions, since the high frequency vibration are generated by a different mechanism, in fact they are related to the impulses coming from the impacts of tread blocks with the road and their vibrations. In static condition this kind of excitation cannot be reproduced so the analysis must be performed in a shorter frequency range.

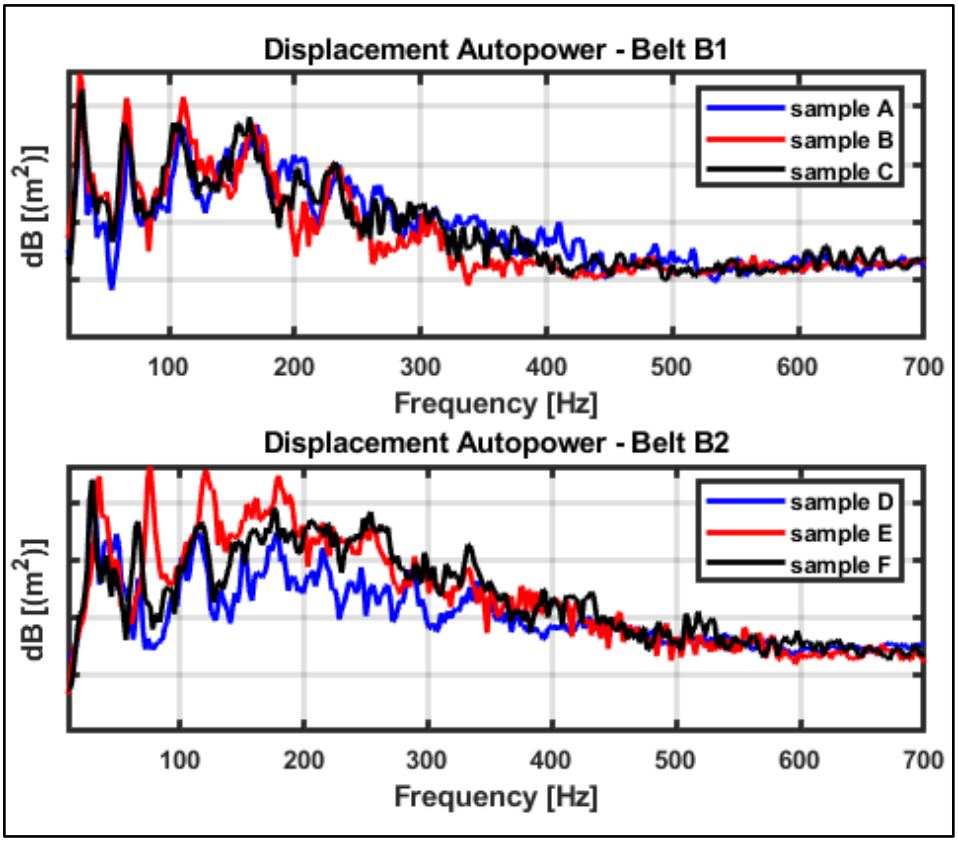

Figure 77 – Comparison of the out-of-plane displacement Autopower for the tested samples described in Table 4

Once the samples have been characterized, it is necessary to define which is the best solution, but with the current information it is not possible to say it, because they should be analysed from a global point of view, i.e. the effect on the rolling tire should be analysed as well as the noise emission. In fact, the effect of all the samples should be evaluated producing a tire for each of the characterized samples and dynamically characterizing all the tires to find the one giving the lower noise emission. This procedure is very expensive in terms of

both time and money and the idea of reducing the number of tests on real tires that this approach wants to introduce would be lacking. So, the two samples with the greatest difference in terms of mobility have been selected to produce the tires to be tested. The idea is to evaluate the noise emission, measure sidewall and tread vibrations and correlate them with the mobility of the slabs. The samples considered are Sample A and Sample B, even if the difference between Sample D and Sample E is higher: according to the company know-how, the combination of Belt B2 with the cap plies obtained using the construction of samples D and E generates tire footprints too different and it would not possible to separate the effect of a different layer (and then of the samples) from that of the footprint. Belt B1, instead, produces minimal differences that are negligible. The complete analysis of the two tires is described in the next paragraph.

4.3. Material optimization validation

In this paragraph the complete process of the correlation of noise emitted from the rolling tires with the dynamic characterization of tires and samples is performed. The comparison considers two tires indicated as Tire A and Tire B. Both the tires have the same belt package, the one previously called B1. Tire A is so-called because it is realized with Sample A, while Tire B has the Sample B as reinforcing layer. The characterization of tires gives the following results:

- in terms of noise emission, the standard Pass-by-Noise test reveals a reduction of 0.8 dB(A) for Tire B with respect to Tire A;
- in terms of vibration, there is an overall reduction of the sidewall vibration level even if the crown's level is slightly increased, likewise the first case study described in Chapter 3.

Since the only difference in tire construction is the different reinforcing layer, a modal analysis on the cord-rubber composites used in the tires must be performed to characterize the two layers. The Operational Modal Analysis (OMA) has been performed instead of the classic Experimental Modal Analysis because it allows to obtain better results. In Figure 77, the samples have been compared looking at the Autopowers of the out-of-plane displacement to be coherent with the analysis performed with all the other samples. However, in this case the modal analysis can be performed considering the whole samples because in the belted slabs the torsional effects are not emphasized, in fact the bending modes are clearly detected unlike the torsional ones that are not excited with the stinger fixed on the centreline. The modal analysis is made considering a subset of the thousands of points measured by the DIC set-up (500 uniformly distributed points are considered to reduce the computational time and mostly the time required to import the data from MatLab to TestLab). Of course, the results obtained considering 500 points have been compared with those of a full analysis and there is a perfect correlation, also because 500 points are more than enough considering the dimensions of the slabs. The results of the OMA on the two belted samples considered are presented in Figure 78.

The modal analysis of the slabs confirms that the mobility of Sample B is higher than that of Sample A and it is confirmed also by the visualization of the ODS (as example only the first two bending modes are plotted). Considering that the cap ply layer is placed under tread, these data should be compared with the vibration measurement on the tire crowns. As anticipated, the characterization of the rolling tires reveals a reduction of sidewall vibrations, but the crown's vibration level is higher: it is in accordance with the measurement on the samples because the mobility of Sample B (corresponding to Tire B) is higher than Sample A. In conclusion, it can be stated that Sample B is better than Sample A because it allows to reduce the noise emission of the rolling tire. All the results are presented in the next figures.

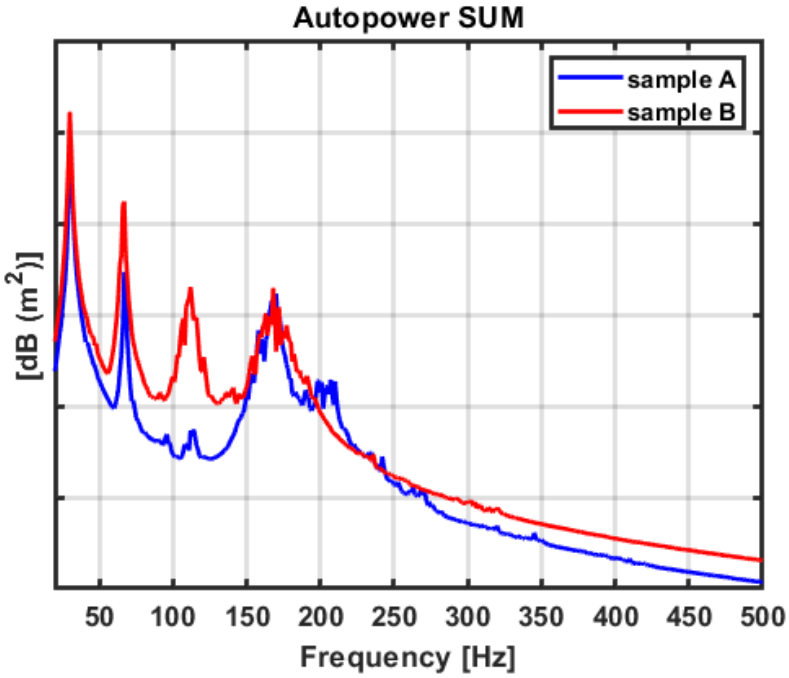

Figure 78 – OMA on samples A and B

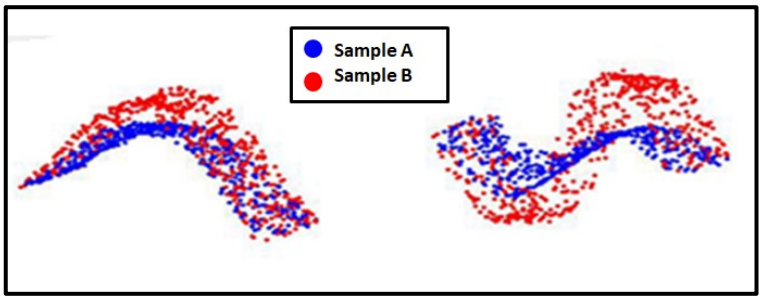

Figure 79 - Mobility comparison for the first two bending modes of samples A and B

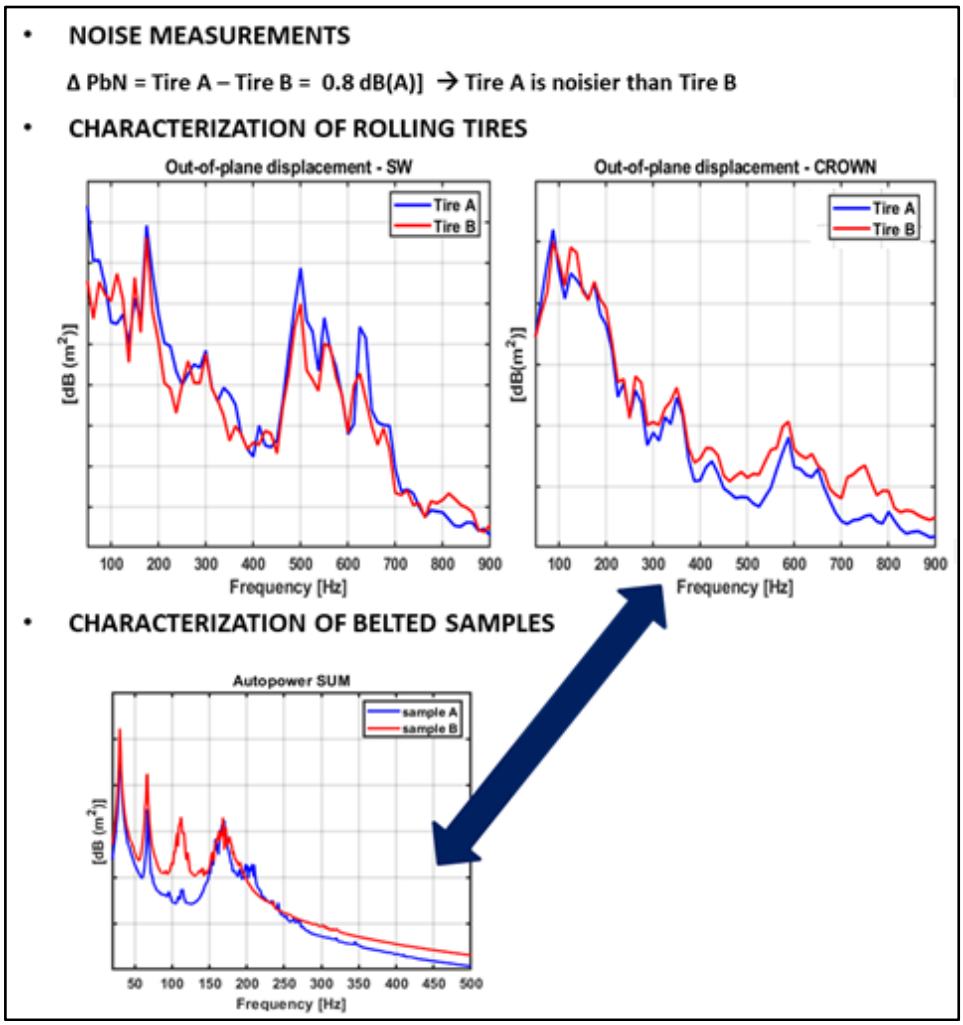

Figure 80 - Analysis of acoustic measurement and dynamic characterization of tires and tire components used for the validation of the material optimization

4.3. Chapter summary

The final chapter is dedicated to the characterization of cord-rubber composite. This activity has two main purposes: to provide the dynamic characterization of tire components and to generate a noise-oriented database of the reinforcing materials. As explained in the

introduction, each tire component is made of a layer of rubber with embedded cords. Both the cords and the rubber are deeply characterized and all their properties are well known, but all these data are not useful to predict noise because the characterizations currently available were born for other applications and the parameters they estimate are not noise-oriented.

In this thesis a characterization of the cord-rubber composite is considered and a lot of time have been spent on the definition of the optimal set-up configuration. Different clamping, different excitation and different excitation points have been tested as well as different samples configuration. The samples are realized as if they were extracted from the tire structure, but if only cap ply or body ply samples are produced, they have a very small mass and each change in cord diameter determines an important mass variation that governs the shift of the resonances of the samples. Moreover, due to some technical limitations of the manufacturing process, the samples show an unwanted torsional behaviour even if the attention is focused on the bending modes that are supposed to be the most important in terms of noise emission and in fact the excitation way in the out-of-plane direction.

The final solution includes samples made of cap ply or body ply layer and the belt package: in this way the mass variation is neglected because the mass of the belts is too much higher than the mass of the other layers and all the properties are determined by the belts. The effect of the final layer has an effect on the mobility. The mobility seems to be the parameter to consider for the classification of the reinforcing materials. The comparison between vibration measurement on rolling tire and samples, combined with acoustic measurement on rolling tire, suggest that a noise reduction can be obtained tire with high crown mobility, and the crown mobility is strictly related to the mobility of the samples studied in this chapter.

This page intentionally left blank.

Chapter 5.

Concluding Remarks

5.1. Conclusions

The main topic of this PhD project is the development and the validation of an innovative set-up to measure the vibrations of a rolling tire and the measurement procedure. The need of such a measurement set-up derives from the automotive industry that is forced to achieve a significant reduction in terms of noise emitted by a rolling tire answering to requirements coming from both the car manufactures and the new regulations. The increasing interest on this topic suggests the tire manufacturers to modify the approach to the problem taking into account the noise emission from the first stages of the development of the new tires. To do this, it is necessary to better understand the mechanisms that generate noise when the tire is rolling. Since one of the most important noise sources are the vibrations, this is the reason why this thesis is focused on the development of such a set-up.

During the last weeks of the project, the same set-up has been used to propose a new dynamic characterization of tire samples in order to define a noise-oriented characterization of the reinforcing materials. This new approach wants to overcome the limits of the current characterization: small samples not representative of tire behaviour, rubber and reinforcing fabric are characterized separately and quasi- static characterization of cord-rubber composites. In this way all the mechanical properties of rubber and reinforcing fabric are well known separately, but they cannot be used to predict the effect on nose emission. Moreover, the current characterization of the cord-rubber composites does not provide useful information since they are characterized by only the in-plane and out-of-plane stiffness, but in such application, it is more important to know how the composites work in the frequency domain. The new approach is based on the dynamic characterization of the cord-rubber composites samples and it can reduce significantly the number of prototype tires to be produced and tested, with a reduction in terms of costs and times, because the effect of a material change on the noise emission can be predicted looking at the mobility of the samples.

As regard the main topic of the thesis, the vibration measurement, an innovative set-up has been developed, optimized and validated. It is based on the 3D-Digital Image Correlation technique and it is used to overcome the limits of the current state of art technique, i.e. the Scanning Laser Doppler Vibrometer. The set-up has been used to perform both static and dynamic measurements and in both the case the LDV has been used for the validation. The vibration measurement in static condition is quite easy to perform and the results show a very good correlation with the LDV measurement. The measurement in

dynamic conditions has required a long optimization process, since there are no references in literature suggesting the best configuration and the influence of several parameters needed to be studied. The main problem is related to the amplitude of the frequency range of interest related to the resolution of the current fast cameras. The frequency range of interest for a rolling tire is very wide and its related to the rolling speed. In fact, if the low frequency carcass vibrations and the high frequency vibration responsible of the so-called pattern noise have to be studied together, it must be used an instrument which can measure in the range 0 – 1000 Hz. Moreover, the groups of vibrations are significantly different from each other since the first one deals with high amplitude vibrations that involves the whole tire structure, while the high frequency vibrations are characterized by small displacements localized in the contact patch area. With the available set-up, it is not possible to measure in this wide range, but according to the vibration group of interest, different configurations of the set-up must be used. In particular, a different framing is required: the low frequency vibration can be measured with a full-tire view, while the high frequency vibrations require a closer view on the contact patch area because the resolution of the system is increased and the small displacement characterizing these vibrations are correctly measured as demonstrated by the comparison with LDV. In this way, the DIC's feature to be a full-field technique cannot be completely exploited, but it is not a problem because it has been demonstrated that the contact patch area is the most representative region of tire in terms of vibrations and then of noise emission.

The DIC set-up can be used for other several tire applications, some of them can be found in literature. In this work a procedure to characterize four regions of tire sidewall and attach them has been developed. It has been used to study the contributions of sidewall regions, but also to provide a tool useful data for the validation of the FEM models simulating tire vibrations: one of the main problems of the LDV measurement is the low number of measurement points and their spatial density, not high enough to be compared to those of a FEM model. Moreover, it must be considered that the acquisition time is directly proportional to the number of measurement points. For example, the acquisition of the 80-points circumference, used in this work for the validation, takes about 15 minutes. To validate a FEM model, thousands of points are needed, so the acquisition would last a couple of hours with a significant variation in terms of boundary conditions and the stationarity of the phenomenon cannot be guaranteed (variation of inflation pressure, tire temperature and room temperature cannot be neglected). For sure, the only contact patch data cannot be used for the validation of the models, so a procedure to measure different area of the sidewall and reattach them during post-processing using a phase reference sensor must be used. The DIC measurement is almost instantaneous and a single acquisition provides thousands of points with a spatial density comparable with that of a FEM model.

The biggest innovation introduced in terms of tire vibrations, is the measurement on the crown of a real patterned tire, not possible with other techniques. In this case, only the closer view can be adopted because the excitation rapidly decays due to the high damping of the tread compound. The new information coming from the tread area and the comparison with sidewall, have been used to analyse some construction changes and to provide the development engineers the guidelines for the design of a noise-oriented tire.

The comparison of DIC data with those of LDV shows a good correlation between the results obtained from both the techniques. The LDV sensitivity is a little bit higher than the DIC and this is the reason why there is a slight difference in terms of vibration amplitude.

It could be eliminated reducing the framed area, but, in this first stage of the analysis, the company requirement was the development of a system able to compare different tires, rather than the evaluation of the exact displacement values, so it is preferable to have a little bit higher measurement area and a little bit lower accuracy. For sure in the future will be produced fast cameras with higher frame rates and higher resolution than the current one and this problem will be overcome.

As regard the second topic, a completely new approach to the study of tire noise has been proposed to predict the effect of reinforcing materials on noise emission. It is based on the dynamic characterization of the cord-rubber composite samples of tire components such as cap ply or body ply layers. The samples are characterized using an electro-dynamic shaker and measuring samples responses using the DIC set-up. Being a completely new activity, a lot of time and a lot of tests have been performed to define the optimal configuration of the samples. The first attempts, in fact, have been made on too lightweight samples giving a shift of the resonances related to the mass variations of the samples only. Every change, both in rubber and cord type, does not give the expected variations, the only parameters that match the frequency shifts are the mass and the thickness of the samples. The results are not supported by the numerical results obtained considering a sandwich beam with both the edges fixed: maybe it depends on the particular configuration of the samples, that is a sandwich, but it does not have several layers, but it has some cords embedded into two rubber layers and probably in this configuration the mass variations are the most important. Further investigations would be necessary, but there is another problem that suggest modifying the samples: the tested samples the resonances are shifted, but there are no variations in terms of amplitude, that is desired effect. For this reason, the structure of the samples has been modified introducing also the belt package. In the final configuration, the main properties are determined by the belt package and the effect of different additional layers is a variation in terms of displacement amplitude. The first results are promising since a correlation between noise emission, rolling tire vibration measurement and samples characterization has been found: the samples with higher mobility belong to tires with high crown mobility which are the tires with lower noise emission, as demonstrated by a teste case reported. According to these first results, it seems that the mobility is the parameter to consider when a noise-oriented reinforcing material wants to be used. If the noise generated by a rolling tire can be correlated to the dynamic characterization of a single tire component, it can be understood how consistent the reduction of the costs related to the production of prototypes and their tests will be.

5.2. Future works

As regard the dynamic characterization of the rolling tire, a lot of work in terms of set-up optimization has been done, but there are some aspects that could be improved. For example, the measurement on tire crown. The current set-up allows to measure quite easily the central ribs, in fact in most the cases only some frames are not automatically correlated

by the algorithm and a manual procedure is needed. It increases a little bit the time processing, but it is currently the unique way to perform this kind of measurement. The number of uncorrelated frames is strictly related to the quality of the speckle pattern: during this PhD project a first improvement has been done covering the central ribs with a black adhesive paint increasing both the contrast of white dots and the definition of their outlines. However, this is a countermeasure studied for the available printer, that probably is not the best solution. In the future, other painting systems can be tested and compared or it could be used a speckle projected on the tire. In this way the problem of speckle deletion due to friction could be overcome and for example several measurements could be performed and attached in order to increase the number of averages and reduce the measurement noise. As regard the measurement on the external ribs the situation is more complex due to the lugs that generate big shadows and the number of uncorrelated frames is very high. Maybe the solution could be to fill the voids in order to create a smooth and continuous surface. However, the research of a material easy to put in the lugs and that leaves the tread blocks free to move at the same time is not easy. The attempts of filling the lugs with a sponge and silicone-like material have been done but they did not work: the sponges tend to detach themselves from the tire and the speckle pattern is not visible; the silicone-like material generate some cleats because it is not easy to fill the voids obtaining a smooth surface. For sure, in order to perform this measurement, other solutions must be defined because it could be used also on winter tires, that have a very complex tread design and full of voids that make the measurement impossible for the moment.

Another application of the DIC could be its connection with a FEM or BEM model for the study of noise propagation: the DIC generate displacement maps for the measured area so, if a model is defined, these data can be imported and the noise simulation can be performed. It could be a first step in the validation of the acoustic simulation of the rolling tire waiting for the vibrational simulations to be validated too.

As regard the characterization of tire components, more measurements are needed in order to increase the database of characterized materials and confirm the first results. For examples other tires could be produced in order to test the samples with Belt B2, but adopting a dedicated countermeasure to avoid significant differences in terms of tire footprint. Moreover, some improvements on the samples have been identified, for example it is necessary to find the way to produce samples having a slot where the stinger of the shaker can be inserted and also a better clamping system: in this way the excitation point is perfectly the same for all the samples as well as the excitation that is influenced by the constraints.

An important step in terms of measurement simplification could be the definition of the minimum number representative points to be acquired. In this way an alternative measurement set-up could be defined, for example based on LDV or micro-accelerometers if few points must be acquired. All the measurement procedure would be speeded up because a dedicated workstation could be realized reducing the time needed for the set-up preparation that is quite long in the case of DIC set-up.

This page intentionally left blank.

References

[1] G. E. Ayyar, M. M. Khule and M. S. Kajarekar, "Noise Generation Mechanism of Tires," *International Journal of Engineering Research and Development,* vol. 12, no. 10, pp. 29 - 33, October 2016.

[2] S. Vercammen, C. González Díaz, P. Kindt, J. Middelberg, C. Thiry and J. Leyssens, "Experimental characterization of the dynamic behavior of rolling tires," in *Proceeding os ISMA 2012 - USD 2012*.

[3] M. Heckle, «Tyre Noise Generation,» *Wear,* vol. 113, pp. 157 - 170, 1986.

[4] (. C. o. E. R. f. A. T. N. Mitigation, "Research for a quieter Europe in 2020: Updated strategy paper of the CALM II network," 2007.

[5] «https://www.discounttiredirect.com/learn/tire-construction,» [Online].

[6] M. G. Pastore Carbone, J. Parthenios, G. Tsoukleri, S. Cotugno, G. Mensitieri and C. Galiotis, "Assessing micromechanical behaviour of PET cords in rubber matrix composites by laser Raman microscopy," *Composites Science and Technology,* no. 85, pp. 104 - 110, 2013.

[7] U. D. o. T. -. N. H. T. S. Administration, "The Pneumatic Tire," 2005.

[8] D. Osborne, "The role of cap plies in steel belted radial tires," 2003.

[9] T. Vieira, *Tyre-road Interaction: a holistic approach to noise and rolling resistance,* 2018.

[10] U. Sandberg and H. J. A., Tyre/road noise referenve book, INFORMEX, 2002.

[11] A. Fadavi, D. Duhamel, P. Klein and F. Anfosso-Ledee, "Tire/road noise: 3D model for horn effect," in *InterNoise 2000*.

[12] G. J. Kim, K. R. Holland and N. Lalor, "Identification of the Airborne Component of Tyre-induced Vehicle Interior Noise," *Applied Acoustics,* vol. 51, no. 2, pp. 141-156, 1997.

[13] W. Kropp, K. Larsson, F. Wullens, P. Andersson and F. X. Bécot, "The generation of tyre/road noise - mechanisms and models," in *10th International Congress on Sound and Vibration*, Stockholm, Sweden, 7 - 10 July 2003.

[14] J. Winroth , W. Kropp, C. Hoever, T. Beckenbauer and M. Männel, "Investigating generation mechanisms of tyre/road noise by speed exponent analysis," *Applied Acoustics,* vol. 115, pp. 101-108, 2017.

[15] K. Liljegren, *Visual and acoustic tyre tread design,* Master's Thesis Chalmers University of Technology, 2008.

[16] A. Abd_Elsalam et al, "Modal analysis on tire with respect to different parameters," *Alexandria Engineering Journal,* 2016.

[17] R. S. Pieters, «Experimental modal analysis of an automobile tire under static load.,» *DCT rapporten,* vol. 2007.112, 2007.

[18] L. Yam , D. Guan and A. Zhang , "Three-dimensional Mode Shapes of a Tire Using Experimental Modal Analysis," *Experimental Mechanics,* vol. 40, no. 4, pp. 369 - 375, December 2000.

[19] G. Rocca, C. Gonzalez Diaz, J. Middelberg, P. Kindt and B. Peeters, "Experimental Characterization of the Dynamic Behaviour of Tires in Static and Rolling Conditions," in *18th International Congress on Sound & Vibration*, Rio de Janeiro, 2011.

[20] P. J., «A study of radial vibrations of a rolling tire for tyre-road noise characterisation,» *Mechanical Systems and Signal Processing,* vol. 16, n. 6, pp. 1043-1058, 2002.

[21] N. Tsujiuchi, T. Koizumi, Y. Maeda and I. T., "An investigation of Rolling Tire Noise Generated by Vibration," in *IMAC XX*.

[22] M. Pallas, "Tire-road Noise: an Analysis of the Tire Vibrations," in *Ler Congres Francais d'Acoustique*, 1990.

[23] D. Bernhard, T. Bernhard and R. Bernhard, "Accelerometer Measurements of Tire Tread Vibrations and Implications to Wheel-Slap Noise," *Tire Science and Technology,* vol. 41, no. 2, pp. 109-126, April-June 2013.

[24] A. Niskanen and A. J. Tuononen, "Three Three-Axis IEPE Accelerometers on the Inner Liner of a Tire for Finding the Tire-Road Friction Potential Indicators," *Sensors,* vol. 15, pp. 19251-19263, 2015.

[25] Yi Xiong and Xiaoguang Yang, "A review on in-tire sensor systems for tire-road interaction studies," *Sensor review,* 2018.

[26] S. Vercammen , P. Kindt , C. Gonzalez Diaz and W. Desmet , "Analyses on the effects of rolling on the tire dynamics," in *Internoise*, Innsbruck, Austria, 2013.

[27] K. Matsumoto, M. Ishihama, Y. Komagamine and K. Miyoshi, "Analysis of High-frequency Vibration Wave Propagation on Tire Tread Using a Laser Displacement Sensor and FEM Simulation.," in *Annual Spring Congress*, Yokohama, May 2016.

[28] G. Rocca, B. Peeters, C. González Díaz, J. Middelberg and P. Kindt, "Experimental study for high-frequency modal characterization of tires," in *ICVS18 - 18th International Congress on Sound & Vibration*, 2011.

[29] P. Castellini, “Vibration measurements by tracking laser doppler vibrometer on automotive components,” *Shock and Vibration,* vol. 9, pp. 67 - 89, 2002.

[30] B. M. Castellini P., “How to measure actual tire shape in the rolling condition using Scanning LDV,” *Mechanical Systems and Signal Processing,* vol. 24, pp. 736 - 745, 2009.

[31] UNIVPM, «Single tyre experimental (vibrational and acoustic) characterization».

[32] P. Kindt, A. delli Carri, B. Peeters, H. Van der Auweraer, P. Sas and W. Desmet, “Operational Modal Analysis of a rotating tyre subject to cleat excitation,” in *Proceeding of IMAC 28*, 2010.

[33] M. Batel, “Operational Modal Analysis – Another Way of Doing Modal Testing,” *Sound and Vibration Journal,* 2002.

[34] J. Bolton and Y.-J. KIM, “Wave number domain representation of tire vibration,” in *the 29th International Congress and Exhibition on Noise Control Engineering*, Nice, France, 27-30 August 2000.

[35] C. Gonzalez Diaz, P. Kindt, J. Middelberg, S. Vercammen, C. Thiry, R. Close and J. Leyssens, “Dynamic behaviour of a rolling tyre: Experimental and numerical analyses,” *Journal of Sound and Vibration,* vol. 364, pp. 147-164, 2016.

[36] T. Koizumi, N. Tsujiuchi, M. Matsubara and F. Nakamura, “Vibration Analysis of Rolling Tire based on Thin Cylindrical Shell Theory,” in *ISMA*, 2010.

[37] N. Tsujiuchi, T. Koizumi, R. Tamaki and I. Shima , “An Investigation of Rolling Tire Vibration Caused by Road Roughness,” in *IMAC XXII*, 2008.

[38] P. Kindt, F. De Coninck, P. Sas and W. Desmet, “Test setup for tire/road noise caused by road impact excitations: first outlines,” in *Proceedings of ISMA 2006*.

[39] P. Kindt, P. Sas and W. Desmet, “Measurement andanalysisofrollingtirevibrations,” *OpticsandLasersinEngineering,* vol. 47, pp. 443-453, 2009.

[40] P. Kindt, F. De Coninck, P. Sas e W. Desmet, «Analysis of tire/road noise caused by road impact excitations,» *SAE Technical Paper,* 2007.

[41] P. Castellini, F. Giovanucci, G. Nava-Mambretti, L. Scalise and E. Tomasini, “Vibration Analysis of tire treads: a in-plane Laser Vibrometry approach,” in *Proceeding of SPIE - The International Society for Optical Engineering*, 1998.

[42] M. N. Helfrick, C. Niezrecki, P. Avitabile and T. Schmidt, “3D digita limage correlation methods for full-field vibration measurement,” *MechanicalSystemsandSignalProcessing,* vol. 25, pp. 917-927, 2011.

[43] T. Beberniss and D. A. Ehrhardt, “High-speed 3D digita limage correlation vibration measurement: Recent advancements and noted limitations,” *MechanicalSystemsandSignalProcessing,* 2016.

[44] P. Reu et al., “Comparison of DIC and LDV for practical vibration and modal parameters,” *Mechanical Systems and Signal Processing,* 2016.

[45] D. A. Ehrhardt, S. Yang, T. J. Beberniss and M. S. Allen, “Linear and Nonlinear Response of a Rectangular Plate Measured with Continuous-Scan Laser Doppler Vibrometry and 3D-Digital Image Correlation”.

[46] D. A. Ehrhardt, S. Yang, T. J. Beberniss and M. S. Allen, “Mode Shape Comparison Using Continuous-scan Laser Doppler Vibrometry and High Speed 3D Digital Image Correlation”.

[47] T. Botha and P. Els, “Digital image correlation techniques for measuring tyre-road interface parameters: Part 2 - Longitudinal tyre slip ratio measurement,” 2015.

[48] T. A. J., «Digital ImageCorrelationtoanalysestick–slip behaviour of tyre tread block,» *Tribology International,* n. 69, pp. 70-76, 2014.

[49] R. A. Moser, H. J. Sube, J. L. Turner and P. Zakelj, “3D Digital Imaging Correlation: Applications to Tire Testing,” *Tire Science and Technology TSTCA,* vol. 38, no. 2, pp. 100-118, April – June 2010.

[50] A. Mange, J. Baqersad, V. Srivastava and J. More, “Using Digital IMage Correlation to Measure Dynamic of Rolling Tires,” *SAE Technical Paper 2018-01-1217,* 2018.

[51] K. Patil, J. Baqersad and A. Sheidaei, “A Multi-View Digital Image Correlation for Extracting Mode Shapes of a Tire,” in *Conference Proceedings of the Society for Experimental Mechanics Series*, 2017.

[52] R. Moser and J. G. Lightner III, “Using 3D Digital Imaging Correlation Techniques to Validate Tire FEM,” in *SEM Annual Conference*.

[53] W. Kropp, P. Sabiniarz, H. Brick and T. Beckenbauer, “On the sound radiation of a rolling tire,” *Journal of Sound and Vibration,* vol. 331, no. 8, pp. 1789-1805, 9 April 2012.

[54] J. Biermann, O. von Estorff, S. Petersen and H. Schmidt, “Computational Model to Investigate the Sound Radiation from Rolling Tires,” *Tire Science and Technology, TSTCA,* vol. 35, no. 3, pp. 209-225, 2007.

[55] PerkinElmer, Inc., «www.perkinelmer.com/lasoffices,» 2007. [Online].

[56] K. P. Menar and M. N. R., “Dynamic Mechanical Analysis in the Analysis of Polymers and Rubbers,” in *Encyclopedia of Polymer Science and Technology*, John Wiley & Sons, Inc., 2015.

[57] «https://www.smithersrapra.com/testing-services/by-material/rubber-and-elastomer-physical-testing/dma,» [Online].

[58] M. G. Pastore Carbone, "Investigating mechanical behavior of cord-rubber composites by multi-scale experimental and theoretical approach," PhD Thesis, 2011.

[59] N. Pan, "Physical Properties of Twisted Structures. II. Industrial Yarns, Cords, and Ropes," *Journal of Applied Polymer Science,* vol. 83, pp. 610-630, 2002.

[60] A. S. Hockenberger and S. Koral, "Effect of twist on the performance of tire cord yarns," *Indian Journal of Fibre & Textile Research,* vol. 29, pp. 19-24, 2004.

[61] A. Aytaç, B. Yilmaz and V. Deniz, "Effects of Linear Density and Twist Level on the Mechanical Properties of Nylon 6.6 Tyre Cords," *Fibers and Polymers,* vol. 11, no. 2, pp. 309-315, 2010.

[62] T. Takeyama and J. Matsui, "Recent developments with tire cords and cord-to-rubber bonding," *Rubber Chemistry and Technology,* vol. 42, no. 1, pp. 159-256, 1969.

[63] T. S. Solomon, «Systems for tire cord-rubber adhesion,» *Rubber Chemistry and Technology,* vol. 58, n. 3, pp. 561-576, 1985.

[64] Encyclopedia of chemical technology, Kirk-Othmer, 2004.

[65] M. Buytaert, F. Coornaert and W. Dekeyser, "Characterization of the steel tire cord-rubber interface," *Rubber Chemistry and Technology,* vol. 82, no. 4, pp. 430-441, 2009.

[66] M. A. Sutton, J.-J. Orteu and S. H. W., Image Correlation for Shape, Motion and Deformation Measurements - Basic Concept, Theory nd Application, Springer, 2009.

[67] D. Lecompte, H. Sol, J. Vantomme and A. Habraken, "Analysis of speckle patterns for deformation measurements by DIC," in *Proceedings of SPIE - The International Society for Optical Engineering*, 2006.

[68] Correlated Solution, *Speckle Pattern Fundamentals.*

[69] D. Boulahbal, J. Britton, M. Muthukrishnan and F. Gauterin et al., "High frequency tire vibration for SEA models partitioning," *SAE Technical Paper,* no. 2005-01-2556, 2005.

[70] G. M. Revel , M. Martarelli and P. Chiariotti , "A new laser vibrometry-based 2D selective intensity method for source identification in reverberant fields: part I. Development of the technique and preliminary validation," *Measurement Science and Technology,* vol. 21, no. 075107, 2010.

[71] S. Vercammen, C. González Díaz, P. Kindt, J. Middelberg, J. Thiry and C. Leyssens, "Experimental characterization of the dynamic behavior of rolling tire," in *Proceedings of ISMA 2012*.